



REPUBLIC OF YEMEN
MINISTRY OF WATER AND ENVIRONMENT
SANA'A BASIN WATER MANAGEMENT PROJECT

(IDA CREDIT 3774-YEM)

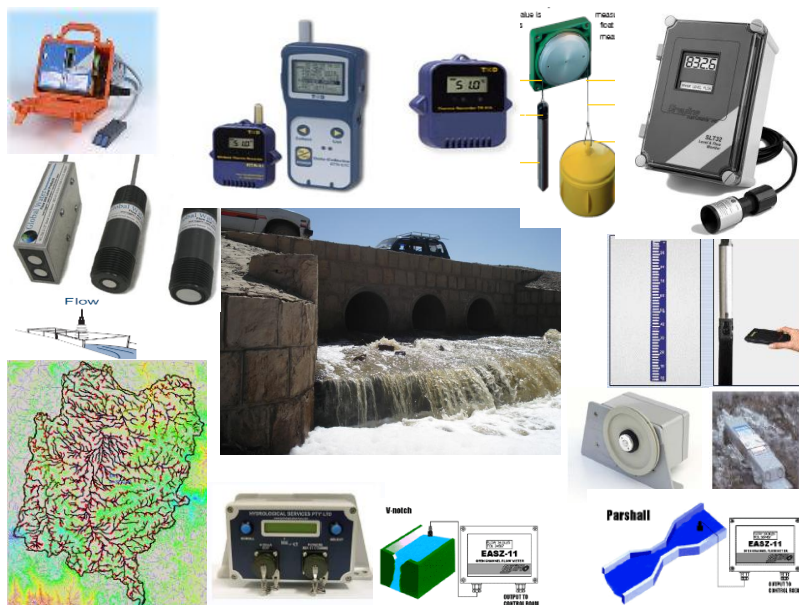
Sub-Component 3(d)

Hydro-geological and Water Resources
Monitoring and Investigations

ACTIVITY 4: HYDROLOGICAL MONITORING AND ANALYSES IN SANA'A BASIN

DRAFT FINAL REPORT
(Part II: Surface Water Report)

by
Dr. Khaled Kheireldin
Regional Consultant



Financed by the World Bank

April, 2008

HYDROSULT Inc.
Consultants, Experts-conseils

TABLE OF CONTENTS

| | |
|--|-----|
| TABLE OF CONTENTS | i |
| LIST OF FIGURES | ii |
| LIST OF TABLES | xii |
| Executive Summary..... | 1 |
| Chapter 1. General Hydrological Features of the Sana'a Basin | 2 |
| 1.1 Introduction..... | 2 |
| 1.2 Sana'a Basin | 2 |
| 1.2.1 Location | 2 |
| 1.2.2 Major Features of the Sana'a Basin | 3 |
| 1.2.3 Sub-Basin Delineation..... | 5 |
| 1.2.4 Water Resources of the Sana'a Basin..... | 5 |
| 1.2.5 Water Use in the Sana'a Basin | 7 |
| 1.2.6 Dams in the Sana'a Basin | 9 |
| Chapter 2. Geospatial Simulation and Analysis of the Sana'a Basin | 11 |
| 2.1 Applied Theoretical Approach..... | 11 |
| 2.2 Stream delineation using GIS..... | 12 |
| 2.2.1 Theory behind GIS-based watershed delineation | 12 |
| 2.2.2 Flow direction | 14 |
| 2.2.3 Flow accumulation, stream grids, and drainage area | 14 |
| 2.2.4 Watershed delineation..... | 15 |
| 2.2.5 Watershed and Stream Delineation Software | 15 |
| 2.2.6 Watershed and Stream Delineation for Sana'a Basin..... | 15 |
| Chapter 3. Delineation of Sub-Basins within the Sana'a Basin | 16 |
| 3.1 Introduction..... | 16 |
| 3.2 Delineation of Sub-Basins and Sub-Sub-Basins..... | 17 |
| Chapter 4. Rainfall Analysis, Development of Intensity Duration Curves and Storm Pattern of the Sana'a Basin..... | 37 |
| 4.1 Storm Design..... | 37 |
| 4.1.1 IDF within Sana'a Basin | 38 |
| 4.2 Developing of Storm Pattern for the Sana'a Basin | 56 |
| 4.2.1 Recorded Rainfall | 56 |
| 4.2.2 Storm Pattern for Darselm Station..... | 57 |

| | | |
|------------|--|-----|
| Chapter 5. | Determination of Suitable Locations for Surface Water Monitoring in the Sana'a Basin | 58 |
| 5.1 | Introduction..... | 58 |
| 5.2 | Land Use Map..... | 59 |
| 5.3 | Soil Map | 60 |
| 5.4 | Determination of Surface Water Monitoring Station Locations | 62 |
| Chapter 6. | Field Visits and Final Selection of Surface Runoff Monitoring Stations | 72 |
| 6.1 | Determination of Locations for Surface Water Monitoring Stations..... | 72 |
| 6.2 | Surface Runoff Monitoring Station for Wadi Sanhan | 73 |
| 6.3 | Surface Runoff Monitoring Station for Wadi Ghyaman | 77 |
| 6.4 | Surface Runoff Monitoring Station for Wadi Shahik..... | 80 |
| 6.5 | Surface Runoff Monitoring Station for Wadi Sawan..... | 85 |
| 6.6 | Surface Runoff Monitoring Station for Wadi Al-Foros | 89 |
| 6.7 | Surface Runoff Monitoring Station for Wadi Al-Sirr | 94 |
| 6.8 | Surface Runoff Monitoring Station for Wadi Thoma | 98 |
| 6.9 | Surface Runoff Monitoring Station for Wadi Khulaga..... | 103 |
| 6.10 | Surface Runoff Monitoring Station for Wadi Mawrid..... | 109 |
| 6.11 | Surface Runoff Monitoring Station for Wadi Miliki | 112 |
| 6.12 | Surface Runoff Monitoring Station for Wadi Iqbal | 115 |
| 6.13 | Surface Runoff Monitoring Station for Wadi Zahr..... | 118 |
| 6.14 | Surface Runoff Monitoring Station for Wadi Hizayaz | 121 |
| 6.15 | Surface Runoff Monitoring Station for Wadi Al-Kharid | 124 |
| 6.16 | Surface Runoff Monitoring Station for Wadi Al-Kharid Bridge..... | 131 |
| 6.17 | Surface Runoff Monitoring Station for Sana'a Basin Wastewater Treatment Plant and the Wastewater Passage | 133 |
| 6.18 | Final Surface Runoff Monitoring Stations | 146 |

LIST OF FIGURES

| | | |
|------------|--|---|
| Figure 1-1 | Location of the Sana'a Basin | 3 |
| Figure 1-2 | Map of the major features of the Sana'a Basin including Sana'a City..... | 4 |
| Figure 1-3 | Digital Elevation Map of Sana'a Basin (basin boundary is represented by the thick black line)..... | 4 |
| Figure 1-4 | The 22 sub-basins of the Sana'a Basin..... | 5 |

| | | |
|-------------|--|----|
| Figure 1-5 | Satellite Image of the Sana'a Basin where the geological outcropping system can be differentiated. | 6 |
| Figure 1-6 | Surface geological map of the Sana'a Basin | 6 |
| Figure 1-7 | Density of groundwater wells within the Sana'a Basin..... | 8 |
| Figure 1-8 | Arable land as surveyed in 1986 and actual cultivated land in 2001..... | 8 |
| Figure 1-9 | Typical view of sandstone outcropping areas within the Sana'a Basin | 9 |
| Figure 1-10 | Typical view of the alluvial plain areas within the Sana'a Basin..... | 9 |
| Figure 2-1 | Representation of a DEM, outlet pour point and watershed boundary (left); hydrological grids used for watershed delineation (right)..... | 14 |
| Figure 2-2 | a) Eight-direction pour point model, numerical depiction of a flow-direction grid; b) Flow accumulation grid values with values above threshold highlighted showing a derived stream network, c) Grid representation of a watershed boundary stream network outlet | 14 |
| Figure 2-3 | Delineation of the Sana'a Basin - red arrow indicates the outlet of the entire basin at Wadi Al-Khared..... | 16 |
| Figure 3-1 | Flow chart showing the different steps that are involved in the design of a surface water monitoring network for the Sana'a Basin..... | 17 |
| Figure 3-2 | Identification of the different sub-basins within the Sana'a Basin | 18 |
| Figure 3-3 | Ghayman basin delineation and streamline delineation map..... | 18 |
| Figure 3-4 | Ghayman sub-basin delineation and area of each sub-basin..... | 19 |
| Figure 3-5 | Hamadan and As-Sabarah basin delineation and streamline delineation map | 19 |
| Figure 3-6 | Hamadan and As-Sabarah sub-basins delineation and area of each sub-basin..... | 19 |
| Figure 3-7 | Hizyaz basin delineation and streamline delineation map | 20 |
| Figure 3-8 | Hizyaz sub-basin delineation and area of each sub-basin | 20 |
| Figure 3-9 | Bani Hawat basin delineation and streamline delineation map | 21 |
| Figure 3-10 | Bani-Hawat sub-basin delineation and area of each sub-basin..... | 21 |
| Figure 3-11 | As-Sirr basin delineation and streamline delineation map..... | 21 |
| Figure 3-12 | As-Sirr sub-basin delineation and area of each sub-basin..... | 22 |
| Figure 3-13 | Al-Mulaikhy and Hamal basin delineation and streamline delineation map | 22 |
| Figure 3-14 | Al-Mulaikhy and Hamal sub-basin delineation and area of each sub-basin..... | 23 |
| Figure 3-15 | Iqbal and Ash Sha'b basin delineation and streamline delineation map | 23 |
| Figure 3-16 | Iqbal and Ash Sha'b sub-basin delineation and area of each sub-basin | 24 |
| Figure 3-17 | Al-Qotob abd MA'adi sub-basin delineation and streamline delineation map | 24 |
| Figure 3-18 | Al-Qotob abd MA'adi sub-basin delineation and area of each sub-basin | 25 |
| Figure 3-19 | Madini and Al-Ghulah basin delineation and streamline delineation map | 25 |
| Figure 3-20 | Madini and Al-Ghulah sub-basin delineation and area of each sub-basin | 26 |

| | |
|--|----|
| Figure 3-21 Madar and Al-Mashamini basin delineation and streamline delineation map | 26 |
| Figure 3-22 Madar and Mashamini sub-basin delineation and area of each sub-basin | 26 |
| Figure 3-23 Qasabah basin delineation and streamline delineation map | 27 |
| Figure 3-24 Qasabah sub-basin delineation and area of each sub-basin..... | 27 |
| Figure 3-25 Al-Furs and Rijam basin delineation and streamline delineation map | 28 |
| Figure 3-26 Al-Furs and Rijam sub-basin delineation and area of each sub-basin | 28 |
| Figure 3-27 Al-Kharid basin delineation and streamline delineation map | 28 |
| Figure 3-28 Al-Kharid sub-basin delineation and area of each sub-basin | 29 |
| Figure 3-29 Khulaqah basin delineation and streamline delineation map | 29 |
| Figure 3-30 Khulaqah sub-basin delineation and area of each sub-basin..... | 29 |
| Figure 3-31 Lasef and Assir basin delineation and streamline delineation map | 30 |
| Figure 3-32 Lasef and Assir sub-basin delineation and area of each sub-basin | 30 |
| Figure 3-33 Al-Mawrid, Al-L'Shash and Hayd basin delineation and streamline delineation map | 31 |
| Figure 3-34 Al-Mawri, Al-L'Shash and Hayd sub-basin delineation and area of each sub-basin..... | 31 |
| Figure 3-35 Akhwar basin delineation and streamline delineation map..... | 32 |
| Figure 3-36 Akwar sub-basin delineation and area of each sub-basin | 32 |
| Figure 3-37 Sa'wan and AR-Rawnah basin delineation and streamline delineation map..... | 33 |
| Figure 3-38 Sa'wan and A-Rawnah sub-basin delineation and area of each sub-basin..... | 33 |
| Figure 3-39 Shahik, Al-Ajbar and Sha'b basin delineation and streamline delineation map | 34 |
| Figure 3-40 Shahik, Al-Ajbar and Sha'b sub-basin delineation and area of each sub-basin..... | 34 |
| Figure 3-41 Thuma and Shiraa basin delineation and streamline delineation map..... | 35 |
| Figure 3-42 Thuma and Shiraa sub-basin delineation and area of each sub-basin..... | 35 |
| Figure 3-43 Yahis and AL-Huqqah basin delineation and streamline delineation map | 36 |
| Figure 3-44 Yahis and Al-Huqqah sub-basin delineation and area of each sub-basin..... | 36 |
| Figure 3-45 Zahr, Harad and Al-Ghayl basin delineation and streamline delineation map | 37 |
| Figure 3-46 Zahr, Harad and Al-Ghayl sub-basin delineation and area of each sub-basin..... | 37 |
| Figure 4-1 Spatial locations of rainfall stations from which rainfall data was collected throughout the basin, showing the Thessien Polygon for each station | 38 |
| Figure 4-2 Test of homogeneity of hydrologic records for Adabat station from 1972 to 1977 | 39 |
| Figure 4-3 Frequency analysis and probability plotting of hydrologic records for Adabat station from 1972 to 1977 | 39 |

| | | |
|-------------|--|----|
| Figure 4-4 | Test of homogeneity of hydrologic records for Al-Salaf station from 1974 to 1994 | 40 |
| Figure 4-5 | Frequency analysis and probability plotting of hydrologic records for Al-Salaf station from 1974 to 1994 | 40 |
| Figure 4-6 | Test of homogeneity of hydrologic records for Astan station from 1990 to 1996 | 41 |
| Figure 4-7 | Frequency analysis and probability plotting of hydrologic records for Astan station from 1990 to 1996 | 41 |
| Figure 4-8 | Test of homogeneity of hydrologic records for Birbasal station from 1991 to 1997 | 42 |
| Figure 4-9 | Frequency analysis and probability plotting of hydrologic records for Birbasal station from 1991 to 1997..... | 42 |
| Figure 4-10 | Test of homogeneity of hydrologic records for Darawan station from 1971 to 1979 | 43 |
| Figure 4-11 | Frequency analysis and probability plotting of hydrologic records for Darawan station from 1971 to 1979 | 43 |
| Figure 4-12 | Test of homogeneity of hydrologic records for Darsalem station from 2000 to 2005 | 44 |
| Figure 4-13 | Frequency analysis and probability plotting of hydrologic records for Darsalem station from 2000 to 2005 | 44 |
| Figure 4-14 | Test of homogeneity of hydrologic records for Maadia station from 1991 to 1996 | 45 |
| Figure 4-15 | Frequency analysis and probability plotting of hydrologic records for Maadia station from 1991 to 1996..... | 45 |
| Figure 4-16 | Test of homogeneity of hydrologic records for Mind station from 1971 to 1978 | 46 |
| Figure 4-17 | Frequency analysis and probability plotting of hydrologic records for Mind station from 1971 to 1978 | 46 |
| Figure 4-18 | Test of homogeneity of hydrologic records for old NWRA station from 1988 to 2001 | 47 |
| Figure 4-19 | Frequency analysis and probability plotting of hydrologic records for old NWRA station from 1988 to 2001 | 47 |
| Figure 4-20 | Test of homogeneity of hydrologic records for Qawaht station from 1986 to 1995 | 48 |
| Figure 4-21 | Frequency analysis and probability plotting of hydrologic records for Qawaht station from 1986 to 1995 | 48 |
| Figure 4-22 | Test of homogeneity of hydrologic records for Samanah station from 1991 to 1996 | 49 |
| Figure 4-23 | Frequency analysis and probability plotting of hydrologic records for Samanah station from 1991 to 1996..... | 49 |
| Figure 4-24 | Test of homogeneity of hydrologic records for Sana'a CAMA station from 1973 to 1979 | 50 |

| | | |
|-------------|---|----|
| Figure 4-25 | Frequency analysis and probability plotting of hydrologic records for Sana'a CAMA station from 1973 to 1979 | 50 |
| Figure 4-26 | Test of homogeneity of hydrologic records for Sana'a Airport station from 1938 to 2001. | 51 |
| Figure 4-27 | Frequency analysis and probability plotting of hydrologic records for Sana'a Airport station from 1938 to 2001..... | 51 |
| Figure 4-28 | Test of homogeneity of hydrologic records for Shibam station from 1974 to 1985 | 52 |
| Figure 4-29 | Frequency analysis and probability plotting of hydrologic records for Shibam station from 1974 to 1985 | 52 |
| Figure 4-30 | Test of homogeneity of hydrologic records for Shuub station from 1974 to 1982 | 53 |
| Figure 4-31 | Frequency analysis and probability plotting of hydrologic records for Shuub station from 1974 to 1982 | 53 |
| Figure 4-32 | Test of homogeneity of hydrologic records for Wallan station from 1978 to 1988 | 54 |
| Figure 4-33 | Frequency analysis and probability plotting of hydrologic records for Wallan station from 1978 to 1988 | 54 |
| Figure 4-34 | 2-year and 100-year rainfall event distribution in the Sana'a Basin | 55 |
| Figure 4-35 | 2-year, 5-year, 10-year, 20-year, 25-year, 50-year and 100-year rainfall event distribution in the Sana'a Basin | 56 |
| Figure 4-36 | 30-minute data collection for Darselm rainfall station over a period of 12 days (August 2006) | 56 |
| Figure 4-37 | 5-minute recorded data for Darselm rainfall station over a continuous period of 100 hours..... | 57 |
| Figure 4-38 | SMADA graphical user interface for determining storm pattern..... | 57 |
| Figure 4-39 | Rainfall hyetograph for storm pattern at Darselm rainfall station, based on pattern type IA..... | 58 |
| Figure 4-40 | Synthetic storm for Darselm station (duration: 5 hours / intensity: 33 mm). | 58 |
| Figure 5-1 | Latest available cropping pattern for the Sana'a Basin (2004/2005) Source: GAFAG draft report | 59 |
| Figure 5-2 | Converted digital map for identifying the cultivation density in the Sana'a Basin..... | 60 |
| Figure 5-3 | Soil map of the Sana'a Basin (Russian study, 1986)..... | 61 |
| Figure 5-4 | Revised soil map (WEC, 2001) | 62 |
| Figure 5-5 | Locations of surface water monitoring stations along Wadi Sanhan | 62 |
| Figure 5-6 | Locations of surface water monitoring stations along Wadi Al-Foros and Rjiam | 63 |
| Figure 5-7 | Locations of surface water monitoring stations along Wadi Al-Kharid..... | 63 |
| Figure 5-8 | Locations of surface water monitoring stations along Wadi Madini and Al Ghulah | 64 |

| | | |
|-------------|---|----|
| Figure 5-9 | Locations of surface water monitoring stations along Wadi Madar and Al Mashamini | 64 |
| Figure 5-10 | Locations of surface water monitoring stations along Wadi Mulaikhy and Hama | 65 |
| Figure 5-11 | Locations of surface water monitoring stations along Wadi Al-Qassaba | 65 |
| Figure 5-12 | Locations of surface water monitoring stations along Wadi Iqbal and Ash Sha'b | 66 |
| Figure 5-13 | Locations of surface water monitoring stations along Wadi Al-Qatab and MA'adi | 66 |
| Figure 5-14 | Locations of surface water monitoring stations along Wadi As-Sirr | 67 |
| Figure 5-15 | Locations of surface water monitoring stations along Wadi Bani Hawat | 67 |
| Figure 5-16 | Locations of surface water monitoring stations along Wadi Zahr and Al Al-Ghay | 68 |
| Figure 5-17 | Locations of surface water monitoring stations along Wadi Ghayman | 68 |
| Figure 5-18 | Locations of surface water monitoring stations along Wadi Hammadan and Al-Sabarah | 69 |
| Figure 5-19 | Locations of surface water monitoring stations along Wadi Khulaga | 69 |
| Figure 5-20 | Locations of surface water monitoring stations along Wadi Hizayaz | 69 |
| Figure 5-21 | Locations of surface water monitoring stations along Wadi Mawrid and Al-Ishash and Hyad | 70 |
| Figure 5-22 | Locations of surface water monitoring stations along Wadi Yahis and Al Haqqah | 70 |
| Figure 5-23 | Locations of surface water monitoring stations along Wadi Lafaf and Asir | 71 |
| Figure 5-24 | Locations of surface water monitoring stations along Wadi Thuma and Shira | 71 |
| Figure 5-25 | Locations of surface water monitoring stations along Wadi Sa'wan and Rawnah | 72 |
| Figure 5-26 | Locations of surface water monitoring stations along Wadi Shahik and Al Ajbar and Sha'b | 72 |
| Figure 6-1 | Location of Wadi Sanhan within the Sana'a Basin (black boundary) | 74 |
| Figure 6-2 | Proposed locations of surface water monitoring stations along Wadi Sanhan through the streamline delineation analysis | 74 |
| Figure 6-3 | View of the crossing structure under the highway at the outlet of Wadi Sanhan where the main monitoring station is located. UTM coordinates are: Left side UTME=426052 and UTMN=1685774 and Right Side UTME=426055 and UTMN=1665790, the section is at elevation 2355 m (AMSL). | 75 |
| Figure 6-4 | Dimensions of the crossing structure at the main monitoring station for Wadi Sanhan | 75 |
| Figure 6-5 | View of the land surface upstream of the crossing structure | 76 |
| Figure 6-6 | Side view of the crossing structure at the location of the main monitoring station in Sanhan | 76 |

| | | |
|-------------|--|----|
| Figure 6-7 | Long view of the stream and the crossing structure | 77 |
| Figure 6-8 | Proposed location for the staff and data logger instrument (wide arrow with brick filling) | 77 |
| Figure 6-9 | Location of Wadi Ghayman within the Sana'a Basin (black boundary) | 78 |
| Figure 6-10 | Proposed locations of surface water monitoring stations along Wadi Ghayman through the streamline delineation analysis | 78 |
| Figure 6-11 | General view of the Ghayman Dam that is located at the outlet of the Ghayman sub-basin - this is the preferred location for the monitoring station of Wadi Ghayman | 79 |
| Figure 6-12 | Upstream view of the dam showing the cultivation in the area | 79 |
| Figure 6-13 | Proposed location for staff gage and data logger instrument (arrow with brick pattern) in the upstream of Ghayman dam | 80 |
| Figure 6-14 | Location of Wadi Shahek within the Sana'a Basin (black boundary) | 81 |
| Figure 6-15 | Proposed locations of surface water monitoring stations along Wadi Ghayman through the streamline delineation analysis | 81 |
| Figure 6-16 | Configuration of the location of the first selected monitoring station site in Wadi Shahek (deemed inappropriate for installation of a monitoring station) | 82 |
| Figure 6-17 | Downstream configuration of the first selected monitoring station site in Wadi Shahek (deemed inappropriate for installation of a monitoring station) | 82 |
| Figure 6-18 | Final proposed location for Wadi Shahek surface runoff station. Coordinates are: left point UTM E 427870 and UTM N 1696144, right point UTM E 427874 and UTM N 1696131 | 83 |
| Figure 6-19 | Dimensions of the culvert openings for the selected location at Shahik | 83 |
| Figure 6-20 | Upstream view of the final proposed location for surface water monitoring station | 84 |
| Figure 6-21 | Proposed location for the surface runoff station at Wadi Shahek | 84 |
| Figure 6-22 | Downstream view from the proposed station showing the cross-section of the downstream area and the culvert alignment under the road | 85 |
| Figure 6-23 | Location of Wadi Sawan within the Sana'a Basin (black boundary) | 86 |
| Figure 6-24 | Proposed locations of surface water monitoring stations along Wadi Sawan through the streamline delineation analysis | 86 |
| Figure 6-25 | Cross-section at the location of the proposed monitoring station | 87 |
| Figure 6-26 | Upstream streambed view of the Wadi Sawan floodway | 87 |
| Figure 6-27 | Downstream streambed view of the Wadi Sawan floodway | 88 |
| Figure 6-28 | Sediment gradation at the selected monitoring station location | 88 |
| Figure 6-29 | Proposed location for staff gage and data logger instrument (arrow with brick pattern) at the outlet stream of Wadi Sawan | 89 |
| Figure 6-30 | Location of Wadi Al-Foros within the Sana'a Basin (black boundary) | 90 |

| | | |
|-------------|--|-----|
| Figure 6-31 | Proposed locations for surface water monitoring stations along Wadi Fors through the streamline delineation analysis | 90 |
| Figure 6-32 | Culvert at the highway intersection near the outlet of Wadi Al-Foros. Flow direction is shown with red arrows. UTM coordinates for this location are UTME=426000 and UTM N =1710625, at an elevation of 2274 m (AMSL)..... | 91 |
| Figure 6-33 | Dimensions of culvert openings..... | 91 |
| Figure 6-34 | Upstream view from crossing structure..... | 92 |
| Figure 6-35 | Upstream view showing shape of stream cross-section..... | 92 |
| Figure 6-36 | Long view showing location of crossing structure (red circle) and flow direction (black arrows)..... | 93 |
| Figure 6-37 | Sediment gradation of streambed upstream of crossing structure | 93 |
| Figure 6-38 | Proposed location for staff gage and data logger instrument (arrow with brick pattern) upstream of crossing structure at Wadi Al-Foros outlet..... | 94 |
| Figure 6-39 | Location of Wadi Al-Sirr within the Sana'a Basin (black boundary)..... | 95 |
| Figure 6-40 | Proposed locations of surface water monitoring stations along Wadi Al-Sirr through streamline delineation analysis | 95 |
| Figure 6-41 | The exiting station installed by component 2. Coordinates of this staff are UTME=423849 and UTMN=1713362, at an elevation of 2253 m (AMSL) | 96 |
| Figure 6-42 | Flow direction, cross-section configuration and ground level at the gage location | 96 |
| Figure 6-43 | Upstream view of streambed at gage location..... | 97 |
| Figure 6-44 | Sediment gradation at gage location | 97 |
| Figure 6-45 | Proposed location for staff gage and data logger instrument (arrow with brick pattern) in main stream of Wadi Al-Sirr floodway | 98 |
| Figure 6-46 | Location of Wadi Thomaa within the Sana'a Basin (black boundary)..... | 99 |
| Figure 6-47 | Proposed locations of surface water monitoring stations along Wadi Thomaa through the streamline delineation analysis | 99 |
| Figure 6-48 | General view of the cross-section at the monitoring station location | 100 |
| Figure 6-49 | Cross-section selected for installation of the staff gage (red curve). Coordinates of the sides are: left side UTME=428835 and UTMN=1726392, at an elevation of 2064 | 100 |
| Figure 6-50 | Cross-section dimensions measured in the field | 101 |
| Figure 6-51 | Upstream view of the stream bed configuration | 101 |
| Figure 6-52 | Top view of the selected cross-section..... | 102 |
| Figure 6-53 | Sediment gradation at cross-section location | 102 |
| Figure 6-54 | Sediment gradation at cross-section location | 103 |
| Figure 6-55 | Proposed location for staff gage and data logger instrument (arrow with brick pattern) in main stream of Wadi Thomaa floodway | 103 |
| Figure 6-56 | Location of Wadi Khulaga within the Sana'a Basin (black boundary) | 104 |

| | | |
|-------------|--|-----|
| Figure 6-57 | Proposed locations of surface water monitoring stations along Wadi Khulaga through the streamline delineation analysis..... | 104 |
| Figure 6-58 | Top view showing location of the crossing structure at the intersection of Wadi Khulaga main floodway and a highway | 105 |
| Figure 6-59 | Downstream view of the wadi after passing the crossing structure | 105 |
| Figure 6-60 | Front view of the box culvert structure at the intersection of the Wadi Khulaga main floodway and a highway. Coordinates of the crossing structure are: for the left side: UTME=437089 and UTMN=1734937, and for the right side: UTME=437117 and UTMN=1734951, at an elevation of 1925 m (AMSL)..... | 106 |
| Figure 6-61 | View of the highway and the downstream side of the floodway..... | 106 |
| Figure 6-62 | Upstream view of the crossing structure | 107 |
| Figure 6-63 | Dimensions of the box culvert..... | 107 |
| Figure 6-64 | Depth of the culvert opening | 108 |
| Figure 6-65 | Upstream view of the main floodway streambed and surrounding environment | 108 |
| Figure 6-66 | Sediment gradation of the stream bed..... | 109 |
| Figure 6-67 | Proposed location for staff gage and data logger instrument (arrow with brick pattern) in the main stream of Wadi Khulaga floodway..... | 109 |
| Figure 6-68 | Location of Wadi Khulaga within the Sana'a Basin (black boundary) | 110 |
| Figure 6-69 | Front view of the bridge at Wadi Mawrid where the surface runoff station is proposed. Coordinates of the crossing structure are: left side UTME=415475 and UTMN=1700396, and right side: UTME=415496 and UTMN=1700393, at an elevation of 2255 m (AMSL) | 111 |
| Figure 6-70 | Downstream view from the bridge | 111 |
| Figure 6-71 | During the measuring of bridge dimensions | 112 |
| Figure 6-72 | Upstream view from the bridge..... | 112 |
| Figure 6-73 | Location of Wadi Miliki within the Sana'a Basin (black boundary) | 113 |
| Figure 6-74 | Front view of the culvert at the highway intersection. Coordinates of the crossing structure are: UTME=415755 and UTMN=1686539, at an elevation of 2331m (AMSL)..... | 113 |
| Figure 6-75 | View of the upstream area in front of the culvert | 114 |
| Figure 6-76 | Culvert dimensions..... | 114 |
| Figure 6-77 | Proposed location for the surface water runoff station for Wadi Al-Muliki | 115 |
| Figure 6-78 | Location of Wadi Iqbal within the Sana'a Basin (black boundary) | 116 |
| Figure 6-79 | Dimensions of the reservoir (under-construction) in the main stream of the Wadi Iqbal floodpath. Coordinates are: 1714085 and UTM E 408986..... | 116 |
| Figure 6-80 | Upstream view of the main stream floodpath leading to the constructed reservoir..... | 117 |
| Figure 6-81 | General view of the reservoir showing the location of the spillway and the flow entrance structure | 117 |

| | | |
|--------------|---|-----|
| Figure 6-82 | Downstream cross-section, including spillway for excess water | 118 |
| Figure 6-83 | Proposed location for the surface water runoff station at Wadi Iqbal | 118 |
| Figure 6-84 | Location of Wadi Zahr within the Sana'a Basin (black boundary) | 119 |
| Figure 6-85 | General view of the Wadi Zahr main stream. Coordinates are: UTM E = 405858 and UTM N = 1707154..... | 119 |
| Figure 6-86 | Cross-section of the Wadi Zahr main stream | 120 |
| Figure 6-87 | Downstream view of the selected cross-section showing the intersection of two main streams at the proposed location for measurement | 120 |
| Figure 6-88 | Final selected location for the Wadi Zahr surface water runoff station | 121 |
| Figure 6-89 | Location of Wadi Hizyaz within the Sana'a Basin (black boundary) | 122 |
| Figure 6-90 | Hizyaz basin and streamline delineation map | 122 |
| Figure 6-91 | View of the urbanization of Wadi Hizyaz | 123 |
| Figure 6-92 | Current status of the proposed monitoring location | 123 |
| Figure 6-93 | Road construction at the proposed monitoring location..... | 124 |
| Figure 6-94 | Google Earth image for the location of the Wadi Al-Kharid outlet surface water runoff station at UTM N = 1739880 and UTM E at 436650 | 125 |
| Figure 6-95 | Location of Wadi Al-Kharid within the Sana'a Basin (black boundary) | 125 |
| Figure 6-96 | Al-Kharid basin streamline delineation map..... | 126 |
| Figure 6-97 | Al-Kharid sub-basin delineation and area of each sub-basin | 126 |
| Figure 6-98 | General fly-over view of Wadi Al-Kharid showing the beginning of the wadi's main stream | 127 |
| Figure 6-99 | Surface bed of Wadi Al-Kharid | 127 |
| Figure 6-100 | Another view of the Wadi Al-Kharid bed surface..... | 128 |
| Figure 6-101 | Wadi AL-Kharid bed configuration | 128 |
| Figure 6-102 | Existing V-Notch weir at Wadi Al-Kharid..... | 129 |
| Figure 6-103 | Backside view of the V-Notch weir at Wadi Al-Kharid..... | 129 |
| Figure 6-104 | V-Notch during field measurements..... | 130 |
| Figure 6-105 | V-Notch weir and its concrete wings..... | 130 |
| Figure 6-106 | Location of wadi water level station in front of V-Notch | 131 |
| Figure 6-107 | View of the bridge openings and piers..... | 131 |
| Figure 6-108 | General view of the bridge across Wadi Al-Kharid..... | 132 |
| Figure 6-109 | View of the upstream surface bed | 132 |
| Figure 6-110 | Details of the monitoring station location..... | 133 |
| Figure 6-111 | Google Earth picture showing the general layout of the Sana'a Wastewater Treatment Plant..... | 134 |
| Figure 6-112 | Aeration basins and trickling filters of Sana'a WWTP | 135 |
| Figure 6-113 | Inlet channel for raw sewage and the parshall flume..... | 135 |

| | | |
|--------------|--|-----|
| Figure 6-114 | Lifting pumps inside Sana'a WWTP | 136 |
| Figure 6-115 | Aerators at work inside the aeration basins of Sana'a WWTP | 136 |
| Figure 6-116 | Trickling filters in Sana'a WWTP | 137 |
| Figure 6-117 | Treated wastewater flowing out from the trickling filter | 137 |
| Figure 6-118 | Sludge drying beds in Sana'a WWTP | 138 |
| Figure 6-119 | Polishing lagoon in Sana'a WWTP | 138 |
| Figure 6-120 | Rectangular siphon of the Sana'a WWTP outlet | 139 |
| Figure 6-121 | Outlet of Sana'a WWTP | 139 |
| Figure 6-122 | Inlet point of Sana'a WWTP | 140 |
| Figure 6-123 | Ultrasound surface water measuring device in Sana'a WWTP | 140 |
| Figure 6-124 | Data logger for the ultrasound device on Sana'a WWTP | 141 |
| Figure 6-125 | Treated wastewater passage | 141 |
| Figure 6-126 | Treated wastewater passage just downstream from Sana'a WWTP | 142 |
| Figure 6-127 | The road culvert in the Bani-Garmouz area. Al-Mosayerka Dam is 1.5 km downstream..... | 142 |
| Figure 6-128 | Upstream view from the Bani Garmouz road culvert | 143 |
| Figure 6-129 | Downstream view of the Bani Garmouz road culvert..... | 143 |
| Figure 6-130 | Flow downstream from the road culvert at Bani Garmouz | 144 |
| Figure 6-131 | Flow downstream from the road culvert at Bani Garmouz | 144 |
| Figure 6-132 | Google Earth image showing the Al-Moseyreka Dam Lake, just downstream from the Bani Garmouz road culvert..... | 145 |
| Figure 6-133 | Google Earth image showing the Al-Masham Dam Lake, just downstream from Al-Mosyeraka Dam | 145 |
| Figure 6-134 | Panorama of Al-Semna Dam Lake, downstream from Al-Masham Dam | 145 |
| Figure 6-135 | Locations of surface water runoff stations for the Sana'a Basin | 147 |

LIST OF TABLES

| | | |
|-----------|--|-----|
| Table 1-1 | List of existing storage and recharge dams within the Sana'a Basin | 11 |
| Table 2-1 | Values of <i>CV</i> for different types of soil and land use..... | 13 |
| Table 4-1 | Developed 2-year, 5-year, 10-year, 20-year, 25-year, 50-year and 100- year yearly rainfall intensity at different rainfall stations inside the Sana'a Basin..... | 55 |
| Table 6-1 | Final locations and coordinates of the Surface Water Runoff Stations for the Sana'a Basin | 146 |

EXECUTIVE SUMMARY

The Sana'a Basin is located in the central highlands of Yemen and covers approximately 3,200 km²; highlands within the region range from 1900 m to more than 3300 m above sea level. The climate of the basin area is characterized by a low, erratic rainfall pattern with an annual average of 250 mm. This activity aims to design a surface water monitoring network covering the Sana'a Basin. From the literature review, it has been concluded that there are no surface runoff monitoring stations in the Sana'a Basin, even though 52 dams are distributed across the basin. Thus, developing a surface water monitoring network for the Sana'a Basin necessitates an intensive work plan that includes the following activities:

- Collection of relevant information and data about the Sana'a Basin;
- Development of an integrated watershed management system for the entire basin (is this true?);
- Selection of locations for surface water monitoring stations throughout the basin;
- Field visits to the different proposed locations to assure their suitability; and
- Final selection of locations for surface runoff monitoring stations.

The work process started by analyzing the digital elevation model for the basin and delineating streamlines of the basin and sub-basins through watershed management models. In this stage, the basin outlet location was determined from the stream delineation. Sub-basin and sub-sub-basin boundaries were then determined using GIS software and the DEM map. In addition, IDF curves and design storms were developed for the basin as a whole. The design storms can be used to model different storm intensities and evaluate their impact on the hydrograph of each stream and its outlet. In addition, land-use maps, surface roughness details and soil maps were used in the watershed management calculations to derive the hydrographs for different locations. The following stage aimed at converting the delineated stream system into a semi-two-dimensional river basin network. This allowed a river network simulation for the streamlines within the entire basin to be performed. Finally, the water depths at different critical locations within the Sana'a Basin were determined. From this intensive activity, a database of stream hydraulic characteristics was developed for the entire basin. The next step in the study was to determine the location of sagging points where surface runoff water is most likely to accumulate and where water will be at a reasonable depth that can allow measurement with the proposed measuring stations. Thus, the final goal of the simulation was to find the locations where water can be collected, and that are at a reasonable depth for measurement. Locations for monitoring stations along each sub-basin were determined according to these criteria. Field visits to selected locations were performed to verify the suitability of each. At many stations, structures considered to be ideal locations for monitoring station installation were identified. Other field visits, however, indicated that it would be difficult or even unfeasible to allocate surface runoff monitoring stations at the selected locations. With the information from these site visits, the final locations for the surface runoff monitoring stations for the basin were determined. In all, locations for 14 monitoring stations were determined, as well as those for three monitoring stations to be installed along treated wastewater passages.

Chapter 1. GENERAL HYDROLOGICAL FEATURES OF THE SANA'A BASIN

1.1 Introduction

The goal of this activity was to design a surface water monitoring network for the entire Sana'a Basin. Following communications with the water resources and irrigation departments of the Ministry of Water and Environment and Ministry of Agriculture, it was concluded that there are no existing surface water measurement stations within the Sana'a Basin. Although there are 52 dams distributed across the basin, surface water monitoring is not currently performed at these sites. In order to establish a monitoring network for surface water within the Sana'a Basin, an intensive work plan was developed that involved the following activities:

- Collection of relevant information and data about the Sana'a Basin;
- Development of an integrated watershed management system for the entire basin (is this true?);
- Selection of locations for surface water monitoring stations throughout the basin; and
- Field visits to the different proposed locations to assure their suitability. In what follows, a detailed description of the different activities and analyses that were performed during the course of this study will be introduced.

1.2 Sana'a Basin

Current trends in water resource management are evolving towards complex, spatially explicit regional assessments. Water management problems have to be addressed with the use of distributed models that can compute runoff on different spatial and temporal scales. The extensive data requirements and the difficulty of building input parameter files, however, have long been an obstacle to the timely and cost-effective use of such complex models by resource managers. The Environmental Modeling Research Laboratory of Brigham Young University, in cooperation with the U.S. Army Corps of Engineers Waterways Experiment Station, has developed an integrated hydrological system tool to facilitate this process. Known as the WMS (expand), it allows for the integration of GIS with hydrological analyses and provides the framework within which spatially distributed data can be collected and used to prepare model input files and evaluate model results. WMS automates the process of transforming digital data into hydrological simulation models and provides a visualization tool to help the user interpret results. The present study introduces the utility of the WMS in joint hydrologic and river system analysis investigations by demonstrating its performance on a diverse basin system like the Sana'a Basin.

Parameters including soil type, land use, and surface roughness, were used in accordance with the digital elevation map of each wadi and geological maps of the region to simulate the physical environment of the watershed. Different scenarios for rainfall intensity were then simulated at the individual wadi level. Also, by interfacing the WMS system with a semi-two dimensional river network model, the delineated stream lines could be simulated as a river network system. The system also allows for the visualization of the spatial distribution of hydrological parameters and conditions across the wadi system. Hydrological information for each basin was compiled by the program, and hydraulic characteristics of individual streamlines were outlined in detail. This allowed for the identification of sagging points where water can be collected in reasonable depths, facilitating the selection of locations for the proposed surface water monitoring stations throughout the basin.

1.2.1 Location

The Sana'a Basin is bounded by four UTM points with the following coordinates: E 390000-N 1670000, E 450000 – N 1670000, E 390000–N 1750000 and E 450000–N 1750000. Figure 1 presents a detailed map of the Sana'a Basin's location within Yemen.

1.2.2 Major Features of the Sana'a Basin

The Sana'a Basin is located in the central highlands of Yemen and covers an area of approximately 3,200 km², with elevations ranging from less than 2,000 m to more than 3,200 m above sea level. The climate of the basin area is characterized by a low and erratic rainfall pattern with average annual precipitation of 250 mm. Sana'a, the capital city of Yemen, is located in the Sana'a plain at an elevation of about 2,200 m above sea level. At the time of the first national census in 1975, the population of the city was 134,588 inhabitants and, by 1986, this number had increased more than three-fold to 424,450. Although the national population growth rate was around 3 percent during that time, the population of the city grew at an annual rate of 11 percent and was projected to continue at a similar rate. This rapid growth is mainly attributed to improved economic conditions which stimulated internal migration from the rural areas. At present, the population of the city is estimated to be over one million and is projected to increase to over 3.4 million by the year 2010.



Figure 1-1 Location of the Sana'a Basin

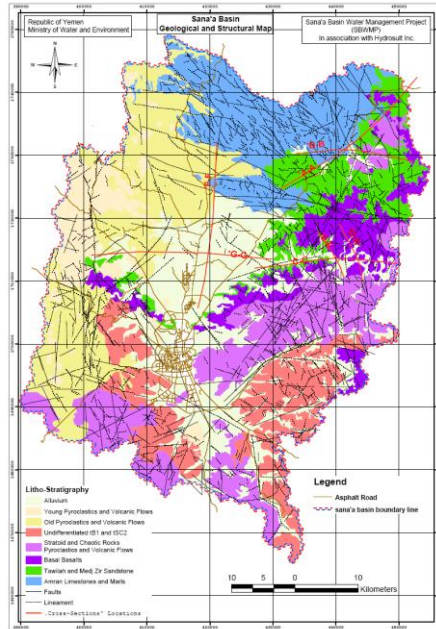


Figure 1-2 Map of the major features of the Sana'a Basin including Sana'a City

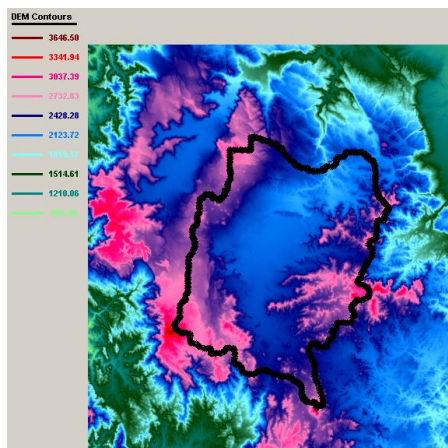


Figure 1-3 Digital Elevation Map of Sana'a Basin (basin boundary is represented by the thick black line)

1.2.3 Sub-Basin Delineation

Previous studies have identified 22 sub-basins within the Sana'a Basin, as shown in Figure 4 (ref). The division of these sub-basins was dependent on the water divide boundaries for each, determined using topographic maps.

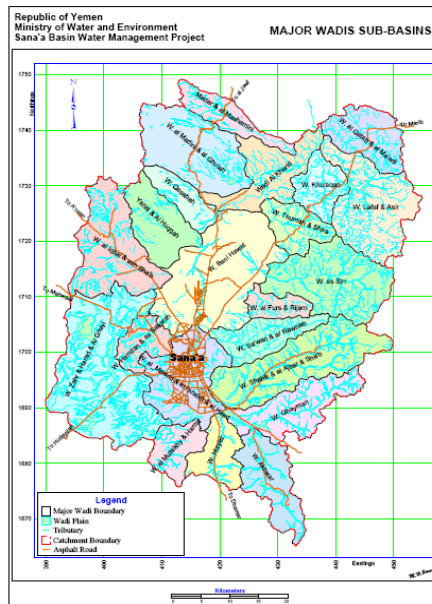


Figure 1-4 The 22 sub-basins of the Sana'a Basin

1.2.4 Water Resources of the Sana'a Basin

The principle source of water in the Sana'a region is groundwater from four aquifer layers, namely alluvial deposits, volcanic units, limestone and Tawilah sandstone. Of the four aquifers, the Tawilah is considered to be the most productive and has the best water quality. The capacity of the Tawilah is estimated at $2,230 \times 10^6 \text{ m}^3$ (total storage), of which only 50 percent is considered withdrawable. In addition to low recharge as a result of low rainfall in the recent past, increased extraction (mainly for agriculture) has resulted in a substantial drop in groundwater levels (3-4 m per year [1]). It is important to realize that, while the total water demand in the Sana'a Basin area was estimated to be $220 \times 10^6 \text{ m}^3$ per year in 1995, recharge estimates for the Tawilah aquifer vary between only $27 \times 10^6 \text{ m}^3$ and $63 \times 10^6 \text{ m}^3$ per year. The large difference between consumption and recharge is being extracted from water in long-term storage, referred to as groundwater mining. The present pattern of water use in Sana'a is clearly unsustainable and, if allowed to continue, depletion of this valuable and scarce resource may be inevitable. Figures 5 and 6 present satellite images for the Sana'a Basin and the surface geology map for the basin respectively. As shown by these two figures, the limestone is in the northern area, while the sandstone spans from the eastern boundary of the basin almost to the western side, forming a crescent shape. The alluvial area is located at low elevation zones following the valley streams. Volcanic zones cover most of the basin area, encircling the basin along the western, southern and eastern boundaries.

Comment [IN1]: Make sure that the statement is accepted by the hydrogeology team

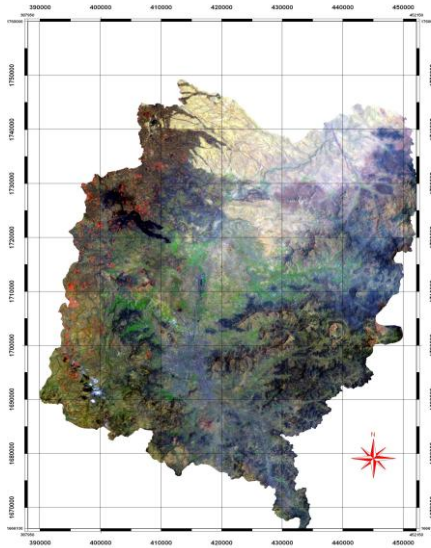


Figure 1-5 Satellite Image of the Sana'a Basin where the geological outcropping system can be differentiated.

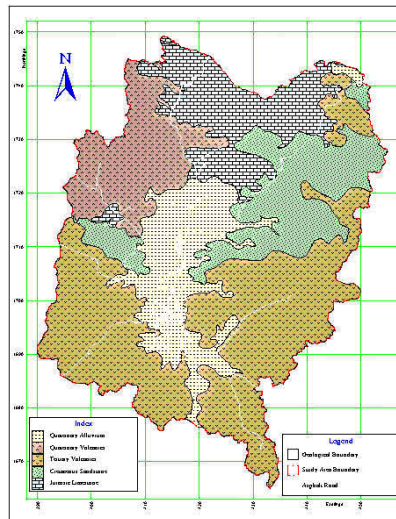


Figure 1-6 Surface geological map of the Sana'a Basin

1.2.5 Water Use in the Sana'a Basin

Groundwater in the region is used to satisfy the water needs of different water-using sectors, namely irrigated agriculture, municipal use and industrial use. Prior to the Yemeni revolution in 1962, agriculture in the Sana'a Basin area was dependent on dry farming practices and spate irrigation. The introduction of drilled boreholes in the 1970s and the identification of the Tawilah Formation as a highly productive aquifer encouraged farmers to use groundwater for irrigation. Figure 7 presents the wells' density map inside the Sana'a Basin, as observed by a WEC (2001) well inventory study. The number of wells per square kilometer ranges from one well per square kilometer up to 51 wells per square kilometer. In 1973, having realized the importance of the Tawilah, the government tried to regulate agricultural water use in the area by passing a law which identified a local protection zone around the NWSA well fields and prohibited further drilling of new wells or cesspits unless permits were obtained. At present, agriculture in the basin consumes about $175 \times 10^6 \text{ m}^3$ per year, which accounts for 80 percent of the total water demand in the area. Moreover, qat and grapes are estimated to consume around 40 and 25 percent respectively of the agricultural water demand in the region. Figures 9 and 10 are photographs of typical cultivated lands in the sandstone mountainous areas and alluvial plains. Figure 8 presents the agricultural land use map for the Sana'a Basin. Cultivation density is considered very high at the alluvial plain and lower densities are found in the remaining 80 percent of the basin area. Qat, grapes, fruit trees and cereal form the cropping pattern in the Sana'a Basin. Qat has the largest cultivation area within the basin. The main reasons behind the over-use of groundwater for irrigation can be summarized as:

- Unclear water rights and thus unregulated extraction,
- Fuel subsidies and low import duties on agricultural equipment,
- High returns on cash crops,
- Inefficient irrigation practices.

Within the Sana'a Basin, it is estimated that the present population is about 2.34 million, of which 1.4 million live in urban areas. Although the per capita consumption rate varies, it is estimated that the total municipal water demand in 1995 was $36.9 \times 10^6 \text{ m}^3$ per year, of which about $29 \times 10^6 \text{ m}^3$ per year was consumed in the urban areas. It was also projected that the total yearly municipal water demand should increase to $138 \times 10^6 \text{ m}^3$ per year by the year 2010 (HWC, 1992c). The industrial water demand was estimated at $4.7 \times 10^6 \text{ m}^3$ per year in 1990 and was projected to increase to $6.2 \times 10^6 \text{ m}^3$ per year in 1995. Van der Gun *et al.* (1987) reported that the government of the Yemen Arab Republic took measures to prevent the further establishment of major water-consuming industries in the Sana'a area and this could explain the low rate of increase in water use compared with the other sectors.

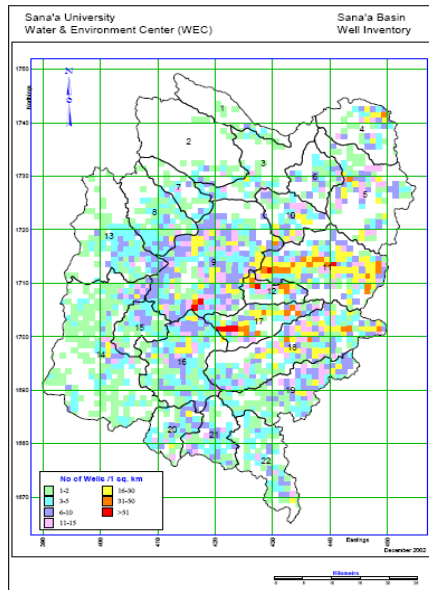


Figure 1-7 Density of groundwater wells within the Sana'a Basin

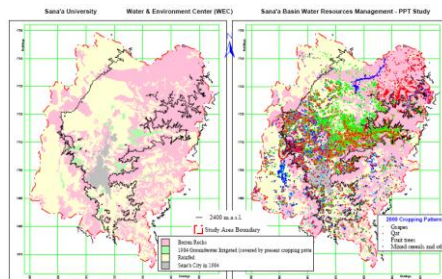


Figure 1-8 Arable land as surveyed in 1986 and actual cultivated land in 2001



Figure 1-9 Typical view of sandstone outcropping areas within the Sana'a Basin



Figure 1-10 Typical view of the alluvial plain areas within the Sana'a Basin

1.2.6 Dams in the Sana'a Basin

About 45 dams were constructed within the Sana'a Basin for water control and flow management. Table 1 presents the basic information required for each dam, including the dam name, district, village, valley name and the geo-reference information.

| No. | Dam Name | District | Wadi | UTM-N | UTM-E |
|-----|--------------|----------|--------------|---------|--------|
| 1 | Al-Musayraka | Arhab | Al-Musayraka | 1725500 | 419375 |
| 2 | Al-Masham | Arhab | Al-Musayraka | 1726450 | 421125 |
| 3 | Simmna | Arhab | Shira'a | 1730275 | 427050 |

| No. | Dam Name | District | Wadi | UTM-N | UTM-E |
|-----|--------------------|----------------|-------------------|---------|--------|
| 4 | Barran | Nihem | Barran | 1739100 | 452700 |
| 5 | Eial Hussein | Nihem | Al-shi'b AlAkhdar | 1742750 | 446675 |
| 6 | Wadi Mahalli | Nihem | Mahalli | 1735100 | 448450 |
| 7 | Beni Naji | Nihem | Beni Naji | 1732925 | 444125 |
| 8 | Al- Jarjur | Nihem | Ukran | 1735400 | 447700 |
| 9 | Al- Hada | Nihem | Al-Hada | 1734200 | 441250 |
| 10 | Al-Hayathem | Nihem | Al-Waker | 1731400 | 437900 |
| 11 | Al-Khalaqa | Nihem | Al-Kalaqa | 1726325 | 438000 |
| 12 | Thoma | Nihem | Thouma | 1721400 | 436950 |
| 13 | Dhuraima | Nihem | Sullaha | 1726325 | 441600 |
| 14 | Al-Ghaida | Nihem | Sullaha | 1724450 | 440875 |
| 15 | Al-Rakab | Nihem | Sullaha | 1726425 | 441425 |
| 16 | Arisha /Mahajer | Nihem | Arisha | 1726200 | 433325 |
| 17 | Al-Jae'f | Beni Al-Hareth | Al-Jae'f | 1718700 | 344950 |
| 18 | Beryan | Beni Husheish | Beryan | 1705100 | 433700 |
| 19 | Mukhtan | Beni Husheish | Mukhtan | 1700650 | 428300 |
| 20 | Ghayman | Beni Bahlul | Ghayman | 1687900 | 429500 |
| 21 | Shahek | Khawlan | Tane'm | 1701275 | 438400 |
| 22 | Tozan | Hamdan | Al-Bargug | 1713800 | 400600 |
| 23 | Eram | Hamdan | Eram | 1709800 | 403200 |
| 24 | Rei'an | Hamdan | Al-Watia | 1703450 | 401250 |
| 25 | Beit Redam | Beni Matar | Al-Halila | 1684250 | 399600 |
| 26 | Beit Redam | Beni Matar | Al-Halila | 1684175 | 398725 |
| 27 | Kamaran | Shahan | Beit Bous | 1688700 | 413925 |
| 28 | Artel | Shahan | Artel | 1687250 | 413880 |
| 29 | Higrat Al-Dhabaina | Sanhan | Al-Higra | 1673725 | 432940 |
| 30 | Al-Gishb | Sanhan | Al-Higra | 1675000 | 433250 |
| 31 | Ni'edh | Sanhan | Sed Ni'edh | 1667150 | 430300 |
| 32 | Assirein | Sanhan | Akhwar | 1671000 | 432225 |
| 33 | Sayan | Sanhan | Sayyan | 1679225 | 427725 |
| 34 | Dharah | Sanhan | Al-Ghail | 1677800 | 433100 |
| 35 | Allujma | Beni Bahlul | Allujma | 1693950 | 433500 |
| 36 | Shi'b Al-Jawza | Sanhan | Sir Shi'b | 1696350 | 425100 |
| 37 | Arisha /Qatran | Nihem | Araman | 1729500 | 435250 |
| 38 | Al-Qudha | Nihem | Shi'b Al-Ghuwail | 1729450 | 448850 |
| 39 | Beni Ghalib | Nihem | Lasaf | 1729900 | 448300 |
| 40 | Ghawlat Assim | Nihem | Ghaulat Assim | 1725375 | 448800 |

| No. | Dam Name | District | Wadi | UTM-N | UTM-E |
|-----|-------------------|---------------|---------------|---------|--------|
| 41 | Al-Khunazer | Beni Husheish | Wadi Khunazer | 1703250 | 423950 |
| 42 | Al- Rejam | Beni Husheish | Reiam | 1709450 | 430750 |
| 43 | Dar El-Heid | Sanhan | Barash | 1695450 | 422175 |
| 44 | Al-Khalas | Arhad | Beit Murait | 1737900 | 429850 |
| 45 | Al-Rakab / Subaha | Beni Matar | Al-Rakab | 1694100 | 406575 |

Table 1-1 List of existing storage and recharge dams within the Sana'a Basin

Chapter 2. GEOSPATIAL SIMULATION AND ANALYSIS OF THE SANA'A BASIN

2.1 Applied Theoretical Approach

In 1972, the U.S. Soil Conservation Service (SCS) suggested an empirical model for rainfall abstractions which is based on the potential for the soil to absorb a certain amount of moisture. The SCS curve number method is a simple, widely used and efficient method for determining the approximated amount of runoff from a rainfall, even in a specific area. Although the method is designed for a single storm event, it can be scaled to find average annual runoff values. The statistical requirements for this method are very low, limited to rainfall amount and curve number. The curve number is based on the area's hydrologic soil group, land use, treatment and hydrologic condition. The basic assumption of the SCS curve number method is that, for a single storm, the ratio of actual soil retention after runoff begins to potential maximum retention is equal to the ratio of direct runoff to available rainfall. This relationship, after algebraic manipulation and inclusion of simplifying assumptions, results in the following equation where curve number (CN) represents a convenient representation of the potential maximum soil retention, S.

$$S = \frac{25400}{C_N} - 254 \text{----- 1}$$

Typical values for the SCS Curve Number C_N as a function of soil type, land use and degree of saturation can be found in most texts on hydrology. In some texts, the values of C_N may be quoted as a function of the percentage of impervious area. These are usually calculated as a weighted average, assuming $C_{N-impervious} = 98$ and $C_{N-pervious}$ is equal to the value for 'Pasture in good condition'. Table 1 shows the C_N values for various soil types A, B, C or D. Values of C_N estimated in this way are intended to be applied to the total catchments, assuming other parameters to be the same for both pervious and impervious areas. Many programs compute the runoff from the pervious and impervious fractions separately and then add the two hydrographs. In such cases, it is most important that one cannot use a composite value of C_N since this would 'double count' the impervious fraction and greatly exaggerate the runoff prediction.

The effective rainfall is computed by the equation:

$$Q(t) = \frac{(P(t) - I_a)^2}{(P(t) + S - I_a)} \text{----- 2}$$

where:

- $Q(t)$ = accumulated depth of effective rainfall to time t
- $P(t)$ = accumulated depth of rainfall to time t

- I_a = initial abstraction
- S = potential storage in the soil

All of the terms in equation 2 are in units of millimeters or inches. Note that the effective rainfall depth or runoff will be zero until the accumulated precipitation depth $P(t)$ exceeds the initial abstraction I_a . Moreover, the original SCS method assumed the value of the initial abstraction I_a to be equal to 10-20% of the storage potential S . On the basis of field observations, this potential storage S (millimeters or inches) was related to a 'curve number' C_n which is a characteristic of the soil type, land use and the initial degree of saturation known as the antecedent moisture condition. Table 2 presents the values of C_n under different conditions.

2.2 Stream delineation using GIS

2.2.1 Theory behind GIS-based watershed delineation

Although a watershed area is easy to conceptualize and delineate on a paper map, GIS delineations are less labor intensive, more reproducible, and less dependent on subjective judgment. The GIS delineation process starts with a grid representation of topography called a digital elevation model (DEM, Figure 3 – Chapter 1). In the current study, the Sana'a Basin DEM map was obtained from the Shuttle Radar Topographic Mission (SRTM). The Shuttle Radar Topography Mission (SRTM) obtained elevation data on a near-global scale to generate the most complete high-resolution digital topographic database of the Earth. SRTM consisted of a specially modified radar system that flew onboard the Space Shuttle Endeavour during an 11-day mission in February 2000. The SRTM data will cover the entire globe with a 3-arc second (approx. 90 m) digital elevation model. SRTM is an international project spearheaded by the National Geospatial-Intelligence Agency (NGA) and the National Aeronautics and Space Administration (NASA). From the DEM, a series of additional grids are produced that represent various hydrologic characteristics of the landscape (see Figure 11).

From these "hydrologic grids", a GIS can delineate watershed boundaries by identifying all locations within a DEM that are uphill of an outlet.

| Land Use Description on Input Screen | Description and Curve Numbers from TR-55 | | | | | |
|--------------------------------------|---|--------------------|--|----|----|----|
| | Cover Description | | Curve Number for Hydrologic Soil Group | | | |
| | Cover Type and Hydrologic Condition | % Impervious Areas | A | B | C | D |
| Agricultural | Row Crops - Straight Rows + Crop Residue Cover- Good Condition ⁽¹⁾ | | 64 | 75 | 82 | 85 |
| Commercial | Urban Districts: Commercial and Business | 85 | 89 | 92 | 94 | 95 |
| Forest | Woods ⁽²⁾ - Good Condition | | 30 | 55 | 70 | 77 |
| Grass/Pasture | Pasture, Grassland, or Range ⁽³⁾ - Good Condition | | 39 | 61 | 74 | 80 |
| High Density Residential | Residential districts by average lot size: 1/8 acre or less | 65 | 77 | 85 | 90 | 92 |
| Industrial | Urban district: Industrial | 72 | 81 | 88 | 91 | 93 |

| Land Use Description on Input Screen | Description and Curve Numbers from TR-55 | | | | | |
|--------------------------------------|--|--------------------|--|----|----|----|
| | Cover Description | | Curve Number for Hydrologic Soil Group | | | |
| | Cover Type and Hydrologic Condition | % Impervious Areas | A | B | C | D |
| Low Density Residential | Residential districts by average lot size: 1/2 acre lot | 25 | 54 | 70 | 80 | 85 |
| Open Spaces | Open Space (lawns, parks, golf courses, cemeteries, etc.) ⁽⁴⁾ Fair Condition (grass cover 50% to 70%) | | 49 | 69 | 79 | 84 |
| Parking and Paved Spaces | Impervious areas: Paved parking lots, roofs, driveways, etc. (excluding right-of-way) | 100 | 98 | 98 | 98 | 98 |
| Residential 1/8 acre | Residential districts by average lot size: 1/8 acre or less | 65 | 77 | 85 | 90 | 92 |
| Residential 1/4 acre | Residential districts by average lot size: 1/4 acre | 38 | 61 | 75 | 83 | 87 |
| Residential 1/3 acre | Residential districts by average lot size: 1/3 acre | 30 | 57 | 72 | 81 | 86 |
| Residential 1/2 acre | Residential districts by average lot size: 1/2 acre | 25 | 54 | 70 | 80 | 85 |
| Residential 1 acre | Residential districts by average lot size: 1 acre | 20 | 51 | 68 | 79 | 84 |
| Residential 2 acres | Residential districts by average lot size: 2 acre | 12 | 46 | 65 | 77 | 82 |
| Water/Wetlands | | 0 | 0 | 0 | 0 | 0 |

Table 2-1 Values of C_n for different types of soil and land use

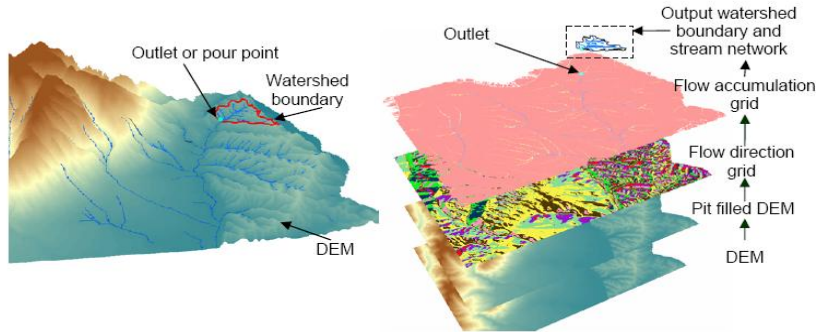


Figure 2-1 Representation of a DEM, outlet pour point and watershed boundary (left); hydrological grids used for watershed delineation (right)

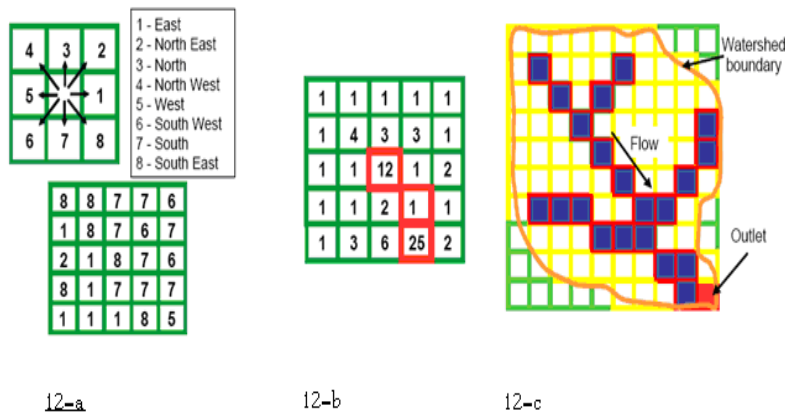


Figure 2-2 a) Eight-direction pour point model, numerical depiction of a flow-direction grid; b) Flow accumulation grid values with values above threshold highlighted showing a derived stream network, c) Grid representation of a watershed boundary stream network outlet

2.2.2 Flow direction

The direction of flow from each grid cell to its downhill neighbor is calculated from the pit-filled DEM. The flow direction is calculated by examining the eight neighbors of a cell and determining the neighbor with the steepest downhill slope. This direction is then coded as a value in a new "flow direction" grid (Figure 2-2-a). This process is repeated to create a grid with flow-directions coded for the entire landscape as shown in the filled squares in Figure 2-2-a.

2.2.3 Flow accumulation, stream grids, and drainage area

With the flow-direction grid, it is possible to sum the number of uphill cells that "flow" to any other cell. This summing can be done for all cells within a grid to create a "flow-accumulation" grid in which each cell-value represents the number of uphill cells flowing to it (Figure 2-2-b). Because a cell

represents a geographic area (i.e. each cell of a 90-meter resolution grid is 8100 m²), the flow-accumulation grid can be multiplied by this area to calculate the total drainage area. In addition, a grid representing a stream network can be created by querying the flow-accumulation grid for cell values above a certain threshold. For example, in Figure 2-2-b, a cell receiving flow from more than 12 other cells is defined as a stream channel.

2.2.4 Watershed delineation

The hydrologic grids discussed in sections are then used to delineate watershed boundaries (xxxFigure 2-2-c). By following a flow direction grid backward, we can determine all of the cells that drain through a given outlet (yellow cells in Figure 2-2-c). These can then be selected and converted to a polygon representing the watershed. The stream grid is necessary to ensure that the cell selected as an outlet is on the modeled "stream" and not on the adjacent hill slope.

2.2.5 Watershed and Stream Delineation Software

The Watershed Modeling System (WMS) was used in the current study. It is a comprehensive graphical modeling environment for all phases of watershed hydrology and hydraulics. WMS includes powerful tools to automate modeling processes such as automated basin delineation, geometric parameter calculations; GIS overlay computations (CN, rainfall depth, roughness coefficients, etc.), cross-section extraction from terrain data, and many more! With the release of WMS 7, the software now supports hydrologic modeling with HEC-1 (HEC-HMS), TR-20, TR-55, Rational Method, NFF, MODRAT, and HSPF. Hydraulic models supported include HEC-RAS and CE QUAL W2. 2-D integrated hydrology (including channel hydraulics and groundwater interaction) can now be modeled with GSSHA. All this in a GIS-based data processing framework will make the task of watershed modeling and mapping easier than ever before. The program's modular design enables the user to select modules in custom combinations, allowing the user to choose only those hydrologic modeling capabilities that are required. Additional WMS modules can be purchased and added at any time. The software will dynamically link to these subsequent modules at run time — automatically adding additional modeling capability to the software.

2.2.6 Watershed and Stream Delineation for Sana'a Basin

The WMS software has been applied to determine the basin delineation and watershed outline for the entire Sana'a Basin. Several trials were adopted until the outlet point for the entire Sana'a Basin was determined. The location of the outlet point can be defined as: UTM (E)=436713 m and UTM (N)=1740306 m and the ground elevation at this point is 1921.50 m (Above Mean Sea Level (AMSL)). Thus, at this point, all the surface runoff within the entire basin is concentrated at this location. The basic information that describes the morphological aspects of the Sana'a Basin is as follows:

- Basin area = 3243.13 km²
- Basin average slope = 0.1160 m/m
- Average overland flow = 751.259 m
- Percentage of north/south Aspects = 0.52 , 0.48
- Basin length = 75218.27 m
- Basin perimeter = 433390 m
- Shape factor = 1.74 mi²/mi²
- Sinuosity factor = 1.49
- Mean basin elevation = 2422.96 m (AMSL)
- Maximum flow distance = 114239.21 m

- Maximum flow slope = 0.0121 m/m
- Maximum stream length = 112253 m
- Maximum stream slope = 0.0093 m/m
- Coordinates of basin centroid UTM (E) = 422258.15 m
- Coordinates of basin centroid UTM (N) = 1711566.98 m
- Distance from centroid to main stream = 125.45 m

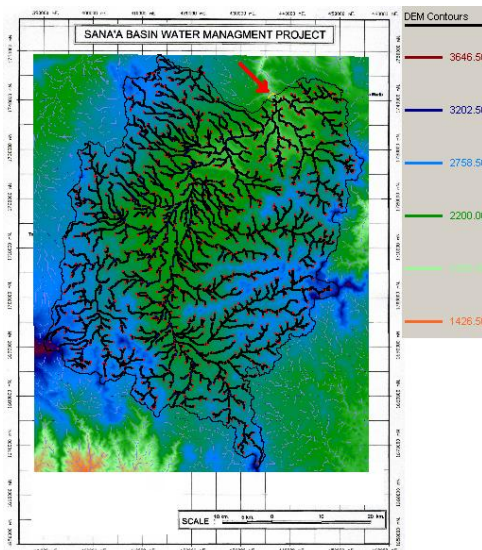


Figure 2-3 Delineation of the Sana'a Basin - red arrow indicates the outlet of the entire basin at Wadi Al-Khared

Chapter 3. DELINEATION OF SUB-BASINS WITHIN THE SANA'A BASIN

3.1 Introduction

In order to complete the design of a surface water monitoring network for the Sana'a Basin, the following information should be very well understood:

- Morphological characteristics of sub-basins and sub-sub-basins;
- Design storm scenarios for different locations throughout the basin;
- Hydrographs of different sub-basins and sub-sub-basins;
- Semi-two-dimensional river-stream network analysis for the sub-basins and sub-sub-basins;
- Locations potentially suitable for surface water monitoring stations;
- Actual suitability of chosen sites based on field visit observations.

These six steps are presented in detail in the flow chart (Figure 14). The process starts by using the DEM map for streamline and watershed delineation of the different sub-basins and sub-sub-basins. Outlet location is also determined during the delineation process. Thus, the sub-basins and sub-sub-basins are outlined in the GIS system and DEM map. Design storms are then selected to test the impact of different storm intensities on the hydrograph of each stream and its outlet. In addition, land-use maps, surface roughness and soil maps will be inputted to the WMS software so that hydrographs can be formulated for different locations within the watershed. The next stage is to apply the delineated stream system to a semi-two-dimensional river-stream network analysis. In order to perform this analysis, HEC-RAS software was applied through the WMS. Once this model is complete, the user can then calculate the expected water depth at different streams within the network. From this information the user can determine the most suitable locations where the surface water monitoring stations can be installed. The stages of this process will be outlined in detail in the following section.

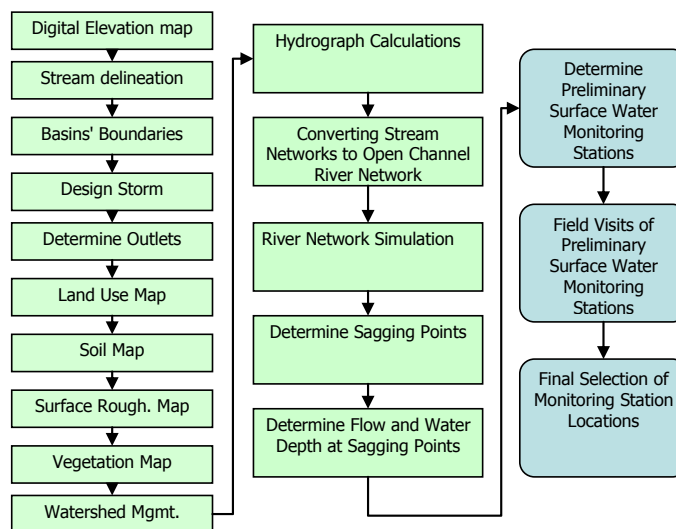


Figure 3-1 Flow chart showing the different steps that are involved in the design of a surface water monitoring network for the Sana'a Basin

3.2 Delineation of Sub-Basins and Sub-Sub-Basins

Using the WMS tool, sub-basins can be divided into individual sub-sub-basins to assist in the study of the morphological behavior of each. The 22 sub-basins of the Sana'a Basin, shown in Figure 15, were thus re-defined and sub-basin boundaries determined. This process found good compatibility between the new boundaries and the previously developed boundaries (which ones?). Only in some local areas was any discrepancy found, but this is unlikely to affect the entire system. Within each sub-basin the sub-sub-basins were then defined. The purpose of this process was to isolate the hydrographs and surface water runoff analyses for each sub-basin through an accurate simulation of the entire physical system. Figure 15 presents the main sub-basins identified. Figures 16 through 59 present the newly developed boundaries of the 22 sub-basins and the sub-sub-basins within each. The figures are superimposed on satellite images of the Sana'a Basin.

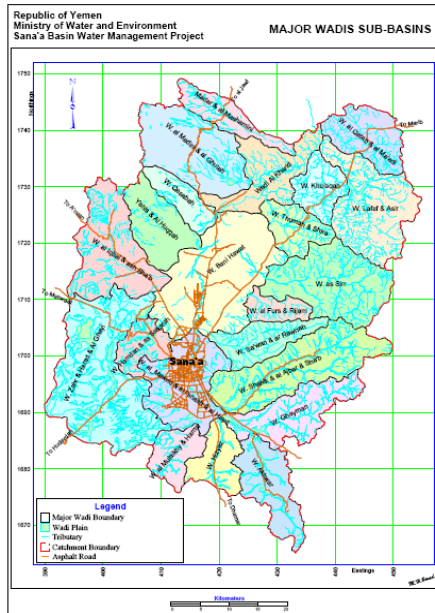


Figure 3-2 Identification of the different sub-basins within the Sana'a Basin

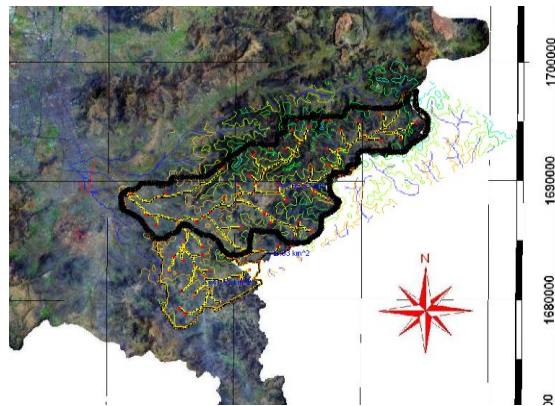


Figure 3-3 Ghayman basin delineation and streamline delineation map

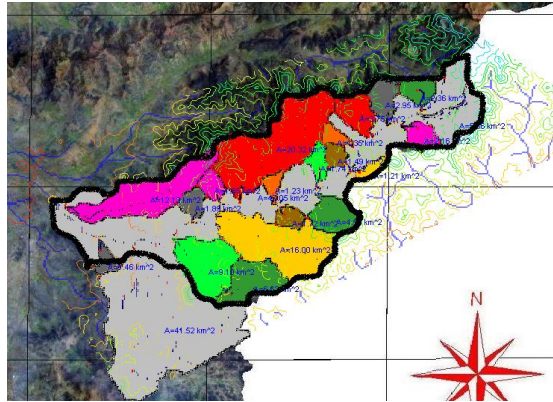


Figure 3-4 Ghayman sub-basin delineation and area of each sub-basin

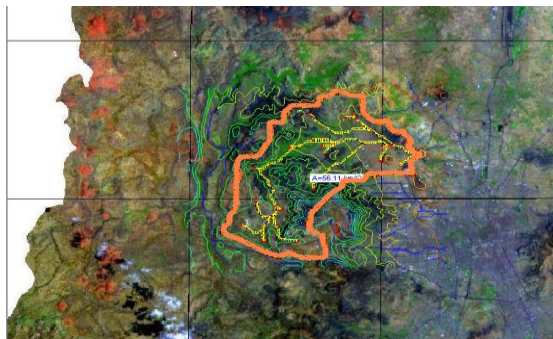


Figure 3-5 Hamadan and As-Sabarah basin delineation and streamline delineation map

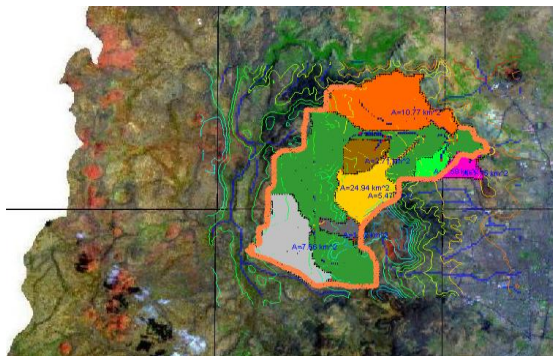


Figure 3-6 Hamadan and As-Sabarah sub-basins delineation and area of each sub-basin

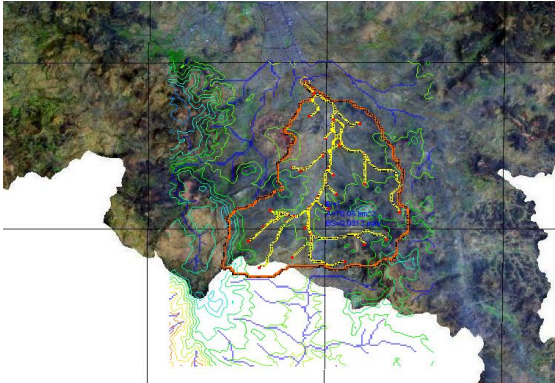


Figure 3-7 Hizyaz basin delineation and streamline delineation map

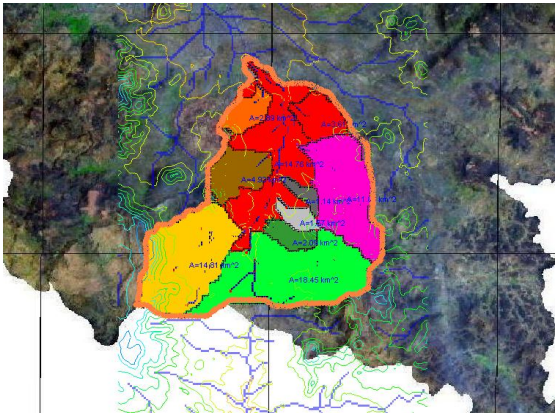


Figure 3-8 Hizyaz sub-basin delineation and area of each sub-basin

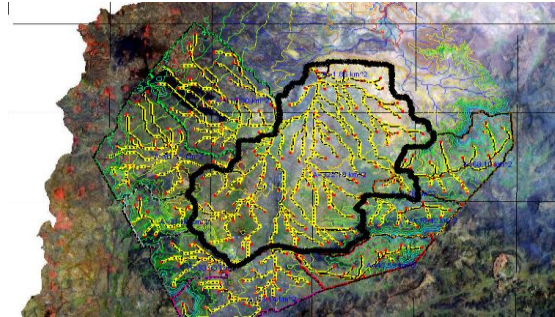


Figure 3-9 Bani Hawat basin delineation and streamline delineation map

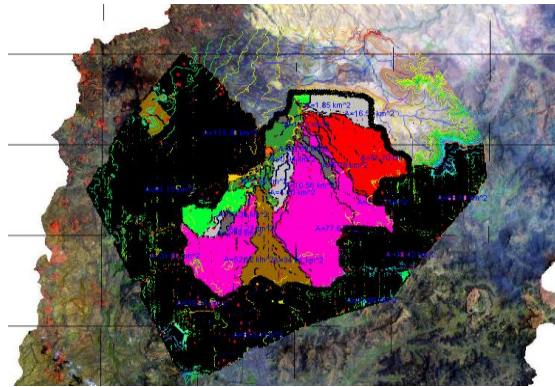


Figure 3-10 Bani-Hawat sub-basin delineation and area of each sub-basin

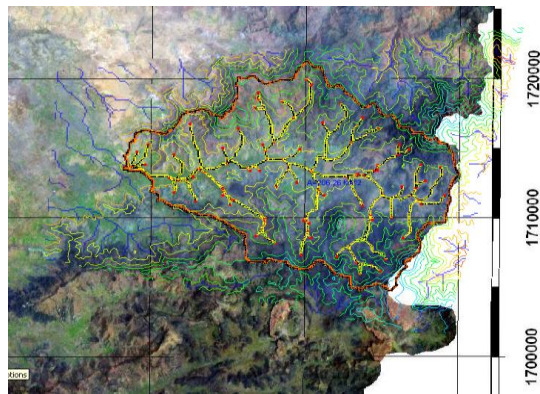


Figure 3-11 As-Sirr basin delineation and streamline delineation map

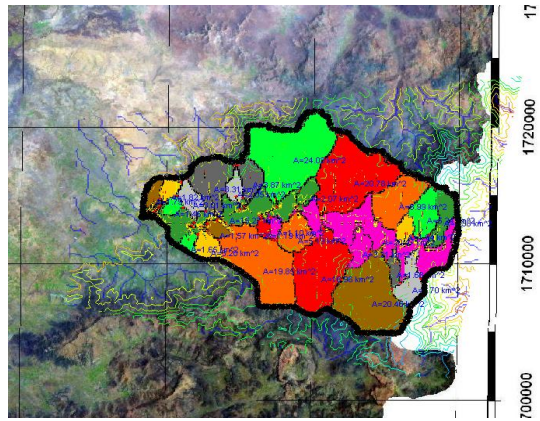


Figure 3-12 As-Sirr sub-basin delineation and area of each sub-basin

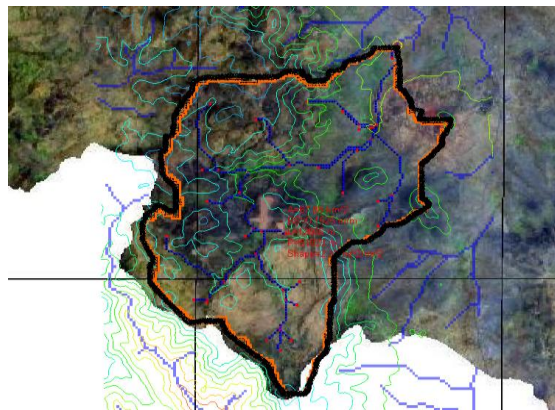


Figure 3-13 Al-Mulaikhy and Hamal basin delineation and streamline delineation map

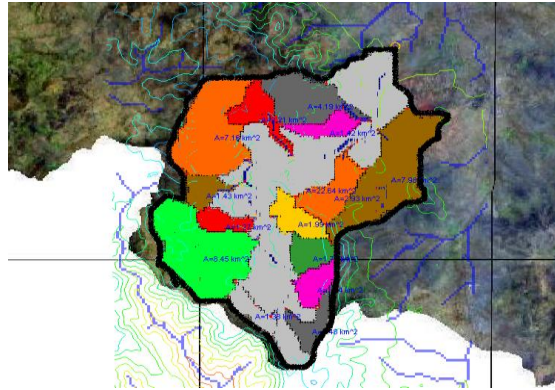


Figure 3-14 Al-Mulaikhy and Hamal sub-basin delineation and area of each sub-basin

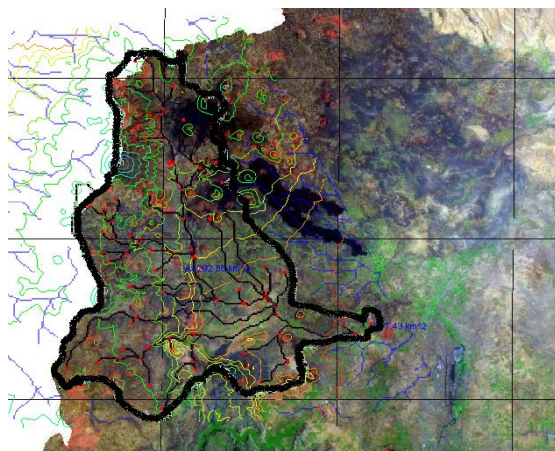


Figure 3-15 Iqbal and Ash Sha'b basin delineation and streamline delineation map

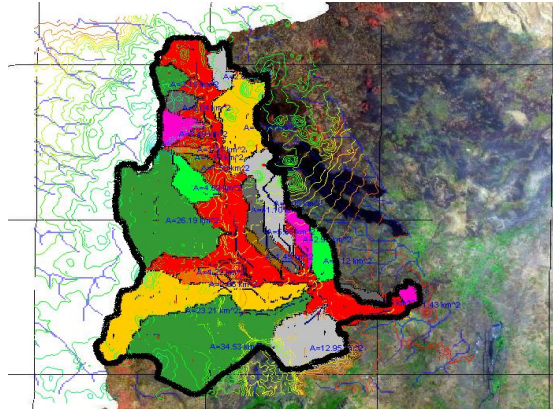


Figure 3-16 Iqbal and Ash Sha'b sub-basin delineation and area of each sub-basin

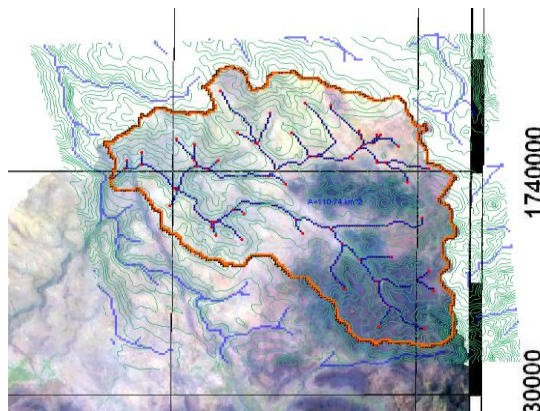


Figure 3-17 Al-Qotob abd MA'adi sub-basin delineation and streamline delineation map

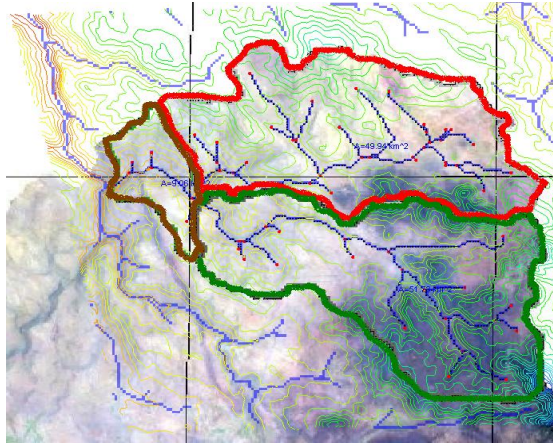


Figure 3-18 Al-Qotob abd MA'adi sub-basin delineation and area of each sub-basin

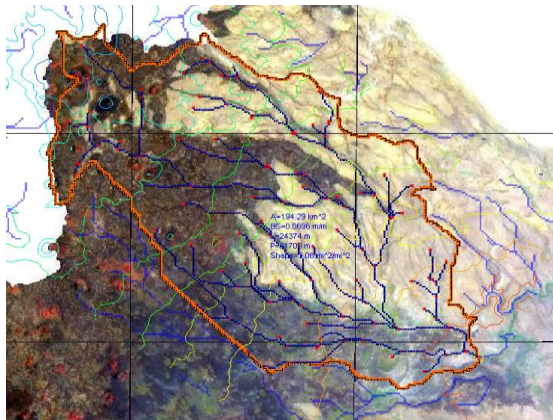


Figure 3-19 Madini and Al-Ghulah basin delineation and streamline delineation map

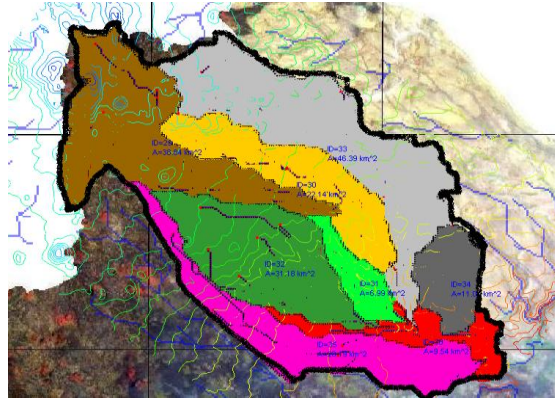


Figure 3-20 Madini and Al-Ghulah sub-basin delineation and area of each sub-basin

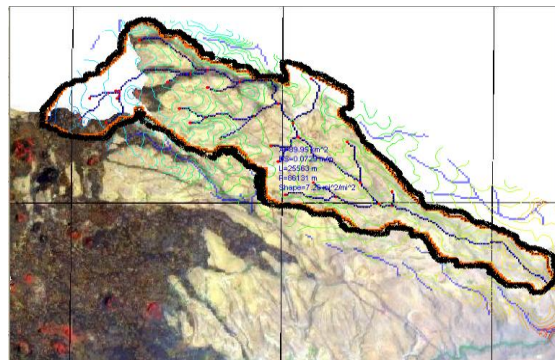


Figure 3-21 Madar and Al-Mashamini basin delineation and streamline delineation map

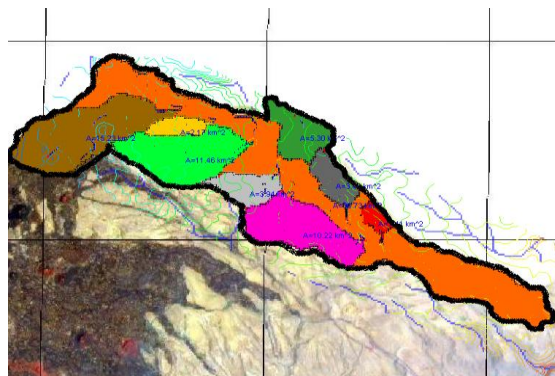


Figure 3-22 Madar and Mashamini sub-basin delineation and area of each sub-basin

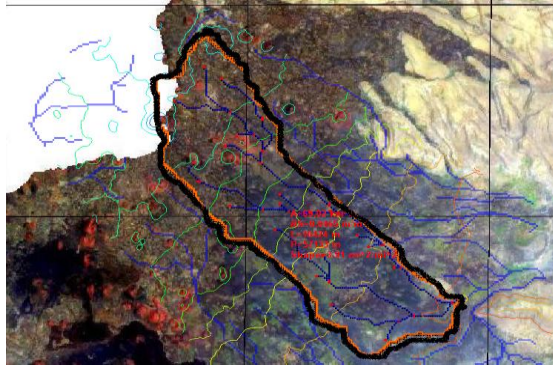


Figure 3-23 Qasabah basin delineation and streamline delineation map

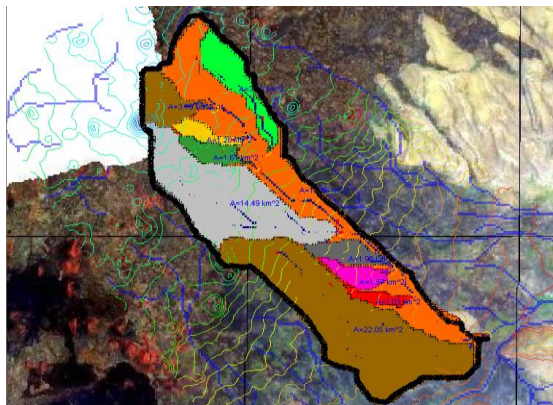


Figure 3-24 Qasabah sub-basin delineation and area of each sub-basin

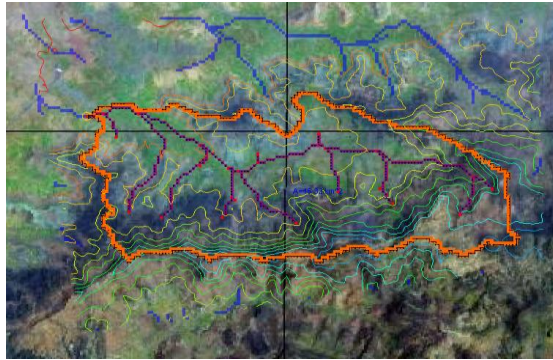


Figure 3-25 Al-Furs and Rijam basin delineation and streamline delineation map

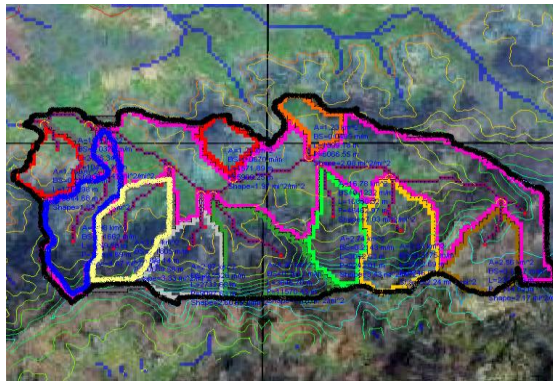


Figure 3-26 Al-Furs and Rijam sub-basin delineation and area of each sub-basin

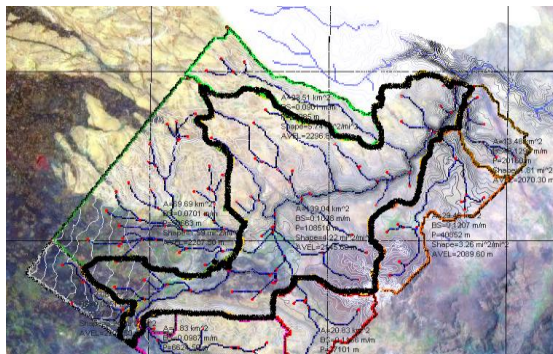


Figure 3-27 Al-Kharid basin delineation and streamline delineation map

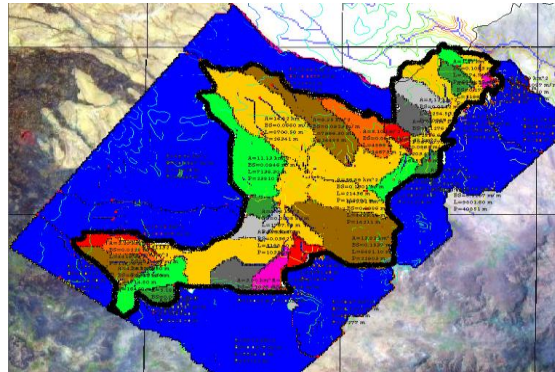


Figure 3-28 Al-Kharid sub-basin delineation and area of each sub-basin

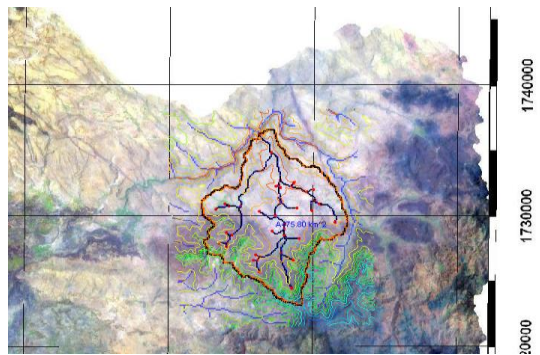


Figure 3-29 Khulaqah basin delineation and streamline delineation map

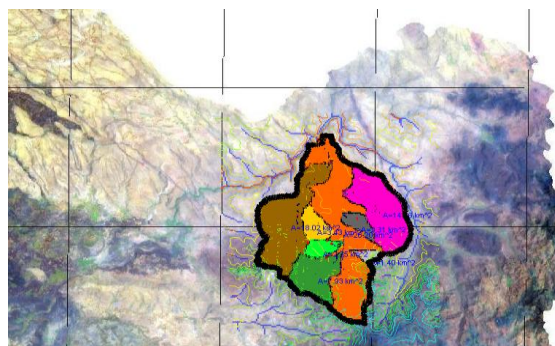


Figure 3-30 Khulaqah sub-basin delineation and area of each sub-basin

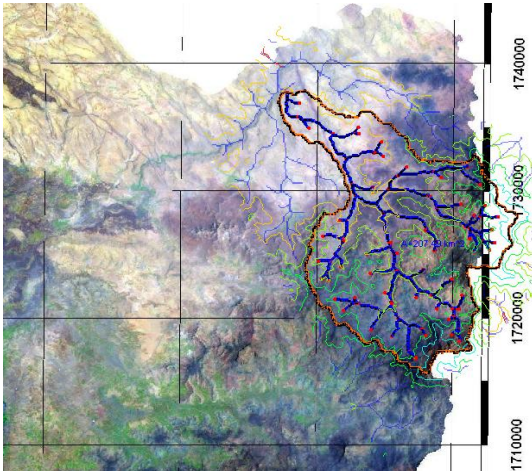


Figure 3-31 Lasef and Assir basin delineation and streamline delineation map

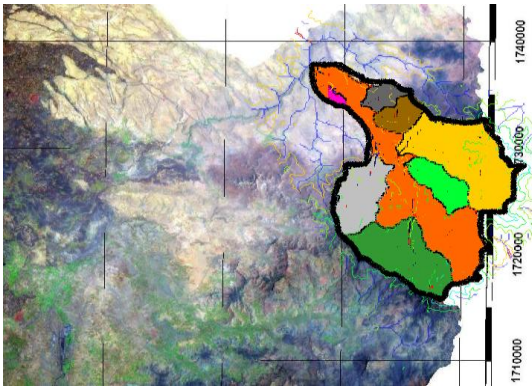


Figure 3-32 Lasef and Assir sub-basin delineation and area of each sub-basin

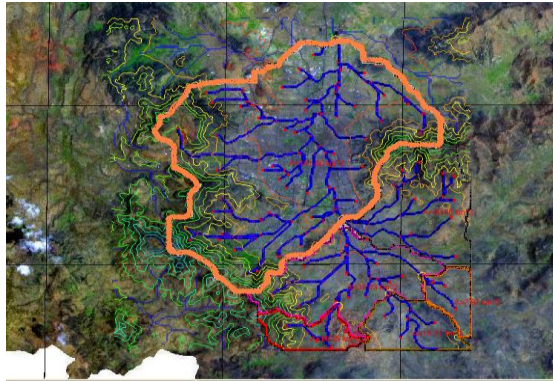


Figure 3-33 Al-Mawrid, Al-L'Shash and Hayd basin delineation and streamline delineation map

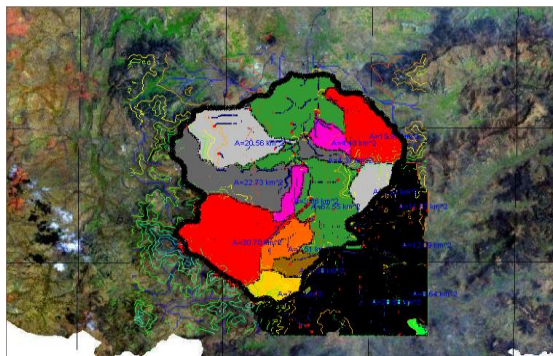


Figure 3-34 Al-Mawri, Al-L'Shash and Hayd sub-basin delineation and area of each sub-basin

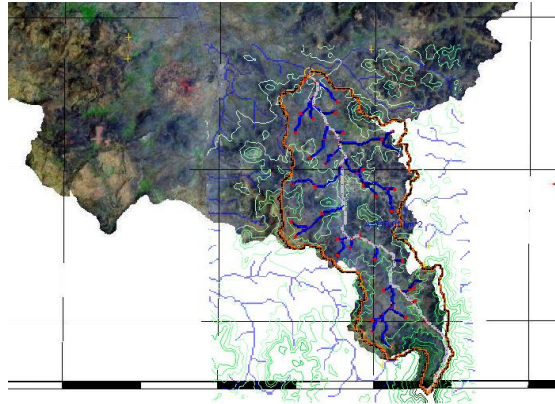


Figure 3-35 Akhwar basin delineation and streamline delineation map

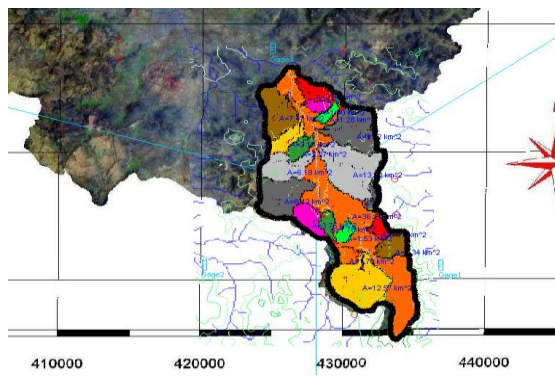


Figure 3-36 Akhwar sub-basin delineation and area of each sub-basin

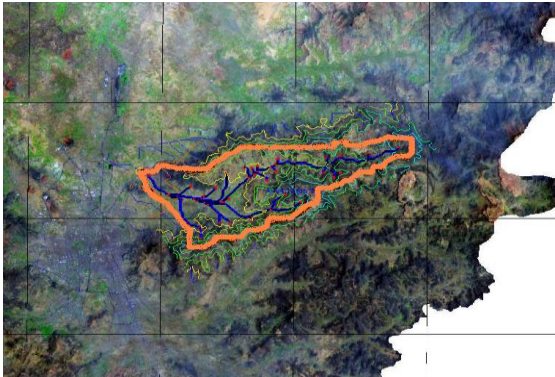


Figure 3-37 Sa'wan and AR-Rawnah basin delineation and streamline delineation map

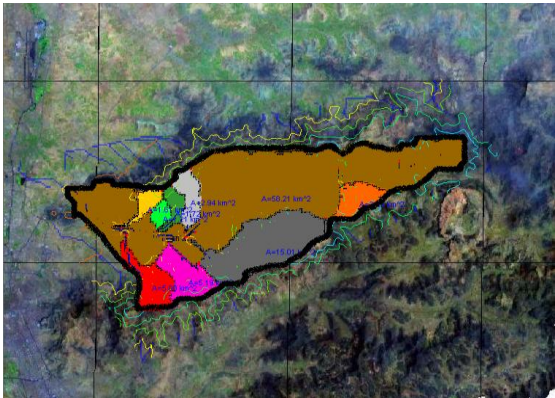


Figure 3-38 Sa'wan and A-Rawnah sub-basin delineation and area of each sub-basin

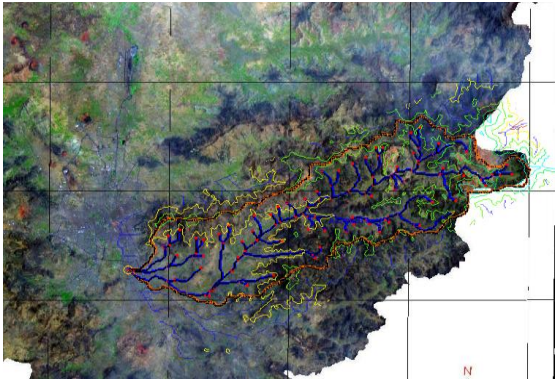


Figure 3-39 Shahik, Al-Ajbar and Sha'b basin delineation and streamline delineation map

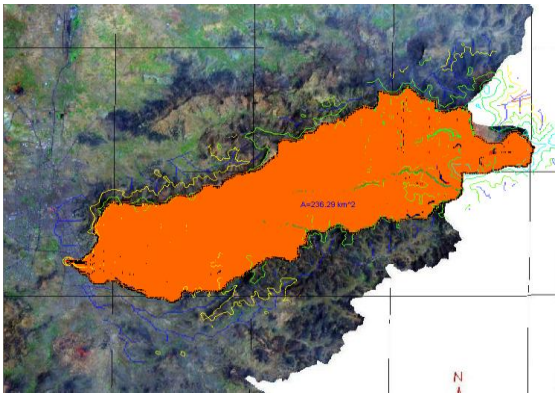


Figure 3-40 Shahik, Al-Ajbar and Sha'b sub-basin delineation and area of each sub-basin

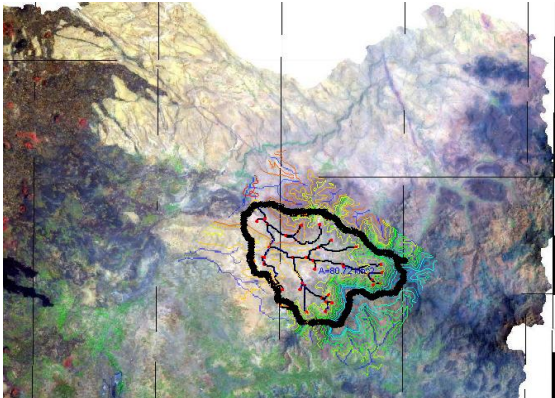


Figure 3-41 Thuma and Shiraa basin delineation and streamline delineation map

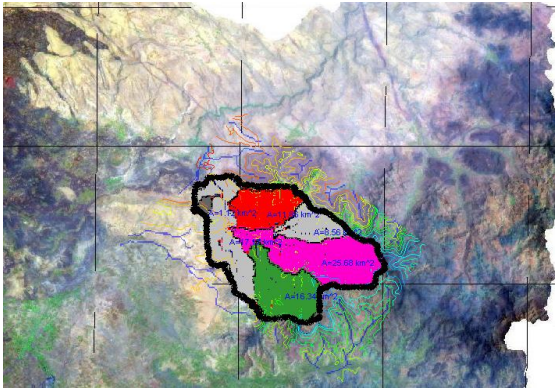


Figure 3-42 Thuma and Shiraa sub-basin delineation and area of each sub-basin

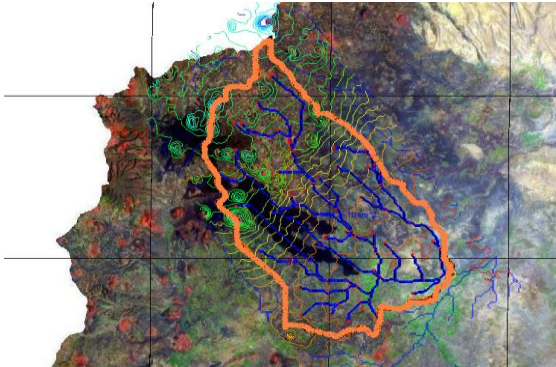


Figure 3-43 Yahis and AL-Huqqah basin delineation and streamline delineation map

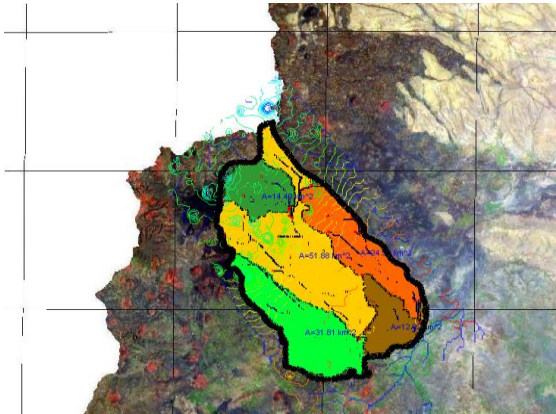


Figure 3-44 Yahis and AL-Huqqah sub-basin delineation and area of each sub-basin

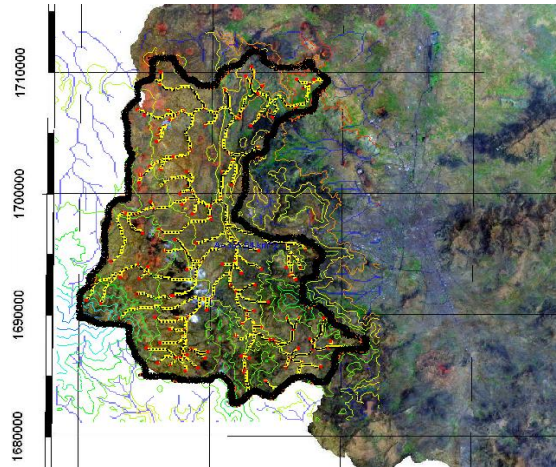


Figure 3-45 Zahr, Harad and Al-Ghayl basin delineation and streamline delineation map

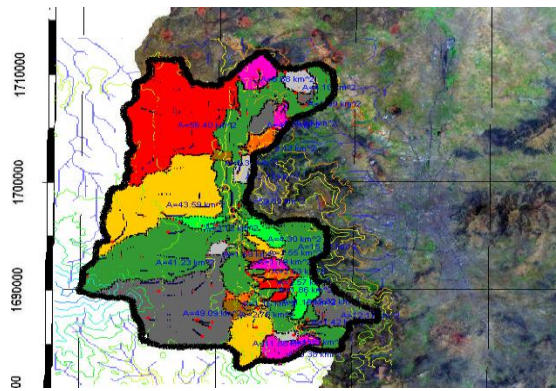


Figure 3-46 Zahr, Harad and Al-Ghayl sub-basin delineation and area of each sub-basin

Chapter 4. RAINFALL ANALYSIS, DEVELOPMENT OF INTENSITY DURATION CURVES AND STORM PATTERN OF THE SANA'A BASIN

4.1 Storm Design

From the literature review, it has been concluded that the analysis of water systems within the Sana'a Basin depends mainly on the yearly average rainfall in the region. However, to interpret the surface water network of the Sana'a Basin, it is necessary to have more detailed information about rainfall patterns within the basin. Thus, a detailed analysis was performed to determine the intensity-duration-frequency curves (IDF) for different locations within the basin. The following section describes the rainfall analysis performed.

4.1.1 IDF within Sana'a Basin

Available IDF curve data from fifteen gauging stations were used to determine specific IDF curves for different areas within the basin. The curves developed are preliminary in nature and should only be used as a preliminary design guide until further refinement is performed and should be refined using actual rainfall data collected during the data collection process presented in Chapter 1. Additional rainfall data collection is recommended and should be used to form the IDF curves and the terrain-weighting factor.

RAINBOW software was used for the purpose of developing the IDF curves for the Sana'a Basin. The program is a menu-driven software designed to test the homogeneity of hydrologic records and to execute a frequency analysis of rainfall and evaporation data. The program is especially suitable for predicting the probability of occurrence of either low or high rainfall amounts, both of which are important variables in the design and management of irrigation systems, drainage networks, networks, and reservoirs.

Figure 60 presents the Thiessen polygon diagram for all the stations that were installed within the Sana'a Basin. Accordingly, in the current study, the IDF for each polygon is developed based on the available data for each station. Thus, some stations were excluded from the calculations, especially those that do not have five years of available data. The rainbow software analysis for the selected reliable stations is presented through the frequency analysis and probability plotting of hydrological data. Figures 61 through 92 introduce the output results.

From the frequency analysis, probability plotting and tests of homogeneity for the hydrological records of the different stations, the IDF for the different stations can be developed. RAINBOW software was applied to calculate the values of the expected 2-year, 5-year, 10-year, 20-year, 25-year, 50-year and 100-year rainfall storm intensity as shown in Table 3. Figures 93 and 94 present the rainfall intensity for 2-year, 5-year, 10-year, 20-year, 25-year, 50-year and 100-year calculated storms.

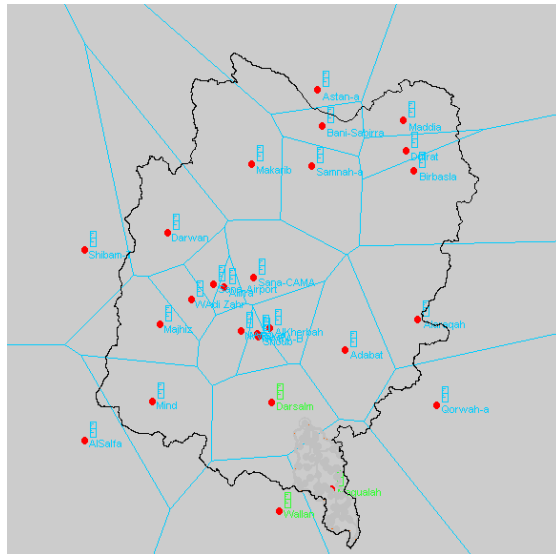


Figure 4-1 Spatial locations of rainfall stations from which rainfall data was collected throughout the basin, showing the Thiessen Polygon for each station

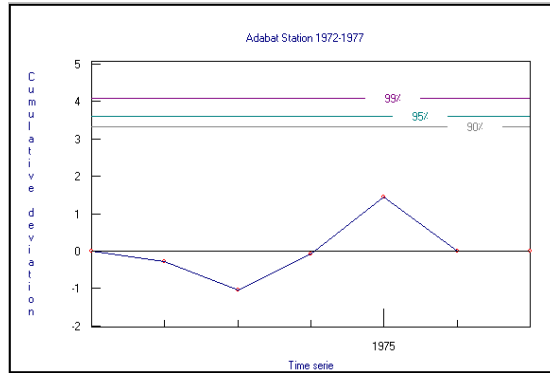


Figure 4-2 Test of homogeneity of hydrologic records for Adabat station from 1972 to 1977

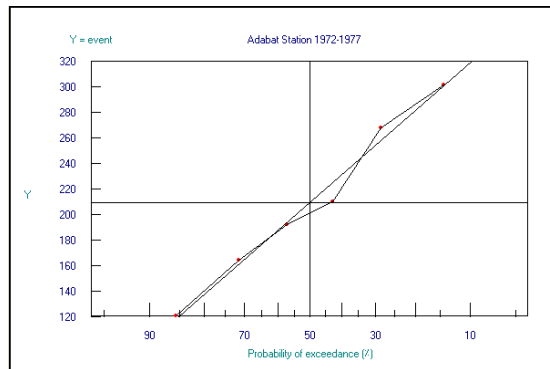


Figure 4-3 Frequency analysis and probability plotting of hydrologic records for Adabat station from 1972 to 1977

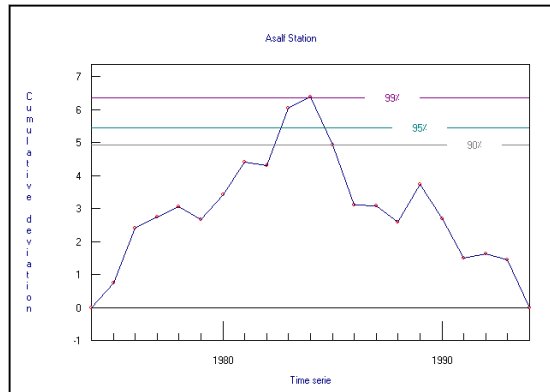


Figure 4-4 Test of homogeneity of hydrologic records for Al-Salaf station from 1974 to 1994

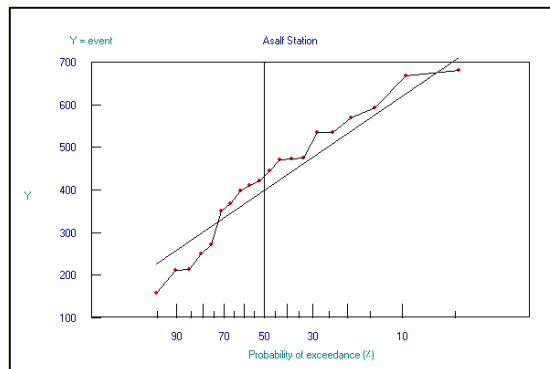


Figure 4-5 Frequency analysis and probability plotting of hydrologic records for Al-Salaf station from 1974 to 1994

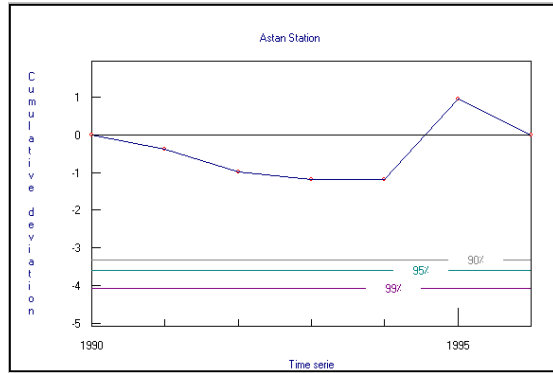


Figure 4-6 Test of homogeneity of hydrologic records for Astan station from 1990 to 1996

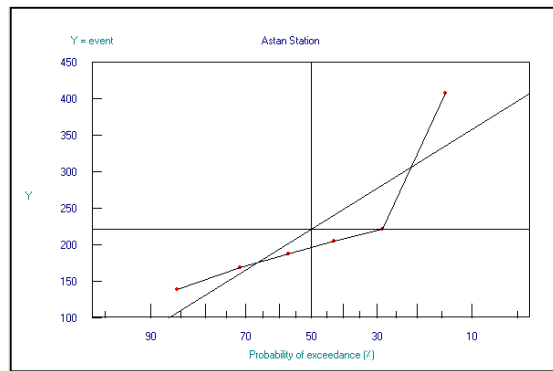


Figure 4-7 Frequency analysis and probability plotting of hydrologic records for Astan station from 1990 to 1996

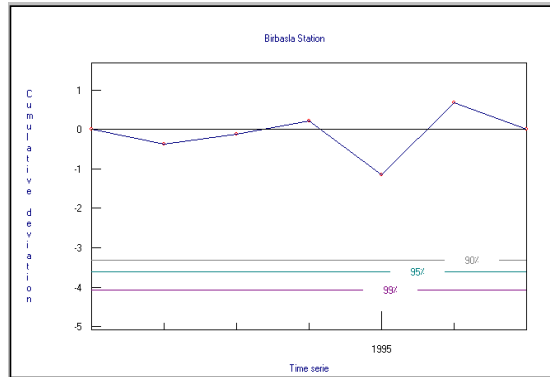


Figure 4-8 Test of homogeneity of hydrologic records for Birbasal station from 1991 to 1997

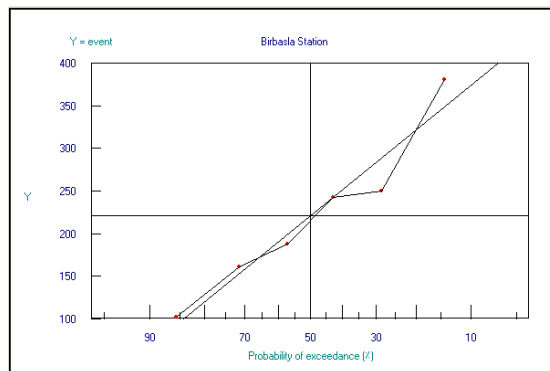


Figure 4-9 Frequency analysis and probability plotting of hydrologic records for Birbasal station from 1991 to 1997

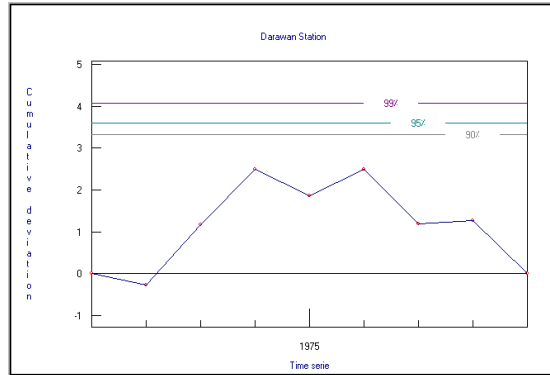


Figure 4-10 Test of homogeneity of hydrologic records for Darawan station from 1971 to 1979

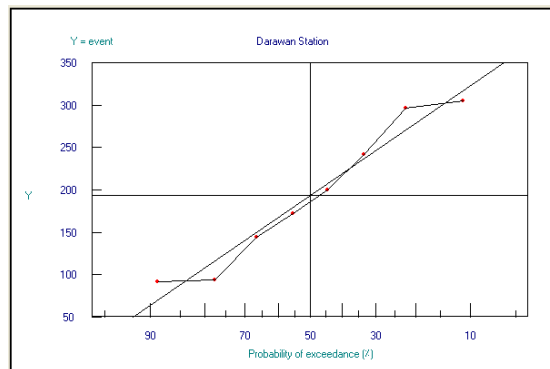


Figure 4-11 Frequency analysis and probability plotting of hydrologic records for Darawan station from 1971 to 1979

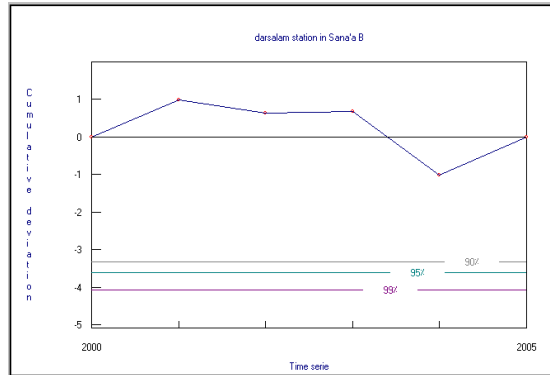


Figure 4-12 Test of homogeneity of hydrologic records for Darsalem station from 2000 to 2005

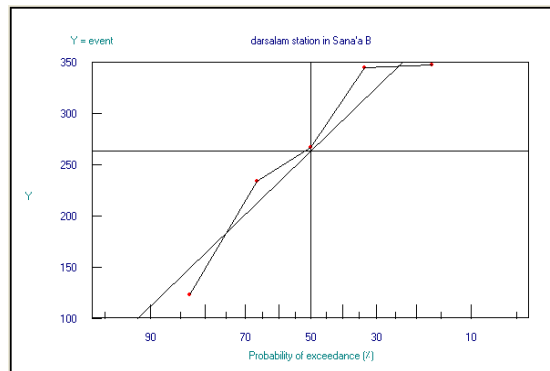


Figure 4-13 Frequency analysis and probability plotting of hydrologic records for Darsalem station from 2000 to 2005

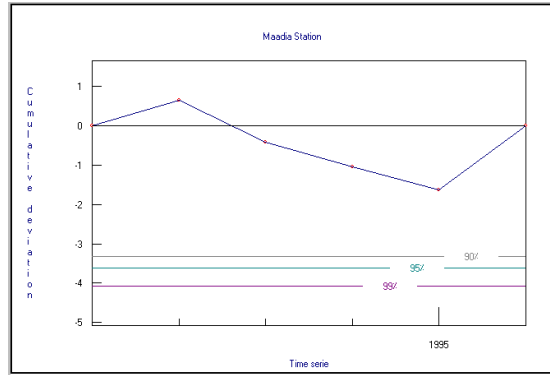


Figure 4-14 Test of homogeneity of hydrologic records for Maadia station from 1991 to 1996

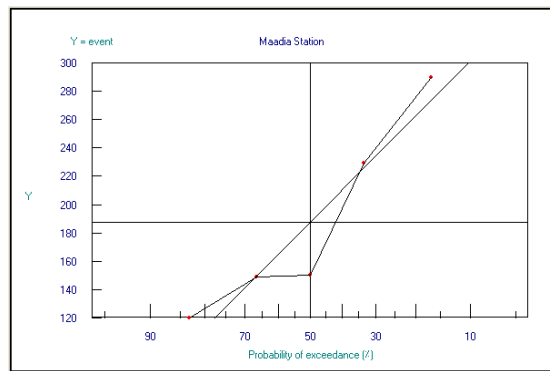


Figure 4-15 Frequency analysis and probability plotting of hydrologic records for Maadia station from 1991 to 1996

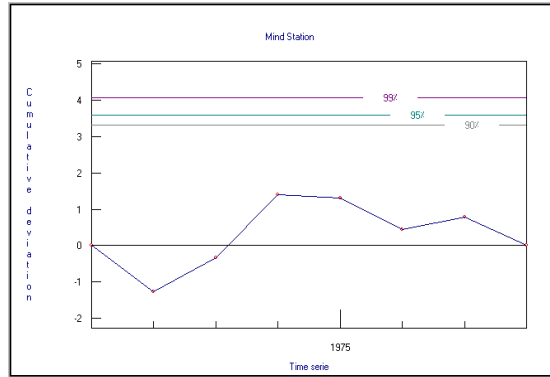


Figure 4-16 Test of homogeneity of hydrologic records for Mind station from 1971 to 1978

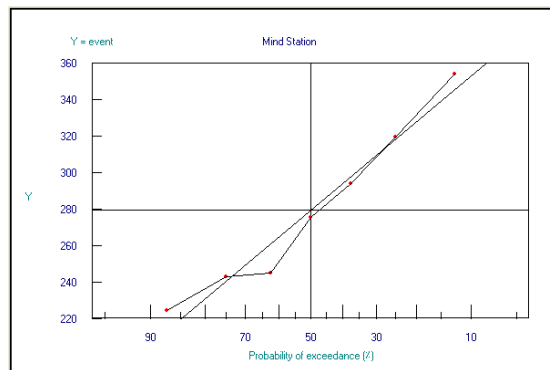


Figure 4-17 Frequency analysis and probability plotting of hydrologic records for Mind station from 1971 to 1978

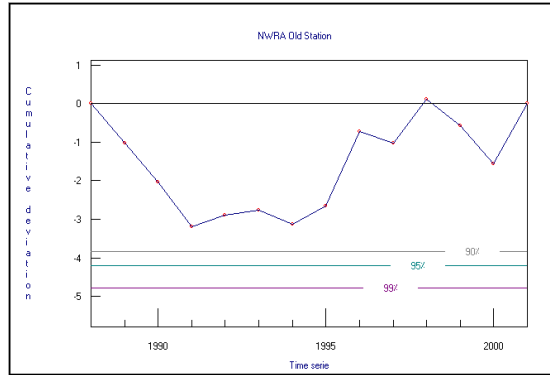


Figure 4-18 Test of homogeneity of hydrologic records for old NWRA station from 1988 to 2001

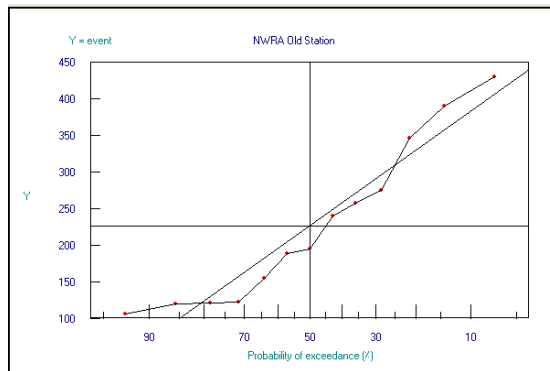


Figure 4-19 Frequency analysis and probability plotting of hydrologic records for old NWRA station from 1988 to 2001

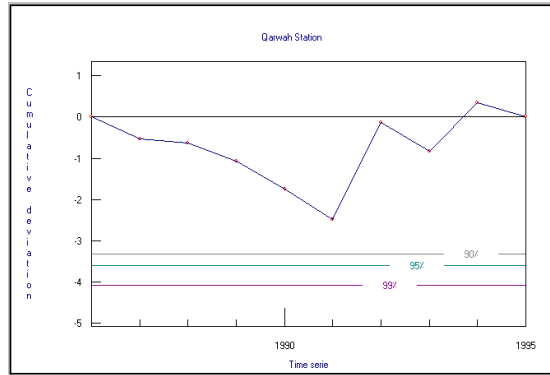


Figure 4-20 Test of homogeneity of hydrologic records for Qawaht station from 1986 to 1995

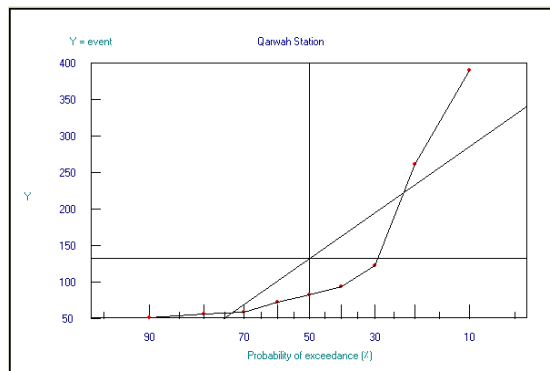


Figure 4-21 Frequency analysis and probability plotting of hydrologic records for Qawaht station from 1986 to 1995

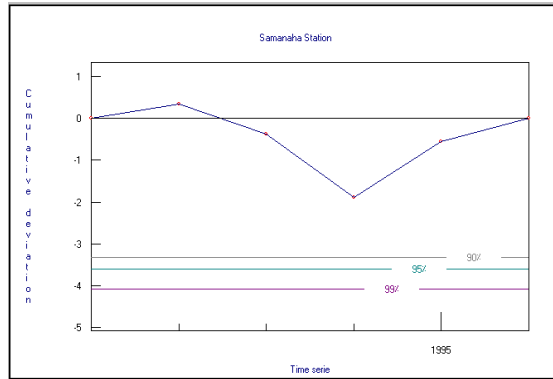


Figure 4-22 Test of homogeneity of hydrologic records for Samanah station from 1991 to 1996

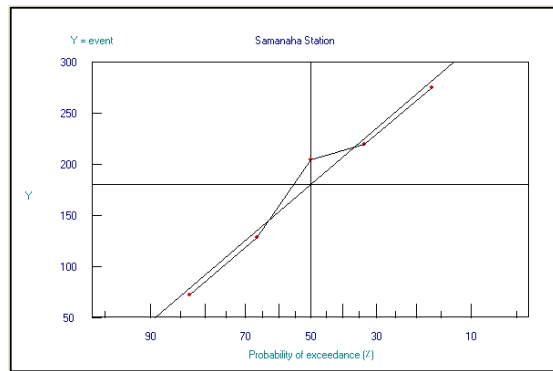


Figure 4-23 Frequency analysis and probability plotting of hydrologic records for Samanah station from 1991 to 1996

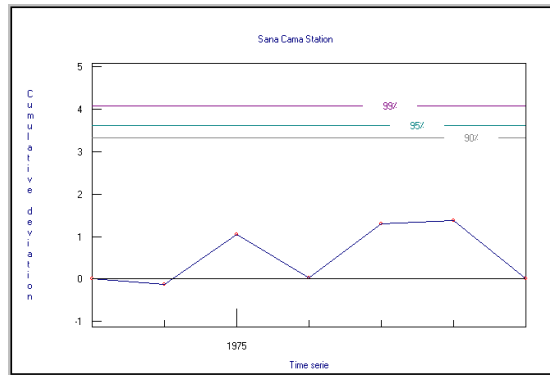


Figure 4-24 Test of homogeneity of hydrologic records for Sana'a CAMA station from 1973 to 1979

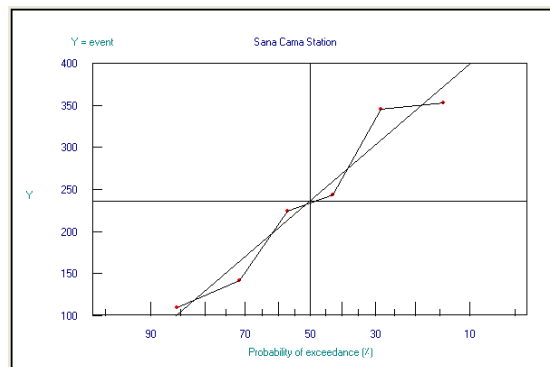


Figure 4-25 Frequency analysis and probability plotting of hydrologic records for Sana'a CAMA station from 1973 to 1979

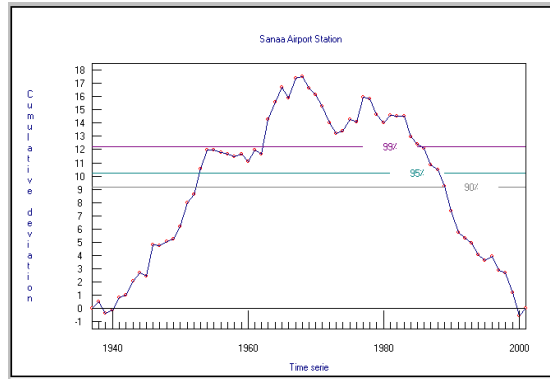


Figure 4-26 Test of homogeneity of hydrologic records for Sana'a Airport station from 1938 to 2001.

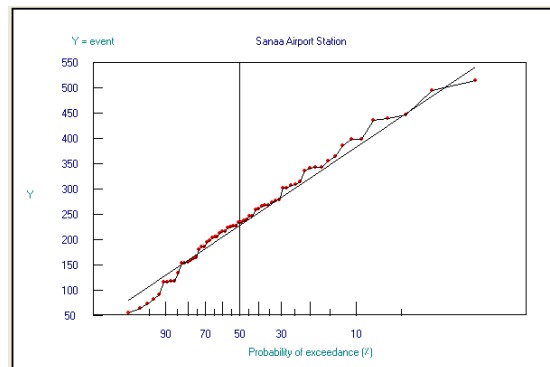


Figure 4-27 Frequency analysis and probability plotting of hydrologic records for Sana'a Airport station from 1938 to 2001.

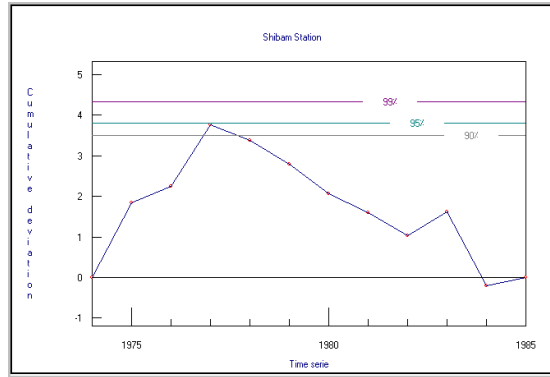


Figure 4-28 Test of homogeneity of hydrologic records for Shibam station from 1974 to 1985

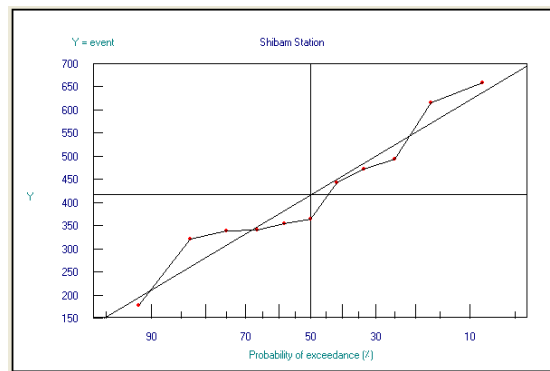


Figure 4-29 Frequency analysis and probability plotting of hydrologic records for Shibam station from 1974 to 1985

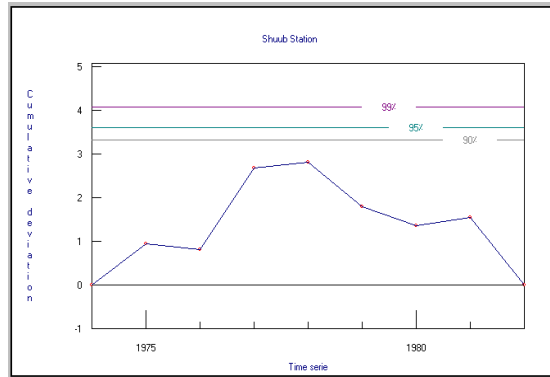


Figure 4-30 Test of homogeneity of hydrologic records for Shuub station from 1974 to 1982

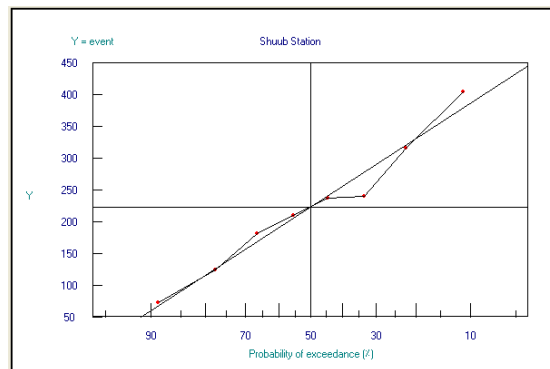


Figure 4-31 Frequency analysis and probability plotting of hydrologic records for Shuub station from 1974 to 1982

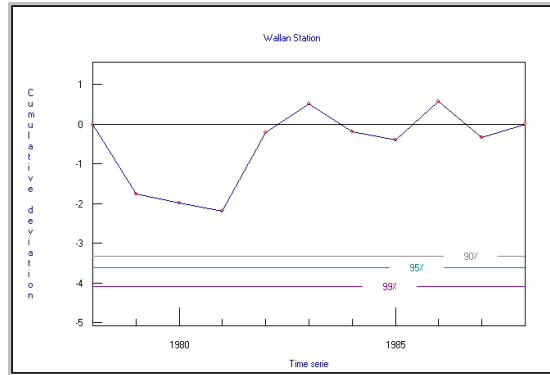


Figure 4-32 Test of homogeneity of hydrologic records for Wallan station from 1978 to 1988

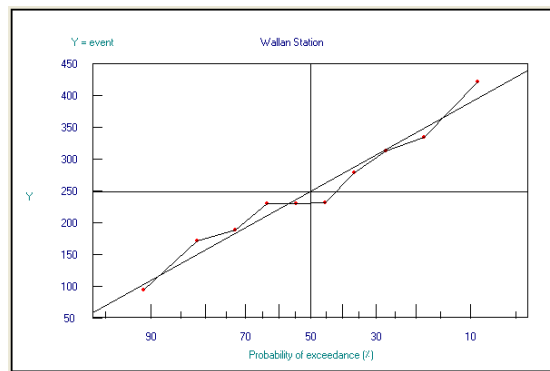


Figure 4-33 Frequency analysis and probability plotting of hydrologic records for Wallan station from 1978 to 1988

| Ser No | Station | UTM E | UTM N | 2 yr | 5 yr | 10 yr | 20 yr | 25 yr | 50 yr | 100 yr |
|--------|----------|--------|---------|------|------|-------|-------|-------|-------|--------|
| 1 | Adabat | 432250 | 1698700 | 210 | 281 | 319 | 350 | 359 | 349 | 408 |
| 2 | Asalf-a | 385800 | 1683400 | 425 | 566 | 640 | 701 | 718 | 769 | 815 |
| 3 | Astan-a | 427550 | 1743027 | 221 | 311 | 359 | 397 | 409 | 441 | 470 |
| 4 | Birbasla | 444000 | 1729284 | 221 | 321 | 374 | 417 | 430 | 466 | 499 |
| 5 | Darawan | 402126 | 1718733 | 193 | 278 | 323 | 360 | 370 | 401 | 428 |
| 6 | Maadia | 442250 | 1737750 | 188 | 262 | 301 | 334 | 343 | 370 | 394 |

| Ser No | Station | UTM E | UTM N | 2 yr | 5 yr | 10 yr | 20 yr | 25 yr | 50 yr | 100 yr |
|--------|---------------|--------|---------|------|------|-------|-------|-------|-------|--------|
| 7 | Mind | 399550 | 1690005 | 279 | 328 | 353 | 374 | 380 | 398 | 413 |
| 8 | Qarwah-a | 447785 | 1689375 | 132 | 233 | 286 | 330 | 342 | 379 | 411 |
| 9 | Samanaha | 426650 | 1730085 | 180 | 268 | 315 | 353 | 364 | 396 | 424 |
| 10 | Sana-Cama | 416700 | 1711150 | 237 | 343 | 399 | 445 | 458 | 497 | 531 |
| 11 | Shibam-T | 383807 | 1715787 | 416 | 551 | 622 | 680 | 697 | 746 | 790 |
| 12 | Shuub | 417500 | 1701000 | 223 | 330 | 386 | 433 | 446 | 485 | 519 |
| 13 | Wallan | 421199 | 1671381 | 249 | 341 | 389 | 429 | 440 | 473 | 503 |
| 14 | Sanaa Airport | 410000 | 1710000 | 234 | 332 | 389 | 440 | 456 | 502 | 545 |
| 15 | NWRA Old | 414581 | 1701935 | 227 | 329 | 383 | 427 | 440 | 477 | 511 |

Table 4-1 Developed 2-year, 5-year, 10-year, 20-year, 25-year, 50-year and 100-year yearly rainfall intensity at different rainfall stations inside the Sana'a Basin

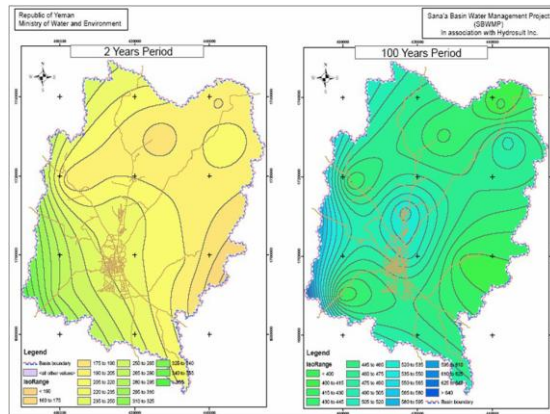


Figure 4-34 2-year and 100-year rainfall event distribution in the Sana'a Basin

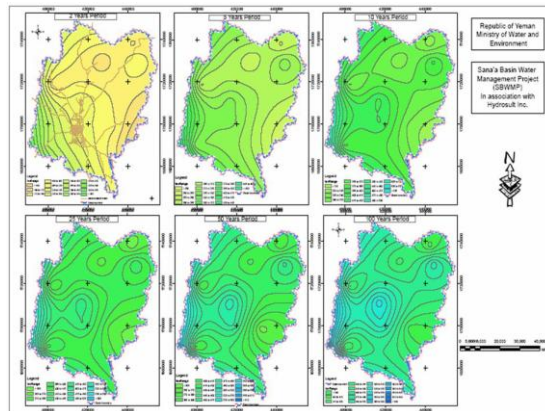


Figure 4-35 2-year, 5-year, 10-year, 20-year, 25-year, 50-year and 100-year rainfall event distribution in the Sana'a Basin

4.2 Developing of Storm Pattern for the Sana'a Basin

The literature review conducted by the current study revealed that storm patterns of the Sana'a Basin have not yet been analyzed. Thus, the aim of the current section is to present the procedure for developing a storm pattern for the Sana'a Basin.

4.2.1 Recorded Rainfall

Previous rainfall records for the Sana'a Basin were principally based on one-day records. This means that the total rainfall during a successive 24 hours is registered only once. In the current study, the monitoring team decided to adjust the rainfall recording stations to record rainfall data every 30 minutes, as presented in Figure 95. The results obtained from the 30-minute recording periods showed reliable data, leading the team to try further reducing the time interval to 5-minute recording periods. This trial also gave good results. Starting in March 2007, all of the rainfall stations were thus adjusted to collect data every 5 minutes, as presented in Figure 96.

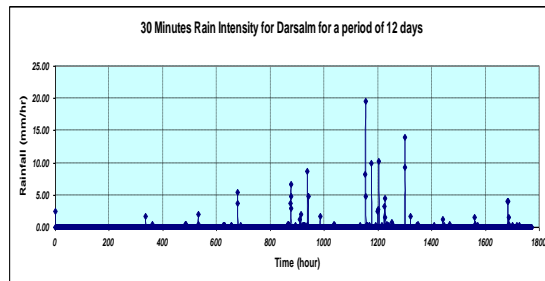


Figure 4-36 30-minute data collection for Darsalm rainfall station over a period of 12 days (August 2006)

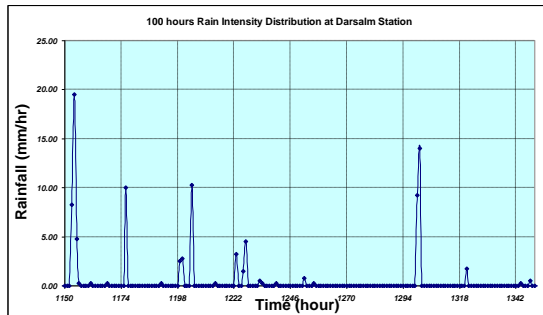


Figure 4-37 **5-minute** recorded data for Darselm rainfall station over a continuous period of 100 hours

4.2.2 Storm Pattern for Darselm Station

SMADA rainfall analysis software was used to develop the storm pattern for Darselm. SMADA currently has many types of dimensionless curves which can be entered: SCS type II, SCS type II Florida modified, and SCS type III. To use these curves, the user must enter duration, time, and total rainfall. The next step is to select the type of curve which the user would like to use. A rainfall pattern will then be created by the program and presented in both graphical and table format. The steps involved in designing a storm pattern for Darselm station were:

- Analysis of the recorded data and determination of the total storm time;
- Identification of the storm period and total rainfall intensity during this period, using the SMADA program;
- Testing of different patterns of storms and selecting an appropriate pattern.

Figure 4-36 and Figure 4-37 present data from the Darselm rainfall station's data logger. Through analyzing this data, it was concluded that most of the storms last approximately five continuous hours, exhibiting various rainfall intensities throughout. Experimenting with the SAMDA program for the available storm patterns, it has been found that storm type IA is the most compatible with the situation of Darselm. More study is needed and will be performed when more data is available for different rainfall seasons. Figure 4-38 and Figure 4-39 present the interface screens of the SMADA software.

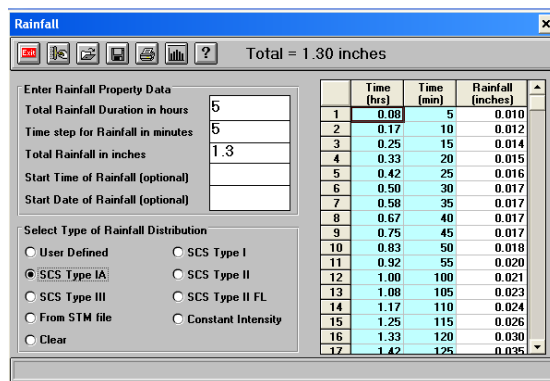


Figure 4-38 SMADA graphical user interface for determining storm pattern

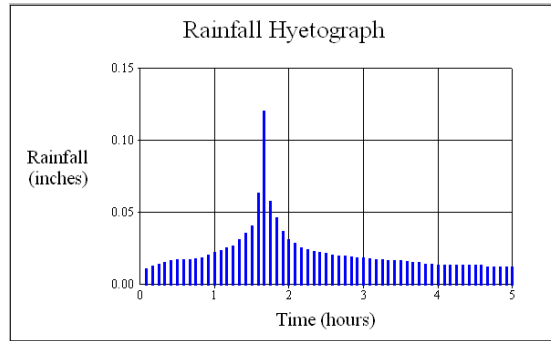


Figure 4-39 Rainfall hyetograph for storm pattern at Darselm rainfall station, based on pattern type IA

The pattern developed for Darselm rainfall station is presented in **Error! Reference source not found.** This storm pattern was used to calculate surface runoff and design hydrographs of basin outlets as part of the planning process for the surface water monitoring stations.

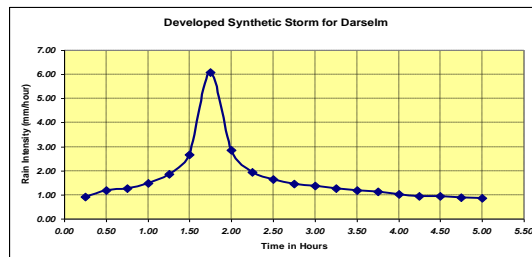


Figure 4-40 Synthetic storm for Darselm station (duration: 5 hours / intensity: 33 mm)

Chapter 5. DETERMINATION OF SUITABLE LOCATIONS FOR SURFACE WATER MONITORING IN THE SANA'A BASIN

5.1 Introduction

The next step in the study focused on determining the location of sagging points in the watershed where surface runoff water is most likely to accumulate to a depth that would allow accurate measurement. The previous step determined the streamline delineation and basin delineation, and this section builds on that information with more detailed study of each sub-basin and the determination of sagging points. This procedure involves several steps, as outlined in Figure 3-1 (Chapter 3). The following section outlines these steps.

5.2 Land Use Map

Digital maps for the entire basin and sub-basins were developed, based largely on collected data from previous studies including the Russian study (1986) and the WEC Study (2001). These maps indicate where cultivated lands and urban areas are located within the basin. Figure 5-1 presents a satellite image overlaid with the land use map for the Sana'a Basin. The land use maps for this study have been developed from this map. This type of digital imagery was converted to GIS using various programs, thus yielding a new GIS attribute image as presented in Figure 5-2.

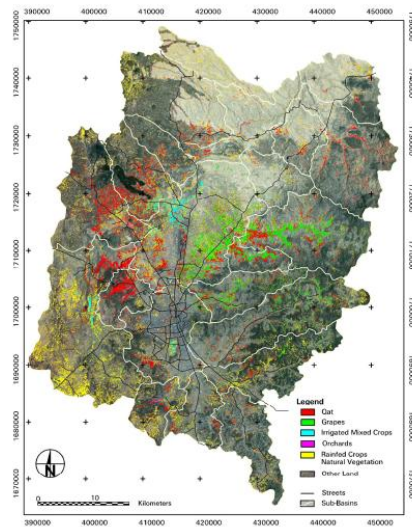


Figure 5-1 Latest available cropping pattern for the Sana'a Basin (2004/2005)
Source: GAFAG draft report

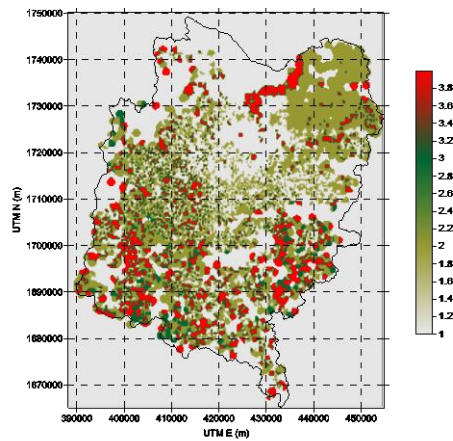


Figure 5-2 Converted digital map for identifying the cultivation density in the Sana'a Basin

5.3 Soil Map

The most important soil map for the Sana'a Basin was developed by the Russian study in 1986. Figure 5-3) is an image of the original map. In that study, soil type was categorized into 12 categories:

- **Type 1** soils are thick, of light loam with a medium loam texture, carbonaceous, solonetz-like and sporadically slightly saline.
- **Type 2** soils are thick, of light loam, medium loam and rarely of sandy loam texture, carbonaceous, mainly solonetz-like and sporadically slightly saline.
- **Type 3** soils are thick to medium thick, of light loam and medium loam texture, carbonaceous, sporadically slightly solonetz-like, saline, and have traces of compactness.
- **Type 4** soils are of thick loam texture, carbonaceous, solonetz-like, mostly saline, with compact horizon depths of more than 30-60 cm.
- **Type 5** soils are thick to medium thick, of loam and rarely clayey texture, carbonaceous, with sporadic traces of compactness.
- **Type 6** soils are thick, of light loam, medium loam and rarely sandy loam texture and carbonaceous.
- **Type 7** soils are thick to medium thick, of light loam and medium loam texture, carbonaceous, slightly eroded, cultivated, slightly solonetz-like, and sporadically slightly saline.
- **Type 8** soils are thick, carbonaceous, of light loam and medium loam texture.
- **Type 9** soils are thick to medium thick, of loam, rarely clayey texture, carbonaceous, sporadically slightly saline, slightly solonetz-like and with traces of compactness.
- **Type 10** soils are thick, of medium loam and rarely heavy loam texture, carbonaceous, artificially terraced, and solonetz-like with compact horizons depths of 30-60 cm.
- **Type 11** soils are rain-fed lands with insufficient moisture, making farming them practically impossible without regular irrigation.

- ***Type 12*** soils are undeveloped (rock outcrops on the surface in combination with immature soils) with a fine earth thickness of 5-30 cm, with high stone content and broken stone.

The WEC (2001) study revised the Russian study map to rectify its over-complexity and developed a new soil map integrating the twelve soil types presented above. The revised soil map is presented in Figure 5-4 (legend is represented in a separate map).

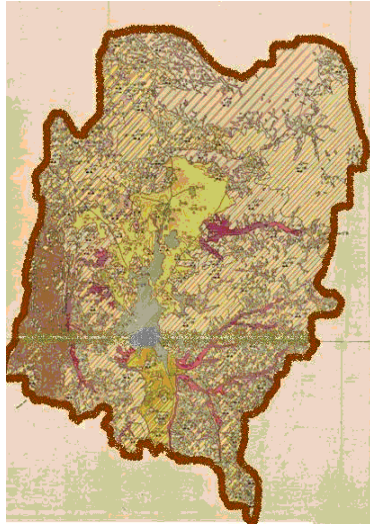


Figure 5-3 Soil map of the Sana'a Basin (Russian study, 1986)

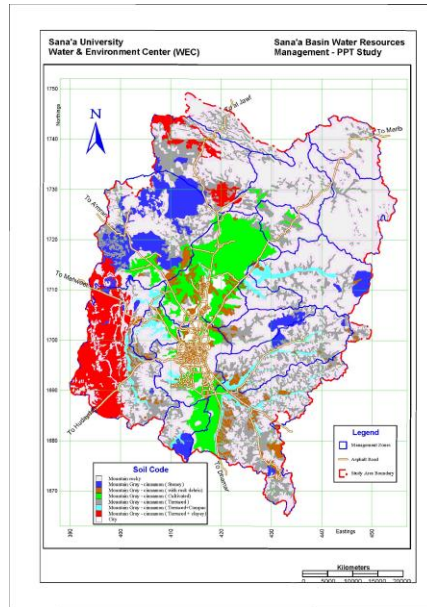


Figure 5-4 Revised soil map (WEC, 2001)

5.4 Determination of Surface Water Monitoring Station Locations

Following the procedure outlined in Figure 3-1 (chapter 3), the following figures were developed to propose locations for surface water monitoring station installation. Figures 104 to 125 present the preliminary locations selected for surface water monitoring stations in each of the 22 sub-basins of the Sana'a Basin. The main feature of this approach is its ability to examine the area as a compilation of individual sub-basins. The final goal of the simulation was to determine locations where water can be collected at reasonable depth for accurate measurement.

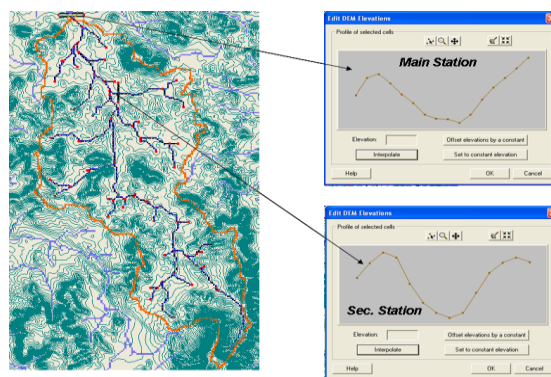


Figure 5-5 Locations of surface water monitoring stations along Wadi Sanhan

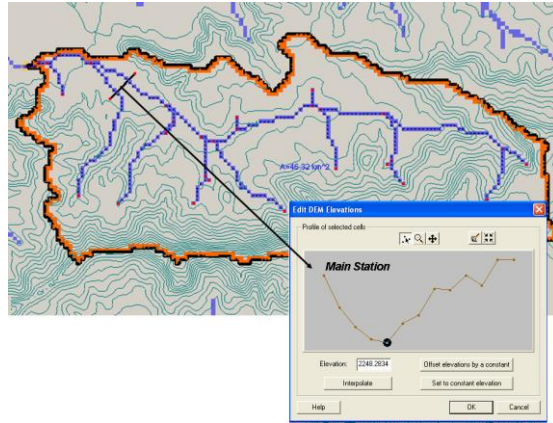


Figure 5-6 Locations of surface water monitoring stations along Wadi Al-Foros and Rjiam

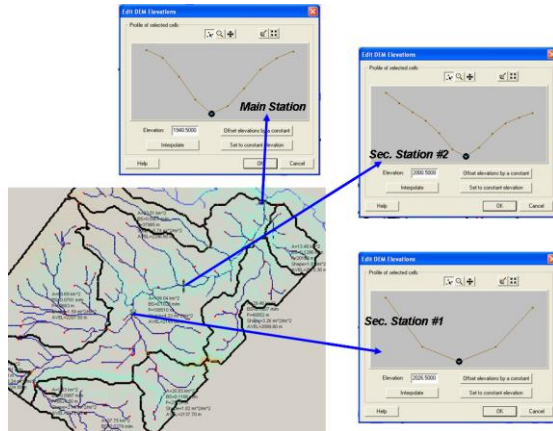


Figure 5-7 Locations of surface water monitoring stations along Wadi Al-Kharid

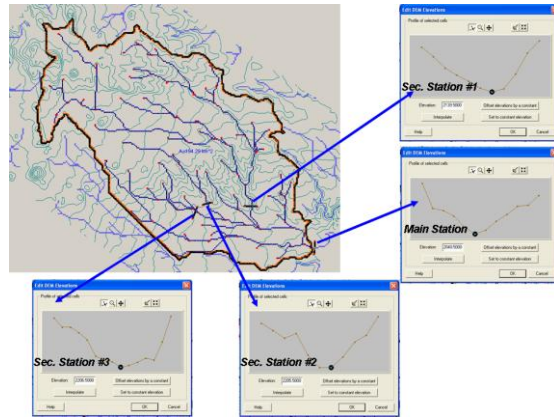


Figure 5-8 Locations of surface water monitoring stations along Wadi Madini and Al Ghulah

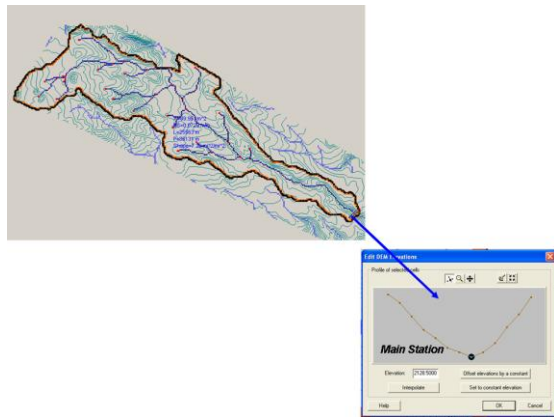


Figure 5-9 Locations of surface water monitoring stations along Wadi Madar and Al Mashamini

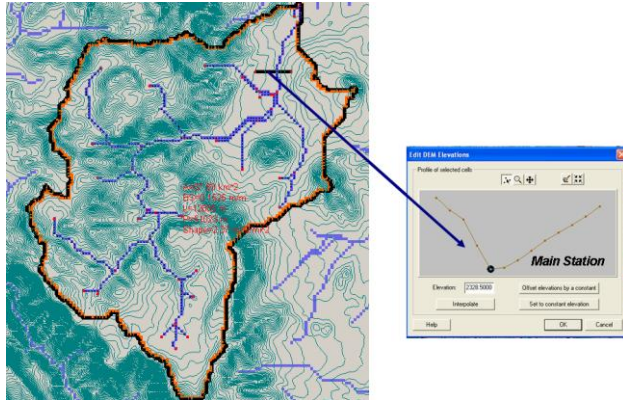


Figure 5-10 Locations of surface water monitoring stations along Wadi Mulaikhy and Hama

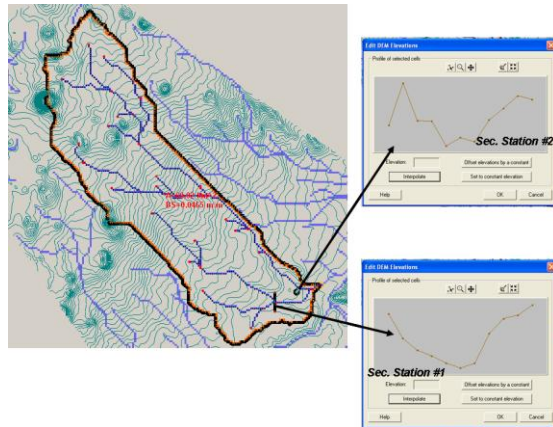


Figure 5-11 Locations of surface water monitoring stations along Wadi Al-Qassaba

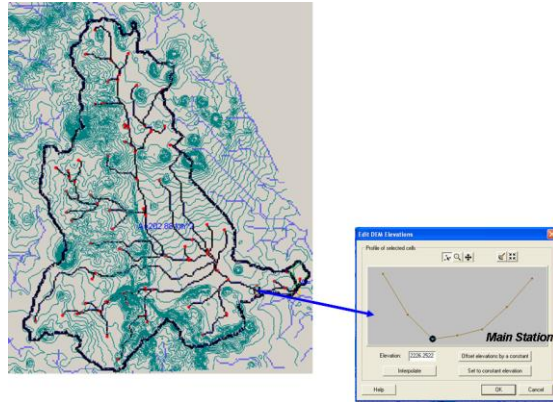


Figure 5-12 Locations of surface water monitoring stations along Wadi Iqbal and Ash Sha'b

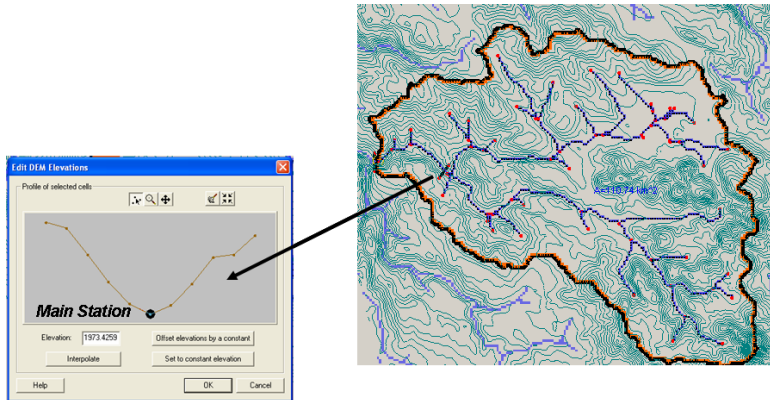


Figure 5-13 Locations of surface water monitoring stations along Wadi Al-Qatab and MA'adi

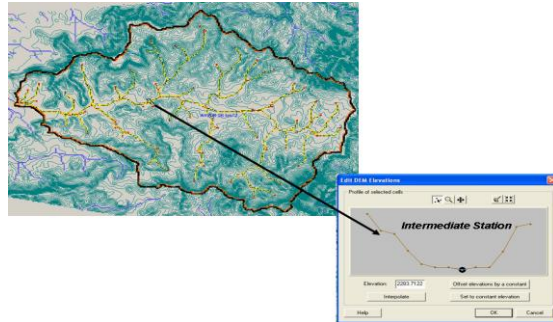


Figure 5-14 Locations of surface water monitoring stations along Wadi As-Sirr

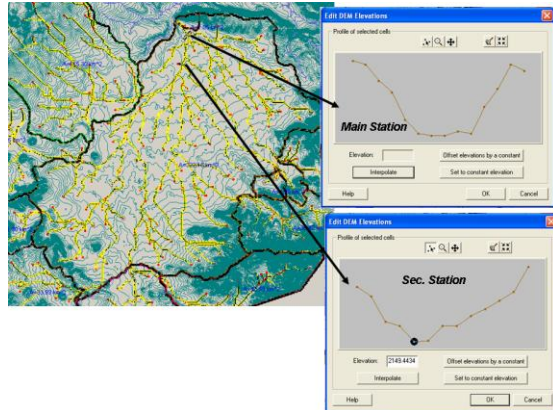


Figure 5-15 Locations of surface water monitoring stations along Wadi Bani Hawat

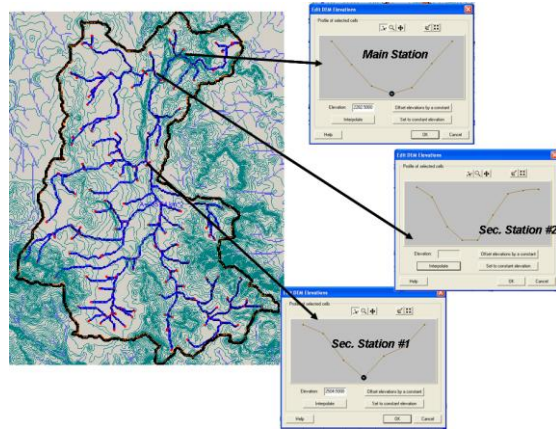


Figure 5-16 Locations of surface water monitoring stations along Wadi Zahr and Al Al-Ghay

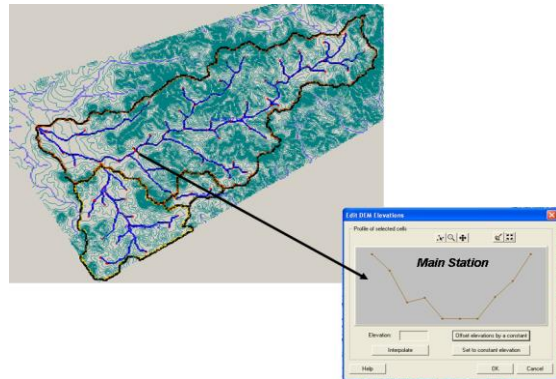


Figure 5-17 Locations of surface water monitoring stations along Wadi Ghayman

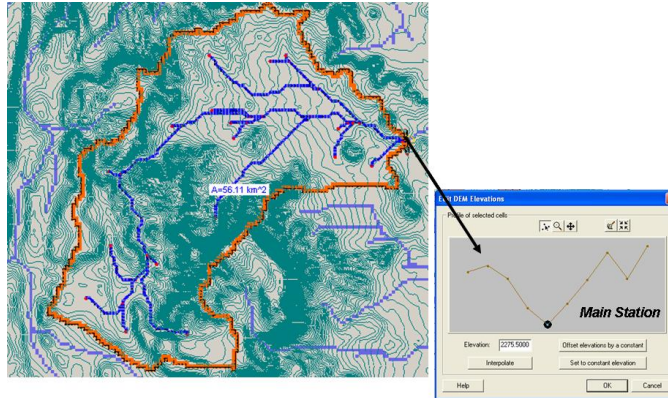


Figure 5-18 Locations of surface water monitoring stations along Wadi Hammadan and Al-Sabarah

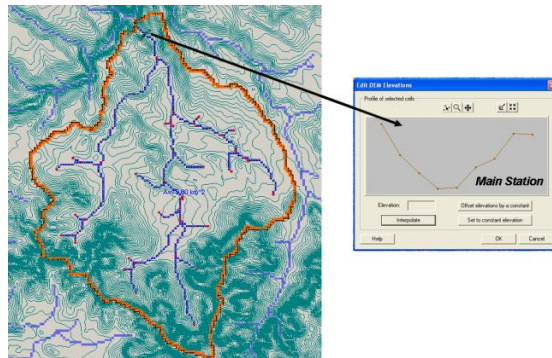


Figure 5-19 Locations of surface water monitoring stations along Wadi Khulaga

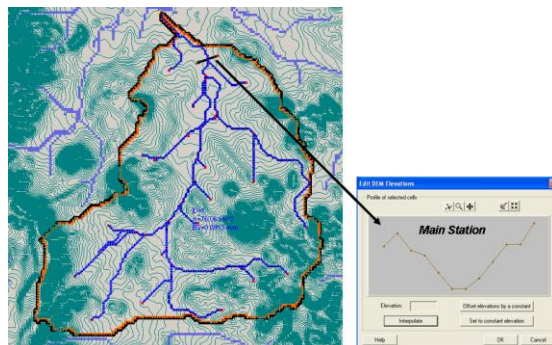


Figure 5-20 Locations of surface water monitoring stations along Wadi Hizayaz

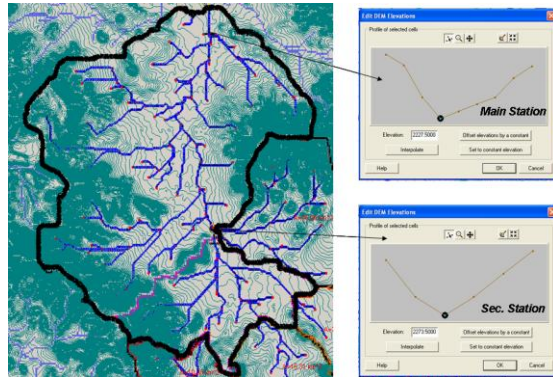


Figure 5-21 Locations of surface water monitoring stations along Wadi Mawrid and Al-Ishash and Hyad

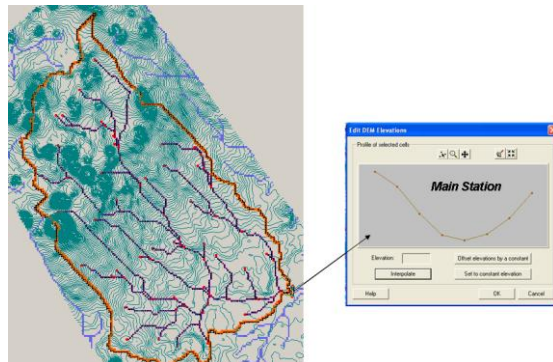


Figure 5-22 Locations of surface water monitoring stations along Wadi Yahis and Al Haqqah

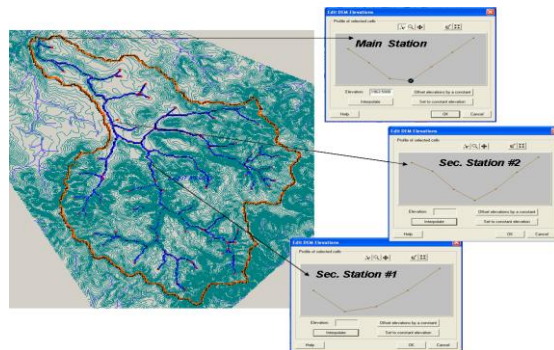


Figure 5-23 Locations of surface water monitoring stations along Wadi Lafaf and Asir

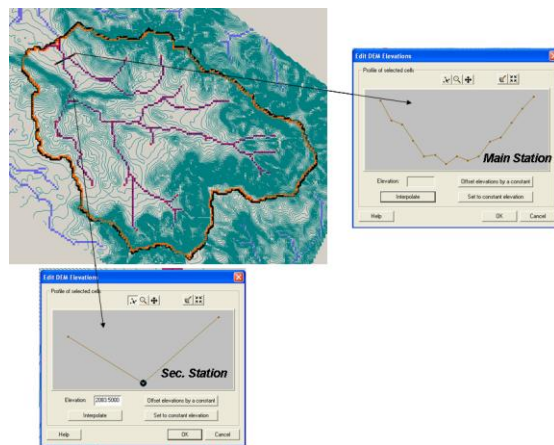


Figure 5-24 Locations of surface water monitoring stations along Wadi Thuma and Shira

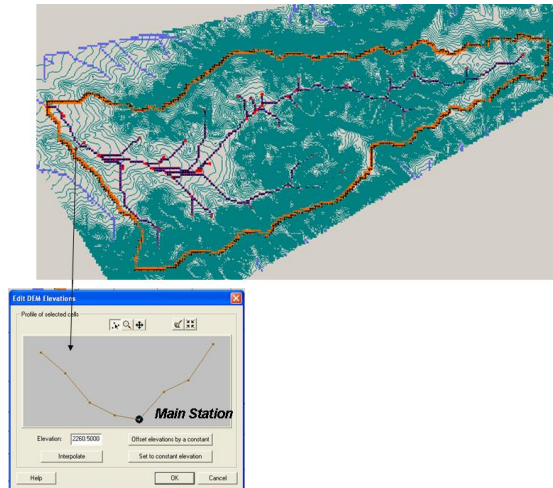


Figure 5-25 Locations of surface water monitoring stations along Wadi Sa'wan and Rawnah

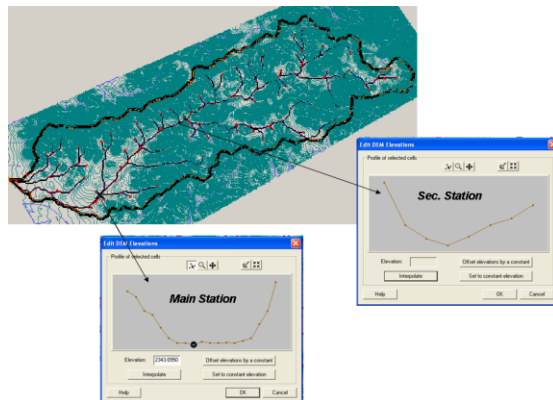


Figure 5-26 Locations of surface water monitoring stations along Wadi Shahik and Al Ajbar and Sha'b

Chapter 6. FIELD VISITS AND FINAL SELECTION OF SURFACE RUNOFF MONITORING STATIONS

6.1 Determination of Locations for Surface Water Monitoring Stations

The preliminary study presented in Chapters 4 and 5 determined a projected location for one monitoring station along each sub-basin. Field visits to the sub-basins were then performed in order to verify these proposed locations. During the field visits, stream-crossing structures were discovered at

some locations that would be considered ideal locations for monitoring station installation. On the other hand, other locations visited were laid out in such a way that the installation of monitoring stations would be difficult or even not feasible. Final locations selected for surface runoff monitoring stations are located on the following wadis/structures:

- Wadi Sanhan,
- Wadi Ghayman,
- Wadi Shahik,
- Wadi Sa'awan,
- Wadi Al Furs,
- Wadi Al-Sirr,
- Wadi Thumah,
- Wadi Khulaga,
- Wadi Mawrid,
- Wadi Miliki,
- Wadi Iqbal,
- Wadi Zahr,
- Wadi Hizayaz,
- Wadi Al-Kharid,
- Al-Kharid Bridge,
- Wastewater Passage,
- At Al-Kharid Bridge.

Figures 126 through 259 present photographs of the selected locations. Each station is documented by photographs overlaid with dimensions. A brief description of each station is presented below.

6.2 Surface Runoff Monitoring Station for Wadi Sanhan

Wadi Sanhan is located in the south-eastern part of the Sana'a Basin as highlighted in Figure 126. Two locations for surface runoff measurements were preliminarily selected based on the spatial analysis performed for this wadi. The first selected site is located in the lower third of the wadi main channel after all the tributaries intersect with the main channel. The second selected site is located almost at the outlet point of the wadi Sanhan. Field visits to the proposed locations revealed that the second site is the most appropriate. At this location, a culvert crosses the main channel of the wadi under an asphalt road. The culvert consists of five circular openings, each with an internal diameter of one meter. The total culvert width is 14.0 meters and the culvert's height is 2.75 meters. The upstream configuration is a flat expanse of land with traces of scattered cultivation. The upstream channel slope is relatively small and the bed consists of fine silt with almost no gravel or boulders. Figures 127 through 133 present field visits photographs for the selected location at Wadi Sanhan. It is proposed that a weir be constructed at the downstream side of the culvert. The weir would be installed flush with the solid apron of the culvert. An ultrasound water level instrument would be installed to measure water level at the weir location.

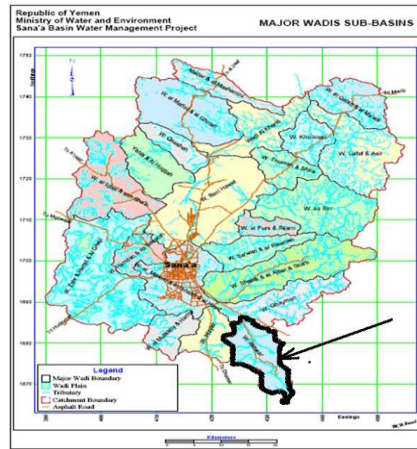


Figure 6-1 Location of Wadi Sanhan within the Sana'a Basin (black boundary)

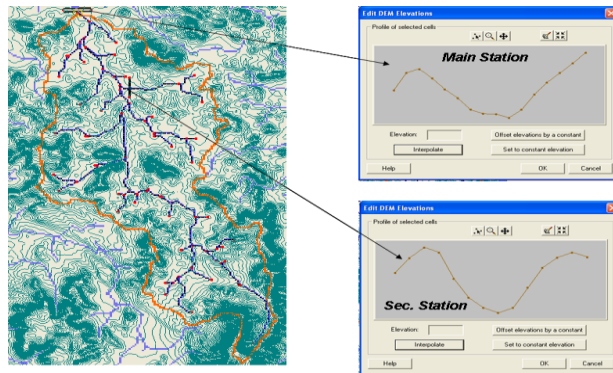


Figure 6-2 Proposed locations of surface water monitoring stations along Wadi Sanhan through the streamline delineation analysis

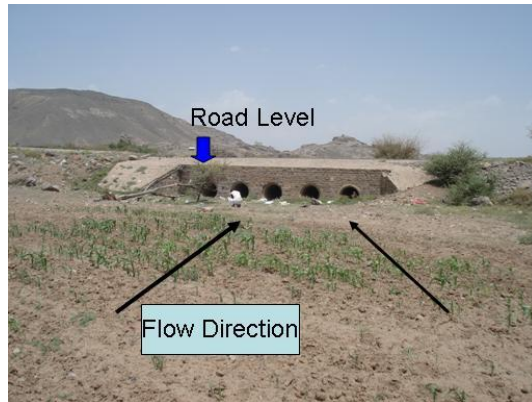


Figure 6-3 View of the crossing structure under the highway at the outlet of Wadi Sanhan where the main monitoring station is located. UTM coordinates are: Left side UTME=426052 and UTMN=1685774 and Right Side UTME=426055 and UTMN=1665790, the section is at elevation 2355 m (AMSL)

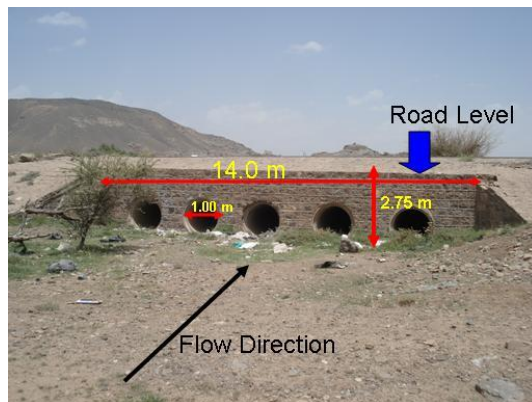


Figure 6-4 Dimensions of the crossing structure at the main monitoring station for Wadi Sanhan



Figure 6-5 View of the land surface upstream of the crossing structure



Figure 6-6 Side view of the crossing structure at the location of the main monitoring station in Sanhan

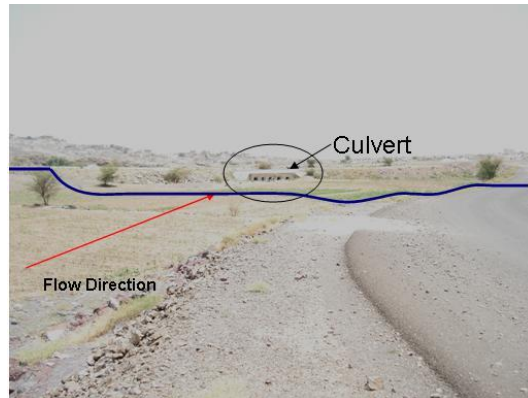


Figure 6-7 Long view of the stream and the crossing structure



Figure 6-8 Proposed location for the staff and data logger instrument (wide arrow with brick filling)

6.3 Surface Runoff Monitoring Station for Wadi Ghayman

Wadi Ghayman is located in the south-eastern part of the Sana'a Basin as shown in Figure 134. Spatial-GIS stream delineation for Wadi Ghayman is presented in Figure 135. Upon examination of the digital maps developed for this region in section 5.4, only one suitable location was found for surface runoff measurements, at a point where a reliable cross-section could be established. However, the selected point was not optimum since it is located upstream of two large streams that intersect with the main Wadi system. After this point of intersection, the wadi starts to widen and leads to a sheet flow over the main streambed, rendering surface runoff flow measurements very difficult. During the field visit, to Wadi Ghayman, it was determined that the best location for the surface water runoff measurement would be on the upstream face of the dam, which is located at the outlet point of the Ghayman basin. Monitoring the water level inside the dam lake would be an appropriate way to approximate the Ghayman sub-basin. Figures 136 through 138 present photographs of selected locations for installation of the surface runoff station in Wadi Ghayman.

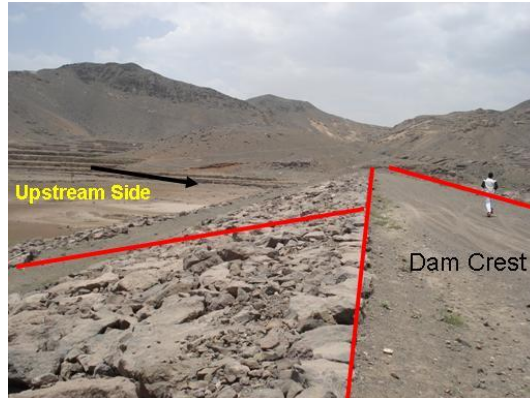


Figure 6-11 General view of the Ghayman Dam that is located at the outlet of the Ghayman sub-basin - this is the preferred location for the monitoring station of Wadi Ghayman

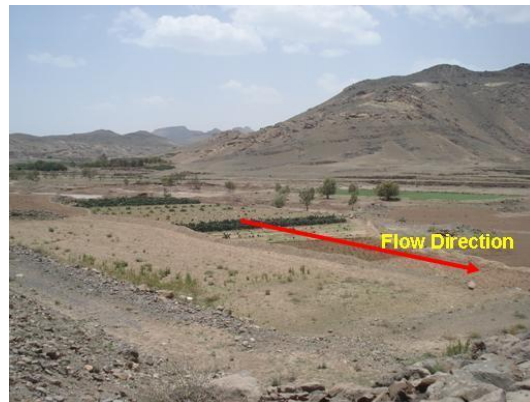


Figure 6-12 Upstream view of the dam showing the cultivation in the area



Figure 6-13 Proposed location for staff gage and data logger instrument (arrow with brick pattern) in the upstream of Ghayman dam

6.4 Surface Runoff Monitoring Station for Wadi Shahik

Wadi Shahik is located in the eastern portion of the Sana'a Basin. The wadi is highlighted in Figure 139. Spatial analysis and streamline delineation show that the wadi consists of two major streams starting in the east and running west. Two sections were selected as potential sites for surface runoff measurement stations and field visits were conducted to select the most appropriate site. The first location, in the western side of the Wadi (Figure 140) was found to be relatively wide, as shown in Figure 141. The wadi outlet channel runs through permanently cultivated land as shown in Figure 142. Thus, this location was not considered for the surface runoff station. Another location, located far upstream of the basin outlet, was pinpointed as more appropriate. The proposed section is spanned by a road culvert located at the selected cross-section. The culvert consists of five openings, each with a 2.5 x 2.5 m square opening. The total culvert width is 13.20 m. The upstream view of the stream shows that the cross-section is naturally developed with a grass-covered bed. The grass height is in the range of 20 to 40 cm. The right side slope of the section is almost vertically cut while the left side slope has the shallow slope of a floodplain. The downstream view shows the same floodplain configuration. Figures 143 through 147 are field visit photographs of the proposed Wadi Shahik surface runoff station. It is proposed that a weir be constructed downstream of the culvert, to be installed flush with the solid apron of the culvert. An ultrasound water level instrument would then be installed to measure water level at the weir location in the same configuration as that of Wadi Sanhan station.

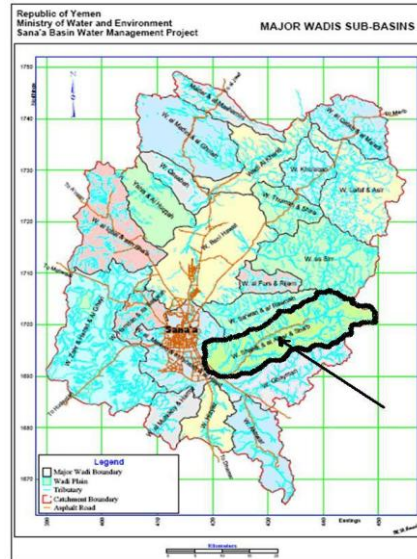


Figure 6-14 Location of Wadi Shahek within the Sana'a Basin (black boundary)

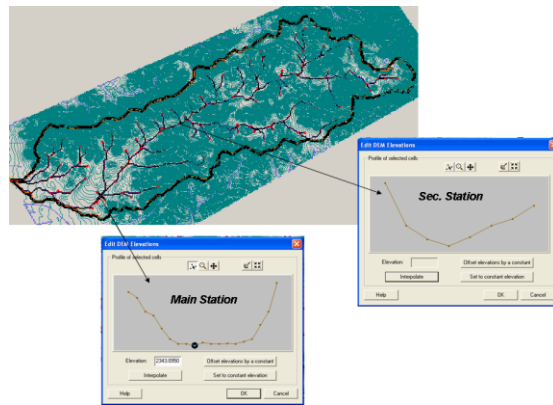


Figure 6-15 Proposed locations of surface water monitoring stations along Wadi Ghayman through the streamline delineation analysis

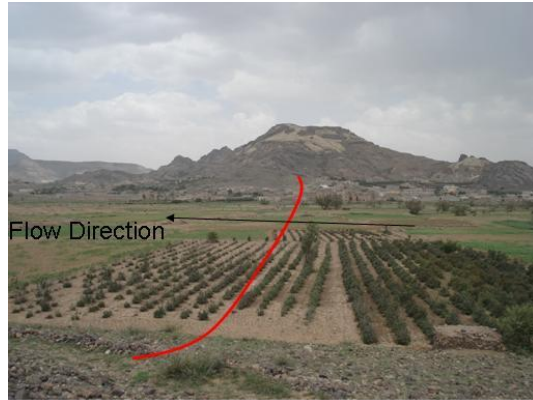


Figure 6-16 Configuration of the location of the first selected monitoring station site in Wadi Shahek (deemed inappropriate for installation of a monitoring station)

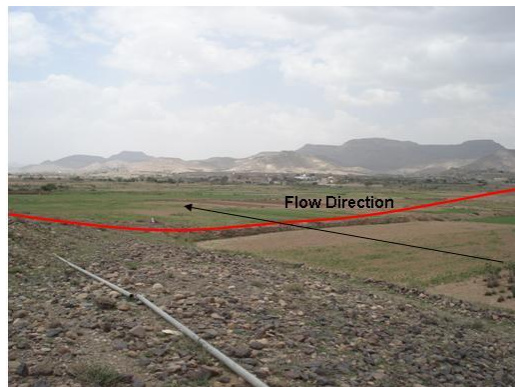


Figure 6-17 Downstream configuration of the first selected monitoring station site in Wadi Shahek (deemed inappropriate for installation of a monitoring station)

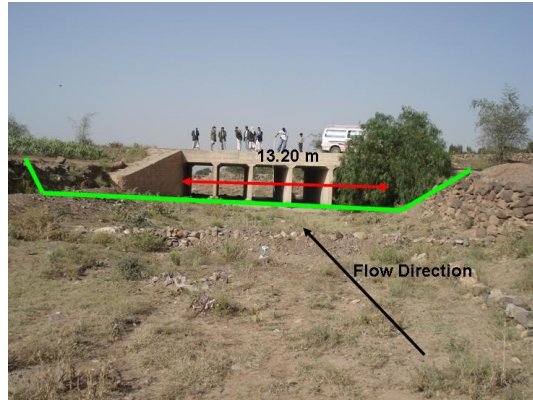


Figure 6-18 Final proposed location for Wadi Shahek surface runoff station. Coordinates are: left point UTM E 427870 and UTM N 1696144, right point UTM E 427874 and UTM N 1696131



Figure 6-19 Dimensions of the culvert openings for the selected location at Shahik

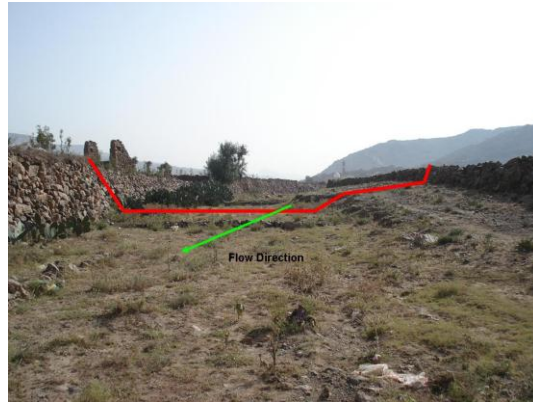


Figure 6-20 Upstream view of the final proposed location for surface water monitoring station



Figure 6-21 Proposed location for the surface runoff station at Wadi Shahek

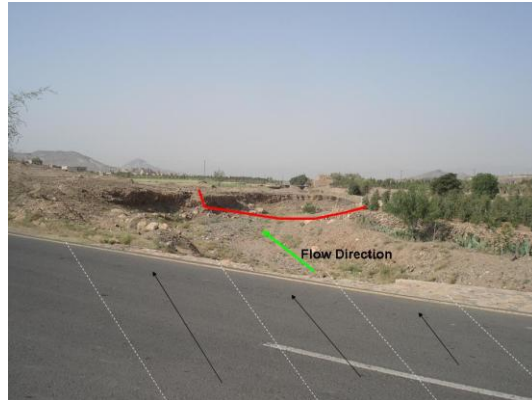


Figure 6-22 Downstream view from the proposed station showing the cross-section of the downstream area and the culvert alignment under the road

6.5 Surface Runoff Monitoring Station for Wadi Sawan

Wadi Sa'awan is located in the eastern side of the Sana'a Basin, as highlighted in Figure 148. The stream network of Wadi Sa'awan (Figure 149) consists of only one major stream until the lower third of the wadi, where six tributaries are found. The outlet of the basin was selected from the spatial analysis to be the most feasible location for the monitoring station. During a field visit to the proposed location, the cross-section at this point was found to be 25 meters in width and 2.5 meters in depth. The upstream bed surface is flat, as shown in Figure 151. The bed surface consists of coarse gravel with a mean diameter, d_{50} , of 20 cm as shown in Figure 153. Figures 150 through 154 were taken during the field visit, at this location. It was proposed to install at this site a wadi gage station equipped with a shaft encoder that can be float operated, or connected to servo mechanical sensors and chart recorders.

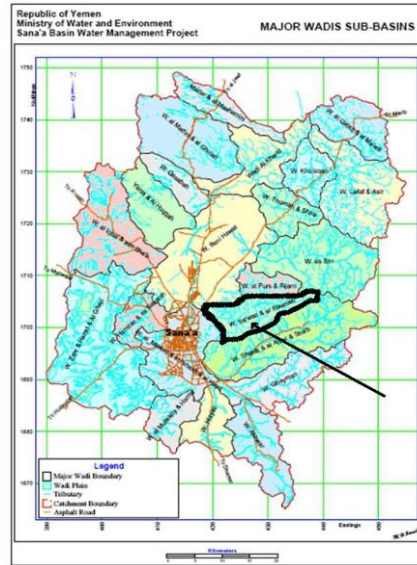


Figure 6-23 Location of Wadi Sawan within the Sana'a Basin (black boundary)

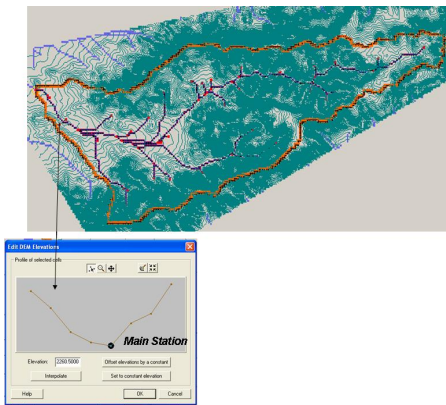


Figure 6-24 Proposed locations of surface water monitoring stations along Wadi Sawan through the streamline delineation analysis

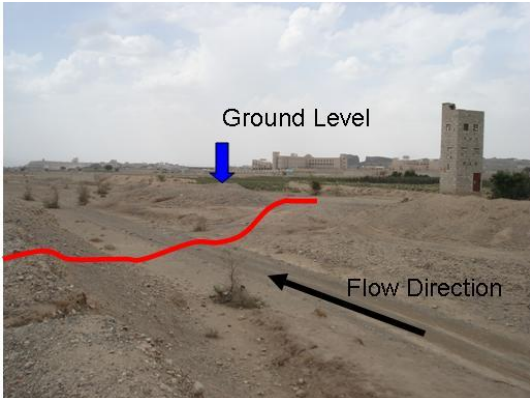


Figure 6-25 Cross-section at the location of the proposed monitoring station

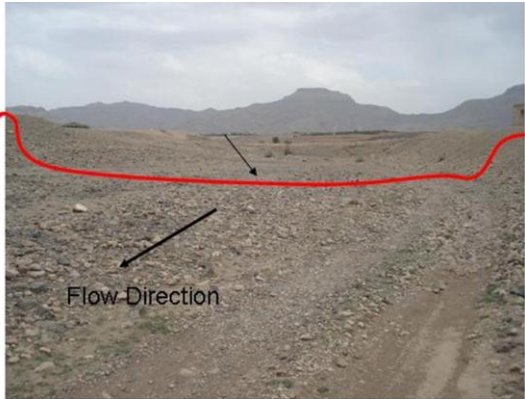


Figure 6-26 Upstream streambed view of the Wadi Sawan floodway



Figure 6-27 Downstream streambed view of the Wadi Sawan floodway



Figure 6-28 Sediment gradation at the selected monitoring station location



Figure 6-29 Proposed location for staff gage and data logger instrument (arrow with brick pattern) at the outlet stream of Wadi Sawan

6.6 Surface Runoff Monitoring Station for Wadi Al-Foros

Wadi Al-Foros is located in the central part of the Sana'a Basin, (Figure 155). The total area of this wadi is 46 km². The spatial analysis stream delineation results show that the wadi has a main stream that flows from east to west. In addition, there are six secondary streams that intersect the main stream. Based on spatial analysis and using the digital elevation map, the proposed location for installing the surface runoff station is illustrated in Figure 156. During the field visit, it was determined that the ideal location would, in fact, be a little downstream of the originally selected section. A culvert consisting of two openings, each 2.8 meters wide and 1.8 meters deep (Figure 158), has been found at the proposed location, as shown in Figure 157. The total width of the culvert is 6.8 meters. The upstream bed is irregularly shaped with scattered weeds and a water supply pipeline, as presented in Figures 159 through 163. The bed surface consists of fine gravel with a d50 of approximately 6 mm.

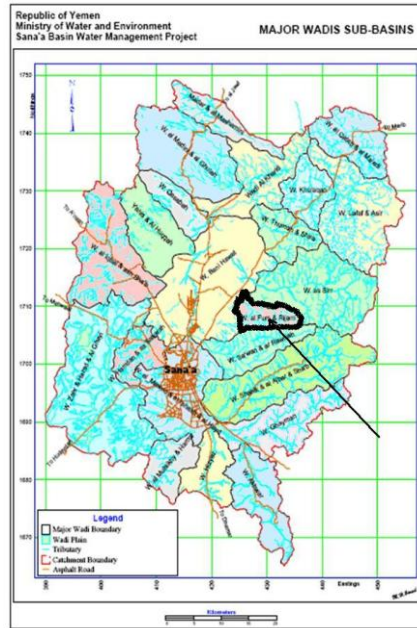


Figure 6-30 Location of Wadi Al-Foras within the Sana'a Basin (black boundary)

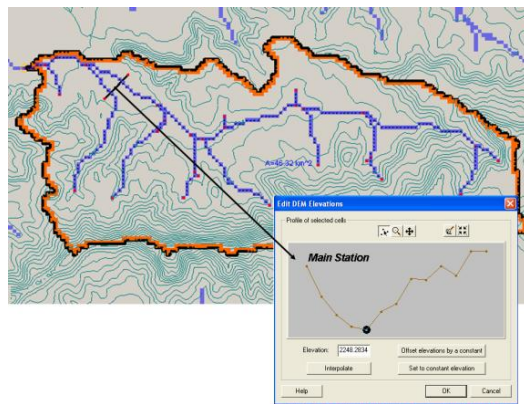


Figure 6-31 Proposed locations for surface water monitoring stations along Wadi Foros through the streamline delineation analysis



Figure 6-32 Culvert at the highway intersection near the outlet of Wadi Al-Foros. Flow direction is shown with red arrows. UTM coordinates for this location are UTME=426000 and UTM N =1710625, at an elevation of 2274 m (AMSL)



Figure 6-33 Dimensions of culvert openings



Figure 6-34 Upstream view from crossing structure

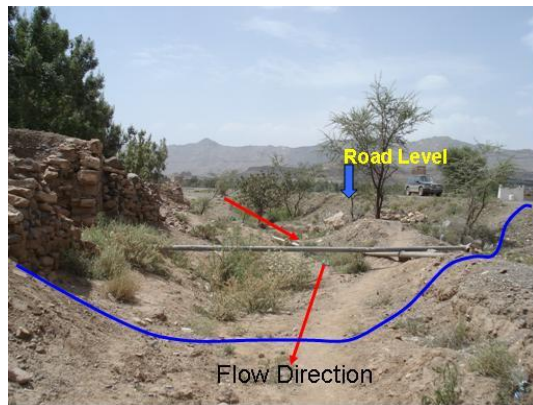


Figure 6-35 Upstream view showing shape of stream cross-section



Figure 6-36 Long view showing location of crossing structure (red circle) and flow direction (black arrows)



Figure 6-37 Sediment gradation of streambed upstream of crossing structure



Figure 6-38 Proposed location for staff gage and data logger instrument (arrow with brick pattern) upstream of crossing structure at Wadi Al-Foros outlet

6.7 Surface Runoff Monitoring Station for Wadi Al-Sirr

Wadi Al-Sirr is a relatively large wadi, with a total area of 206 km² (Figure 164). Spatial analysis shows the stream network to consist of one main stream intersected by about 20 secondary streams. It was determined that the most appropriate location for the monitoring station would be in the lower fifth section of the main stream. A final location for the station was assigned during a field visit to Wadi Al-Sirr main stream. The cross-section at this point is rectangular with a plain bed, and the bed surface consists of coarse to medium sand. Figures 166 through 170 present several photographs of the selected location. It was proposed to install a wadi gauge station equipped with a shaft encoder that can be float-operated or connected to servo mechanical sensors and chart recorders.

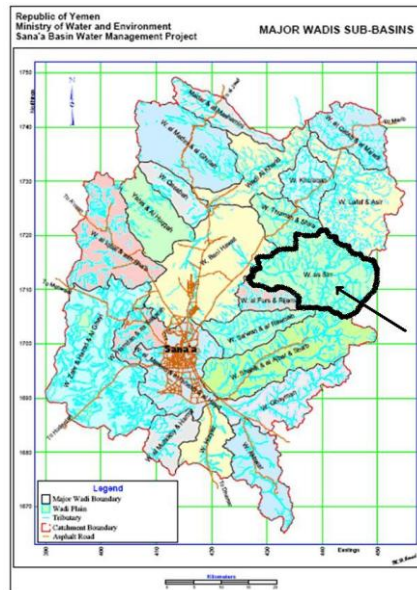


Figure 6-39 Location of Wadi Al-Sirr within the Sana'a Basin (black boundary)

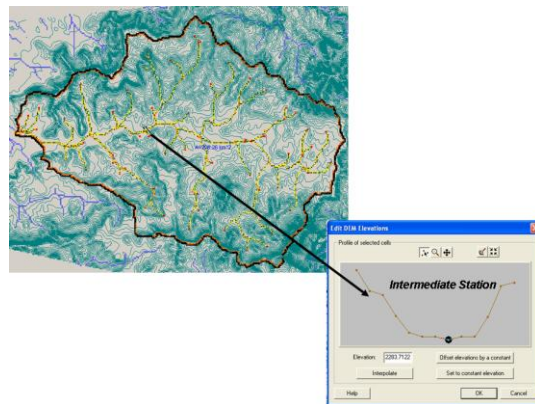


Figure 6-40 Proposed locations of surface water monitoring stations along Wadi Al-Sirr through streamline delineation analysis



Figure 6-41 The exiting station installed by component 2. Coordinates of this staff are **UTME=423849** and **UTMN=1713362**, at an elevation of **2253 m (AMSL)**

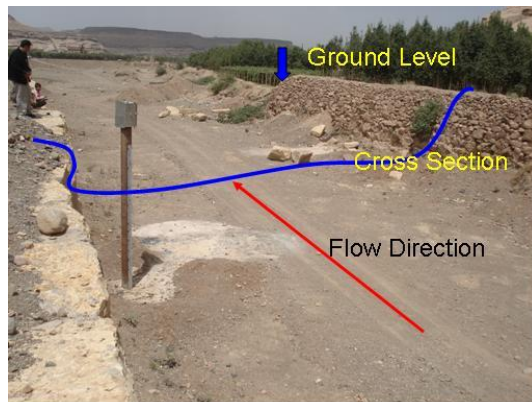


Figure 6-42 Flow direction, cross-section configuration and ground level at the gage location



Figure 6-43 Upstream view of streambed at gage location



Figure 6-44 Sediment gradation at gage location



Figure 6-45 Proposed location for staff gage and data logger instrument (arrow with brick pattern) in main stream of Wadi Al-Sirr floodway

6.8 Surface Runoff Monitoring Station for Wadi Thomaa

Wadi Thomaa is located in the north-eastern part of the Sana'a Basin, highlighted in Figure 171. Spatial analysis shows that the wadi consists of four major streams, which converge into one main channel near the outlet point. Thus, from the digital elevation map, it was determined that the best location for a surface runoff station would be very close to the basin outlet point. The site visit showed that the cross-section is naturally developed as a common natural channel. The cross-section at this point is irregular; the left bank is higher than the right bank by about 3.0 meters. The total cross-section top width is 32.80 meters and the depth starts at 2.0 meters on the right side and decreases to less than 1.0 meter on the left edge (Figure 175). The bed surface consists of coarse gravel and boulders with a mean diameter of 20 cm, interspersed with scattered areas of medium sand (Figure 178). The upstream streambed portion of the channel is covered with coarse gravel and fine boulders, forming braided channels. The expected roughness at this site will be relatively high, based on Chow (1959). Figures 173 through 180 present other views of this location. It is proposed to install a wadi gauging station equipped with a shaft encoder that can be float operated or connected to servo mechanical sensors and chart recorders.

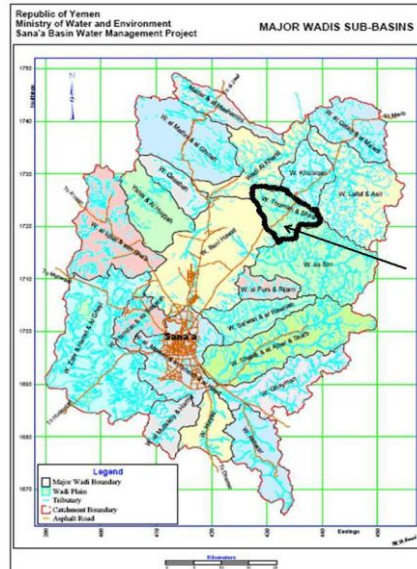


Figure 6-46 Location of Wadi Thoma within the Sana'a Basin (black boundary)

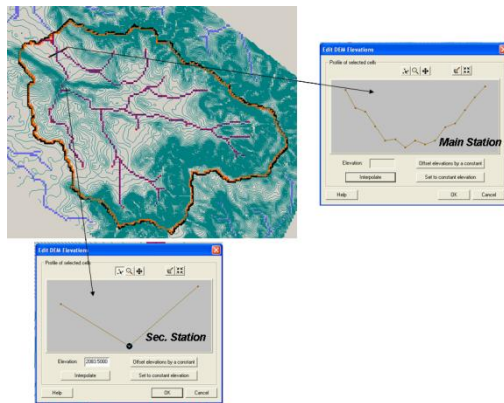


Figure 6-47 Proposed locations of surface water monitoring stations along Wadi Thoma through the streamline delineation analysis



Figure 6-48 General view of the cross-section at the monitoring station location

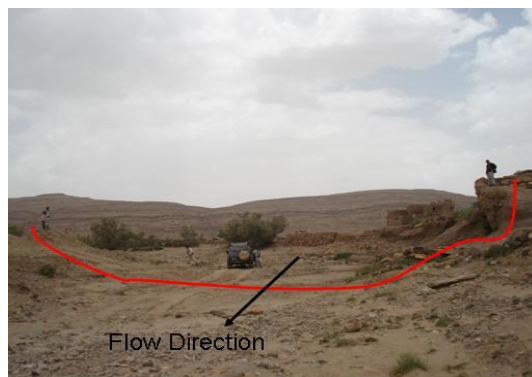


Figure 6-49 Cross-section selected for installation of the staff gage (red curve).
Coordinates of the sides are: left side UTME=428835 and UTMN=1726392, at an elevation of
2064

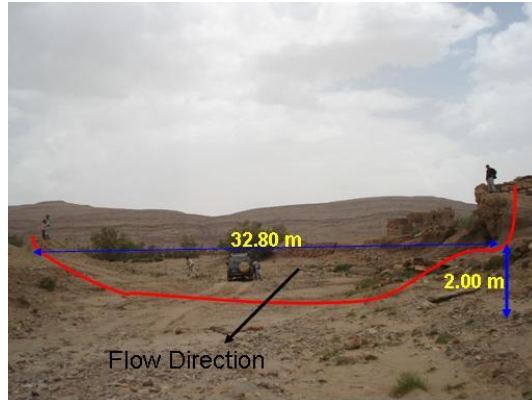


Figure 6-50 Cross-section dimensions measured in the field

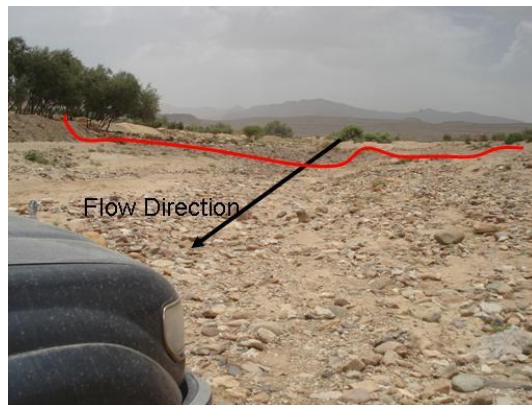


Figure 6-51 Upstream view of the stream bed configuration



Figure 6-52 Top view of the selected cross-section



Figure 6-53 Sediment gradation at cross-section location



Figure 6-54 Sediment gradation at cross-section location

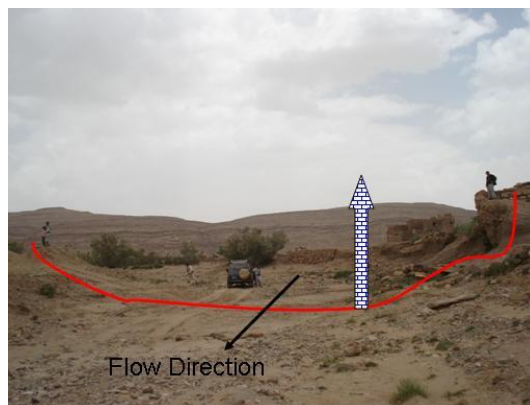


Figure 6-55 Proposed location for staff gage and data logger instrument (arrow with brick pattern) in main stream of Wadi Thoma floodway

6.9 Surface Runoff Monitoring Station for Wadi Khulaga

Spatial analysis using the digital elevation map indicates that the Wadi Khulaga stream network consists of four main streams, with a total area of 75 km² (Figure 181). Two major streams intersect on the upstream side of the wadi, forming one main stream, then another major stream joins the group further down. The last major stream intersects with the main stream close to the basin outlet point, as shown in Figure 182. The proposed location for the surface runoff station is very close to the basin outlet. During the field visit, it was found that a large culvert intersects with the highway at the proposed location. The culvert consists of four openings, each 4.0 m x 3.8 m with a length of 15.0 meters. The total width of the culvert is 15.20 m. The upstream bed consists of fine sand as shown in Figure 191. The upstream cross-section is rectangular with some scattered trees (Figure 184). Figures 183 through 192 present different views of the selected location. It was proposed that a weir be constructed on the downstream side of the culvert. The weir would be attached flush with the solid apron of the culvert. An ultrasound water level instrument would then be installed to measure water level at the weir location in the same configuration as that of the Wadi Sanhan station.

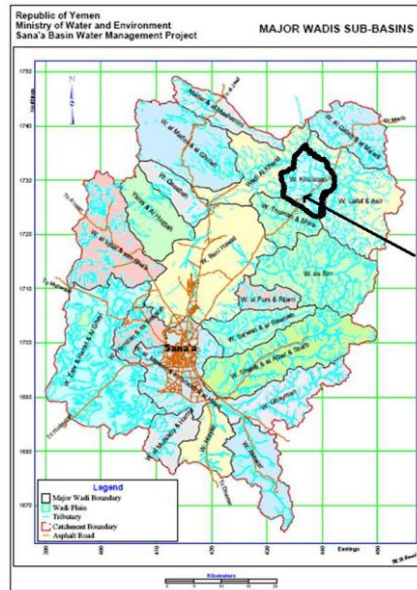


Figure 6-56 Location of Wadi Khulaga within the Sana'a Basin (black boundary)

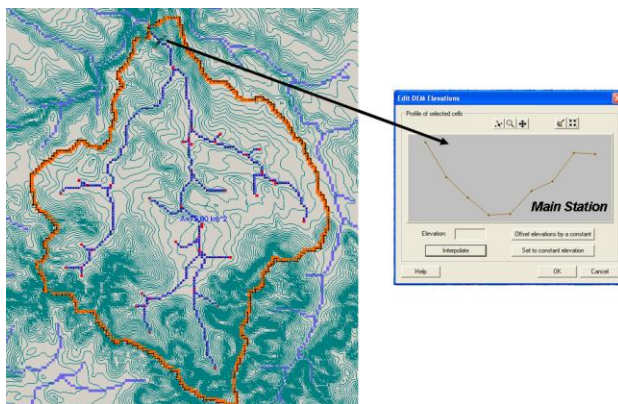


Figure 6-57 Proposed locations of surface water monitoring stations along Wadi Khulaga through the streamline delineation analysis

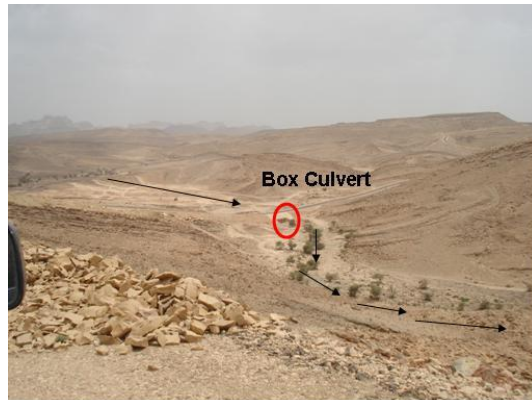


Figure 6-58 Top view showing location of the crossing structure at the intersection of Wadi Khulaga main floodway and a highway

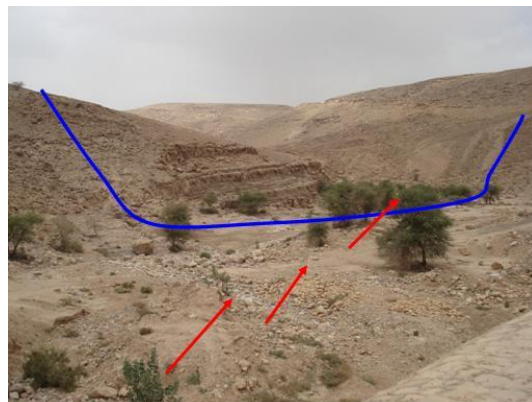


Figure 6-59 Downstream view of the wadi after passing the crossing structure



Figure 6-60 Front view of the box culvert structure at the intersection of the Wadi Khulaga main floodway and a highway. Coordinates of the crossing structure are: for the left side: UTME=437089 and UTMN=1734937, and for the right side: UTME=437117 and UTMN=1734951, at an elevation of 1925 m (AMSL)



Figure 6-61 View of the highway and the downstream side of the floodway



Figure 6-62 Upstream view of the crossing structure



Figure 6-63 Dimensions of the box culvert



Figure 6-64 Depth of the culvert opening

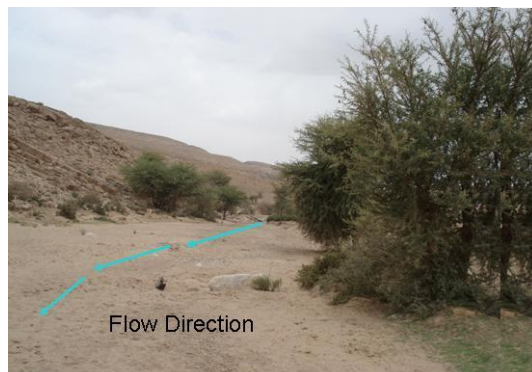


Figure 6-65 Upstream view of the main floodway streambed and surrounding environment



Figure 6-66 Sediment gradation of the stream bed



Figure 6-67 Proposed location for staff gage and data logger instrument (arrow with brick pattern) in the main stream of Wadi Khulaga floodway

6.10 Surface Runoff Monitoring Station for Wadi Mawrid

Wadi Mawrid covers the entire area of Sana'a City, as highlighted in Figure 193. It starts near the south boundary of the city and ends at the west, north and east city boundaries. The City of Sana'a has a storm water collection system that collects all the excess rainfall water from the south, east and west regions into a major storm drain canal that runs across the city from south to north. The collected water is then transferred northward to Wadi Hawat, very close to the city airport. The storm water collection channel is a trapezoidal/rectangular open channel with a paved bed and side walls covered with stone (Figure 194). Spatial analysis will not be used with the same reliability to study the delineated

streamlines within the city boundaries since urbanization makes for unpredictable slopes and flow directions. Spatial analysis detail is presented in Figure 46 and 47 (Chapter 4). Thus, a city road bridge has been selected to be the location of flow measurement for Wadi Mawrid. The upstream view from the selected location is shown in Figure 194, and the downstream view in Figure 195. The selected location is within about 1-2 km of the end of the city's storm water canal, where the channel starts to widen with an unidentified cross-section. In addition, this location is close to the northern boundary of the city, which means that the water volume represents most of the collected water from the city storm drain system within the boundary of Wadi Hawat. Figures 196 and 197 present different views of the selected site. The bridge has two openings, with a total cross-sectional width of 16.80 meters. The channel depth at this location is 3.20 meters. The proposed installation at this point will include a wadi gage station equipped with a shaft encoder that can be float operated or connected to servo mechanical sensors and chart recorders.

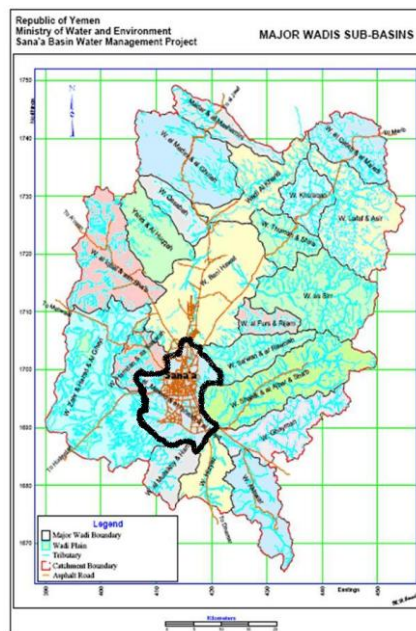


Figure 6-68 Location of Wadi Khulaga within the Sana'a Basin (black boundary)

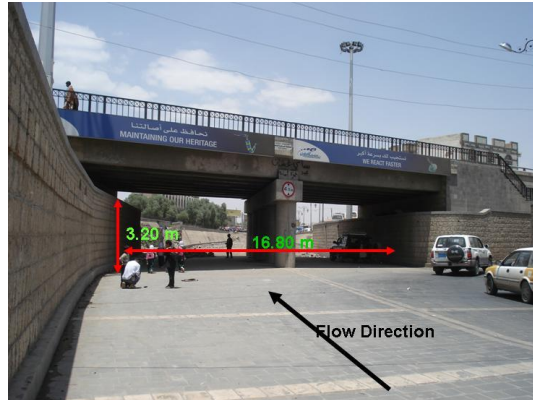


Figure 6-69 Front view of the bridge at Wadi Mawrid where the surface runoff station is proposed. Coordinates of the crossing structure are: left side UTME=415475 and UTMN=1700396, and right side: UTME=415496 and UTMN=1700393, at an elevation of 2255 m (AMSL)



Figure 6-70 Downstream view from the bridge



Figure 6-71 During the measuring of bridge dimensions



Figure 6-72 Upstream view from the bridge

6.11 Surface Runoff Monitoring Station for Wadi Miliki

Wadi Miliki is located in the southern part of the Sana'a Basin as shown in Figure 198. The total area of this wadi is 68 km². Spatial analysis and streamline delineation show that the wadi has one major stream that extends from south to north, that near the middle is diverted 90 degrees towards the east. Then, in the lower third of the wadi, it once again begins flowing from south to north. The digital elevation map shows that the optimum location for the surface runoff station would be close to the outlet of the basin. During the site visit, it was discovered that there is a road culvert close to the selected site at the intersection between a highway and the wadi. The culvert consists of four circular openings, each of which is 1.16 m in diameter. The total width of the culvert is 11.40 m, with a depth of 2.0 m. The upstream area of the channel is cultivated land, flat with some scattered trees. Figures 199 through 202 present some views of the selected site. All the water collected from Wadi Al-Miliki runs across this culvert. It is proposed to construct a weir on the downstream side of the culvert. The weir would be installed flush with the solid apron of the culvert. An ultrasound water level instrument would then be installed to measure water level at the weir location.

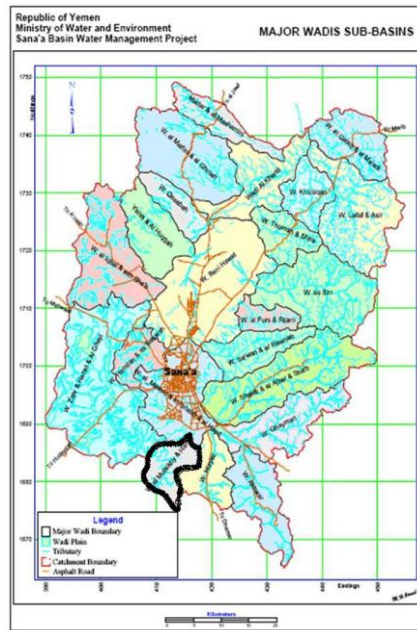


Figure 6-73 Location of Wadi Miliki within the Sana'a Basin (black boundary)

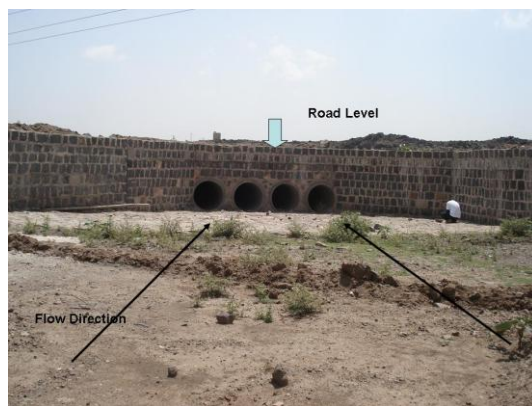


Figure 6-74 Front view of the culvert at the highway intersection. Coordinates of the crossing structure are: UTME=415755 and UTMN=1686539, at an elevation of 2331m (AMSL)



Figure 6-75 View of the upstream area in front of the culvert



Figure 6-76 Culvert dimensions

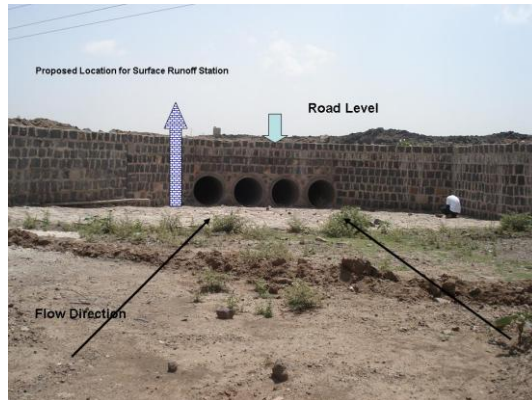


Figure 6-77 Proposed location for the surface water runoff station for Wadi Al-Muliki

6.12 Surface Runoff Monitoring Station for Wadi Iqbal

Wadi Iqbal is located on the west side of the Sana'a Basin, covering a total area of 203 km². Spatial analysis and streamline delineation show that the wadi has about 17 sub-basins, as shown in Figures 28 and 29 (Chapter 4). The digital elevation map shows that the optimum location for a surface runoff station is near the basin outlet. During the field visit, to the proposed location, it was discovered that about 800 m upstream of the selected site, a new in-ground reservoir had been constructed to serve the neighborhood. The reservoir dimensions are 64m x 37m x 5.6 m, for a total volume of 13,260 m³. The reservoir was constructed across the main wadi channel. Figures 204, 206 and 208 show the dimensions of the reservoir from different perspectives. Figures 205 and 206 present general views for the upstream channel section. The reservoir is equipped with a downstream spillway which runs across the original wadi and flows toward the selected cross-section. Figure 206 is the downstream view of the natural spillway channel of the dam. It is proposed to install a wadi gage station equipped with a shaft encoder that can be float operated or connected to servo mechanical sensors and chart recorders. The proposed station would be installed as shown in Figure 208.

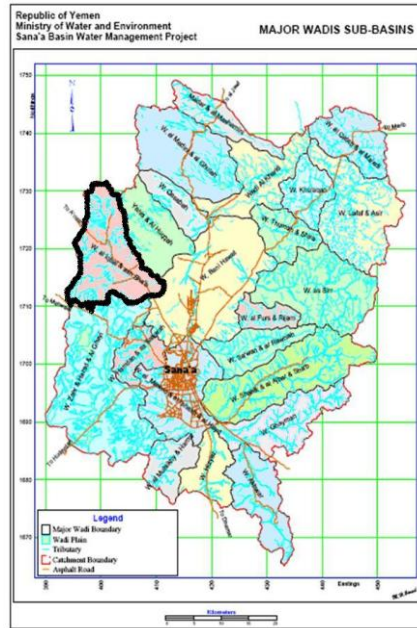


Figure 6-78 Location of Wadi Iqbal within the Sana'a Basin (black boundary)



Figure 6-79 Dimensions of the reservoir (under-construction) in the main stream of the Wadi Iqbal floodpath. Coordinates are: 1714085 and UTM E 408986



Figure 6-80 Upstream view of the main stream floodpath leading to the constructed reservoir



Figure 6-81 General view of the reservoir showing the location of the spillway and the flow entrance structure

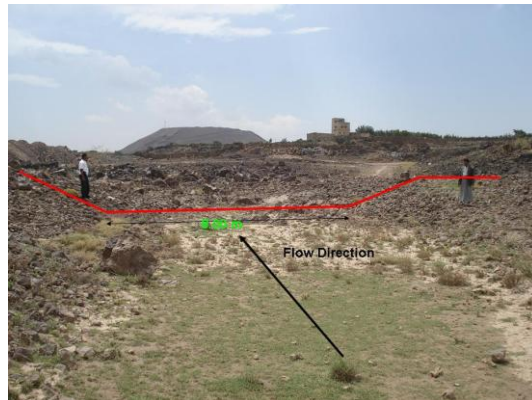


Figure 6-82 Downstream cross-section, including spillway for excess water



Figure 6-83 Proposed location for the surface water runoff station at Wadi Iqbal

6.13 Surface Runoff Monitoring Station for Wadi Zahr

Wadi Zahr is a relatively large wadi with an area of 365 km². The wadi is located on the west side of the Sana'a Basin, as shown in Figure 209. The wadi has many tributaries and about 32 sub-basins, as described in the spatial analysis section of chapter 4 (Figures 58 and 59). After spatial analysis, several locations were proposed as possible locations for the monitoring station. The main section is found just upstream of the basin outlet point. A field visit was conducted to the proposed location where the final position for the station was selected. The Wadi Zahr main channel has a flat bed with a fine sand surface. The channel sides are well defined with stone walls, as shown in Figure 211. The upstream view from the selected location shows the intersection point between two sub-basins. The cross-sectional width at the selected location is 12.0 m and the channel height ranges from 1-2 m, depending on the condition of the side walls. Figures 210 through 213 present different views of the location. It is proposed to install a wadi gage station equipped with a shaft encoder that can be float operated or connected to servo mechanical sensors and chart recorders. The proposed station can be installed as shown in Figure 213.

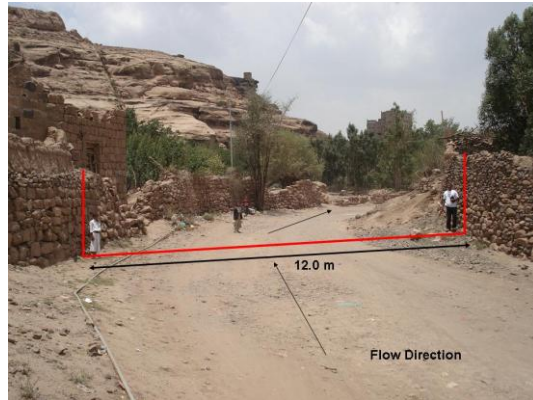


Figure 6-86 Cross-section of the Wadi Zahr main stream



Figure 6-87 Downstream view of the selected cross-section showing the intersection of two main streams at the proposed location for measurement

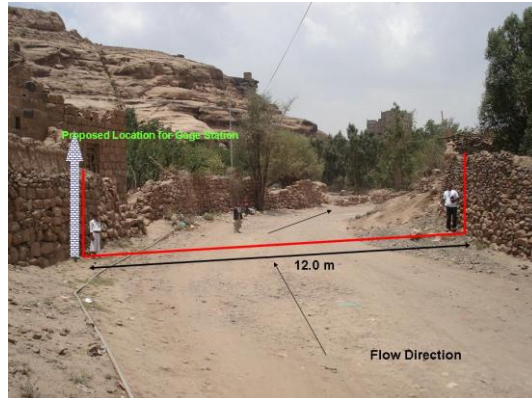


Figure 6-88 Final selected location for the Wadi Zahr surface water runoff station

6.14 Surface Runoff Monitoring Station for Wadi Hizayaz

Wadi Hizayaz is located in the southern part of the Sana'a Basin, covering an area of 76 km². The wadi location within the Sana'a Basin is shown in Figure 214. Streamline delineation analysis shows that the wadi has one major stream and four significant sub-basins, two of which form the far upstream part of the wadi, with the remaining two close to the wadi outlet. Spatial analysis for Wadi Hizayaz is presented in Figures 20 and 21 (Chapter 4). The optimum location for the monitoring station was determined based on the spatial analysis results, as shown in Figure 119 in Chapter 5. Accordingly, a field visit to the proposed location was conducted. During the visit, it was discovered that the wadi has been invaded by urbanization. At the proposed location, there was no clear evidence of any reliable cross-section since buildings and roads were omnipresent. Figures 216 through 218 present the current situation of the streamline system at the proposed location. It is clear that there is no obvious location for the monitoring location.

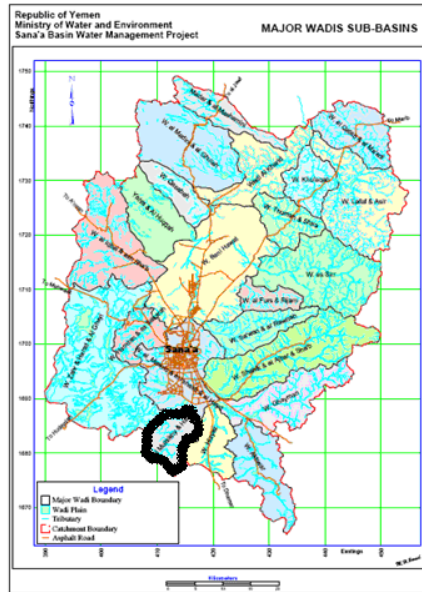


Figure 6-89 Location of Wadi Hizyaz within the Sana'a Basin (black boundary)

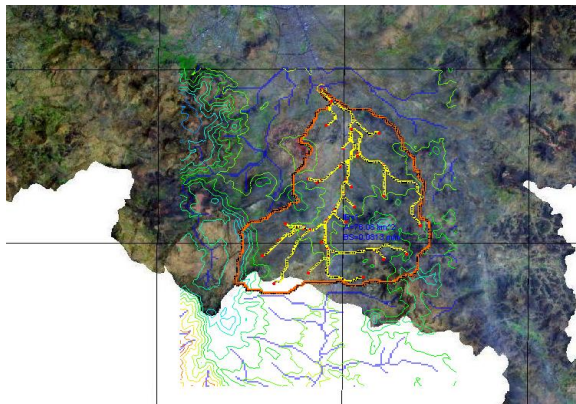


Figure 6-90 Hizyaz basin and streamline delineation map



Figure 6-91 View of the urbanization of Wadi Hizyaz



Figure 6-92 Current status of the proposed monitoring location



Figure 6-93 Road construction at the proposed monitoring location

6.15 Surface Runoff Monitoring Station for Wadi Al-Kharid

Wadi Al-Kharid is located in the northern part of Sana'a Basin with an area of 139 km² as shown in Figure 220. Wadi AL-Kharid contains the outlet point for the entire Sana'a Basin, thus it is considered to be very important for measurement. All collected surface runoff from the entire Sana'a Basin, excluding losses, evaporation and seepage, should end up in Wadi Al-Kharid. Figure 219 presents a Google Earth Image for the Outlet point of Wadi Al-Kharid. Previous studies show that there is a V-notch weir located exactly at the point of the Sana'a Basin outlet. Accordingly, a special field visit was conducted to check this location. From Figures 221 and 222, it can be observed that the Wadi Al-Kharid streamline system consists of one major stream toward the middle of the wadi with many intersecting tributaries. Thus, there are many wadis that connect to the Wadi Al-Kharid main stream: Meder, Al-Qatab, Lafaf and Asir, Yahis, and Al- Qasaba. In addition, during field visits to all of these wadis, it was found that it would be very difficult to install surface water runoff stations at each of the wadis listed above. The topography of the intersections where these wadis join the main stream of Wadi Al-Kharid is very rough. So, the decision was made to install two monitoring stations along the main stream. The first is located approximately at the middle point of the main stream, while the second is at the location of the final weir. Thus, the first monitoring station will measure the three upstream wadis and the second one will measure the next three, taking into consideration that these two locations are also measuring the surface runoff gathered from all of the upstream wadis. A field visit to Wadi AL-Kharid was conducted, but it was impossible to reach the outlet point of Wadi Al-Kharid by car because of the very rough road. Thus, hiking is the only possible way to reach the target location. Figure 223 presents a fly-over view of the first 2-3 km of the Wadi Al-Kharid main stream. As shown in this figure, the main stream runs between two precipices; the outlet is located 6 km from the site of the picture. Figures 224 through 226 show the surface bed configuration, which changes from cobbles to boulders to very large rocks. The water has traced a path through small tunnels developed inside these large rocks. The path is very rough from a topographic point of view. The visit was in the month of December and no traces of water were evident. Finally, the team reached the V-Notch weir installed in the 1980's at the outlet point of Sana'a Basin. Figures 227 through 230 show different views of the weir. Field measurements indicate that the V-Notch dimensions are 125 cm in width and 37 cm in depth. In addition, the streambed upstream of the weir is full of sediment, meaning that water depth in front of the weir will be in the range of 15 cm (considered very small). The vertical distance between the highest and lowest points of the V-Notch is 37 cm. Thus, it is expected that this V-Notch cannot pass more than ...m³/sec. Also, in front of the weir there is a gage station where a water depth instrument had been installed, as shown in Figure 231. No records were found for this instrument location. It is recommended that an ultrasound water level instrument be installed to measure the water level at the weir location. This instrument must

have GSM technology so that data can be transferred directly from this remote area. The installed instrument should therefore be placed in an armed box for instrument safety.



Figure 6-94 Google Earth image for the location of the Wadi Al-Kharid outlet surface water runoff station at UTM N = 1739880 and UTM E at 436650

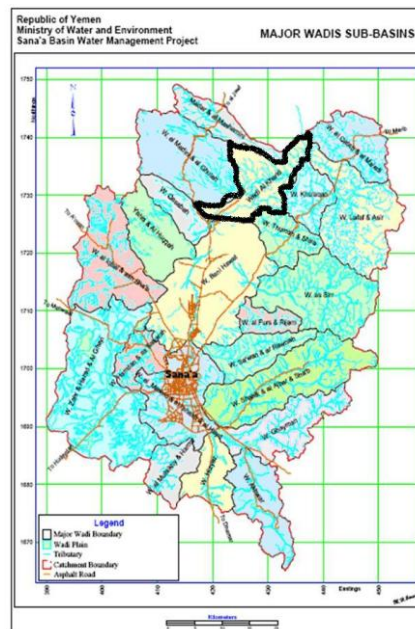


Figure 6-95 Location of Wadi Al-Kharid within the Sana'a Basin (black boundary)

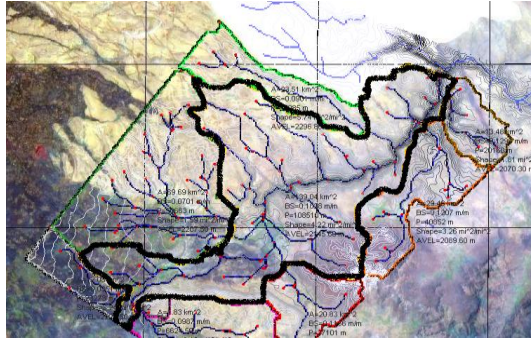


Figure 6-96 Al-Kharid basin streamline delineation map

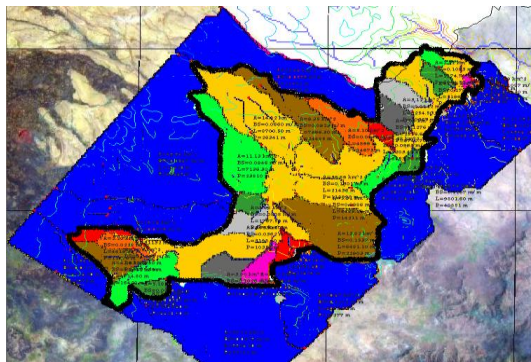


Figure 6-97 Al-Kharid sub-basin delineation and area of each sub-basin



Figure 6-98 General fly-over view of Wadi Al-Kharid showing the beginning of the wadi's main stream



Figure 6-99 Surface bed of Wadi Al-Kharid



Figure 6-100 Another view of the Wadi Al-Kharid bed surface



Figure 6-101 Wadi AL-Kharid bed configuration



Figure 6-102 Existing V-Notch weir at Wadi Al-Kharid



Figure 6-103 Backside view of the V-Notch weir at Wadi Al-Kharid



Figure 6-104 V-Notch during field measurements



Figure 6-105 V-Notch weir and its concrete wings



Figure 6-106 Location of wadi water level station in front of V-Notch

6.16 Surface Runoff Monitoring Station for Wadi Al-Kharid Bridge

As stated in the previous section, an additional surface water monitoring station has been selected at Wadi Al-Kharid Bridge. The bridge will be an ideal location for surface runoff monitoring. Figures 232 through 235 show a general view of the bridge location. Figures 233 and 234 show the upstream bed surface consisting of medium size boulders. This location is suitable for installation of a wadi gage station but there will be an essential need to survey the upstream channel to determine the characteristics of the open channel. It is proposed to install a wadi gage station equipped with a shaft encoder that can be float operated or connected to servo mechanical sensors and chart recorders. The proposed station can be installed as shown in Figure 235.



Figure 6-107 View of the bridge openings and piers



Figure 6-108 General view of the bridge across Wadi Al-Kharid



Figure 6-109 View of the upstream surface bed



Figure 6-110 Details of the monitoring station location

6.17 Surface Runoff Monitoring Station for Sana'a Basin Wastewater Treatment Plant and the Wastewater Passage

Sewage water treatment for the Sana'a Basin is performed at the Sana'a Wastewater Treatment Plant. In general, activated sludge plants use a variety of mechanisms and processes that use dissolved oxygen to promote the growth of biological floc, which then work to produce a substantial removal of organic material. The process traps particulate matter and can, under ideal conditions, convert ammonia to nitrite and nitrate and ultimately to nitrogen gas. The Sana'a Wastewater Treatment Plant also has final clarifiers for improving the secondary treatment effectiveness. Finally, the plant has tertiary treatment as a final stage to raise the effluent quality before it is discharged to the receiving environment. In the Sana'a plant the effluent from the tertiary treatment is directly connected to an effluent polishing lagoon. Figures 236 and 237 show current Google Earth satellite images of the plant and its different components. Shown in this figure are the locations of the plant inlet, screw pumps, aerations tanks, clarifiers, drying bed, polishing lagoon, outlet, and overload-spillway channel. Figure 237 shows an enlarged satellite image of the inlet, screw pumps, aeration tanks and clarifiers. From the field visit, it was concluded that the plant is efficiently operated and the BOD_5 of the effluent is in the range of 40-50 mg/L. The plant's daily capacity is 50,000 m³; however, due to low water volumes, the inflow is loaded with very high biological oxygen demand and total suspended solids. Sana'a City sewer networks have been improved in the last five years, so inflow to the treatment plant has recently increased. During peak flow hours, the plant operators are compelled to open an overload spillway valve to keep the plant from flooding. This water flows out completely untreated. A new wastewater treatment plant for Sana'a City will be added in the coming years. During the field visit, it was discovered that the flow measuring instruments are not currently functional and no records for either the inflow or the outflow were available. Figures 238 through 247 show the different stages of the Sana'a Wastewater Treatment Plant. It is recommended that two new surface water monitoring instruments be installed since the existing flow measurement units are out of order. The first location is at the site of the existing treated flow measuring instrument, installed in the chlorination room. Figures 248 and 249 show the entrance to the chlorination room, the existing ultrasound instrument and the data logger hanging on the wall. It is also essential to measure the untreated sewage that passes through the overload-spillway channel. Accordingly, it is proposed to construct a sharp-crested weir in the overload-spillway channel where an ultrasound water level instrument will be installed to measure water levels at the weir location.

The effluent flow of the Sana'a Wastewater treatment plant runs across the Sana'a Basin for a distance of about 26 km until it reaches Wadi AL-Kharid. Along this path are three dams: Al-Roda, Al-Masham and Al-Semna. The geological formation of this path is very crucial since **it's running is overlaid**

with major faults. Accordingly, it has been found that developing surface water monitoring along this path will be a major benefit for the Sana'a Basin management project. Treated and untreated wastewater flow together in this channel. Figure 251 presents a general view of the first location downstream of the wastewater treatment plant. The channel is about 2.5 meters in width and about 0.50 meter deep. Figure 251 shows the field visit team during the measurement of the channel width and depth. In addition, the surface velocity was measured using floats; the velocity of the channel was found to be in the range of 27 cm/sec. Intensive field visits were performed to explore and check every kilometer of the sewage path. The path runs across agricultural land starting from the treatment plant and running as far as a place named Bani-Garmouz. This path has a length of nearly 15 km. Figure 250 presents a Google Earth image with the passage overlay. At Bani-Garmouz, a road culvert was found underneath an asphalted road. Significant cultivated area is located in the 15 km before this road culvert. Thus, a surface runoff flow measurement station should be allocated to this location to identify how much flow is being withdrawn in the area between the treatment plant and Bani-Garmouz. Figures 252 and 253 document the Bani-Garmouz culvert where the new station will be installed. As shown in these figures, the flow is relatively high - these amounts of flowing water are rarely seen in the Sana'a Basin. Only on certain rainy days can this amount of flow be witnessed, as shown in Figures 254 through 256. Directly downstream of Bani-Garmouz is Al-Mosyerka dam. After a very short distance, the water reaches the Al-Roda dam. Figure 257 shows a Google Earth satellite picture of Al-Mosyerka dam and its lake. Water flow over Al-Mosyerka dam is directly transferred to Al-Masham Dam, which is located about 2.5 km downstream of Al-Roda dam. Figure 258 shows a Google Earth satellite picture of Al-Masham dam and its lake. The outflow from Al-Masham dam then runs through high cliffs until it reaches the Al-Semna dam. At Al-Semna Dam, water is accumulated, forming a relatively large lake. The lake is bordered by large trees and is habitat for many types of birds. Based on field visits, it can be said that AL-Semna Lake forms the end of the treated and untreated wastewater flows. These flow into the lake, shown in Figure 259, which is located in a land depression. There was no evidence of recent flow over the Al-Semna dam spillway. Accordingly, it is highly recommended that a staff gage be installed inside Al-Semna Lake to measure water level fluctuations throughout the year. An intensive survey of the lake boundary and berm should be also be conducted to allow calculation of a mass balance for this lake.



Figure 6-111 Google Earth picture showing the general layout of the Sana'a Wastewater Treatment Plant



Figure 6-112 Aeration basins and trickling filters of Sana'a WWTP



Figure 6-113 Inlet channel for raw sewage and the parshall flume



Figure 6-114 Lifting pumps inside Sana'a WWTP



Figure 6-115 Aerators at work inside the aeration basins of Sana'a WWTP



Figure 6-116 Trickling filters in Sana'a WWTP



Figure 6-117 Treated wastewater flowing out from the trickling filter



Figure 6-118 Sludge drying beds in Sana'a WWTP



Figure 6-119 Polishing lagoon in Sana'a WWTP



Figure 6-120 Rectangular siphon of the Sana'a WWTP outlet



Figure 6-121 Outlet of Sana'a WWTP



Figure 6-122 Inlet point of Sana'a WWTP



Figure 6-123 Ultrasound surface water measuring device in Sana'a WWTP



Figure 6-124 Data logger for the ultrasound device on Sana'a WWTP

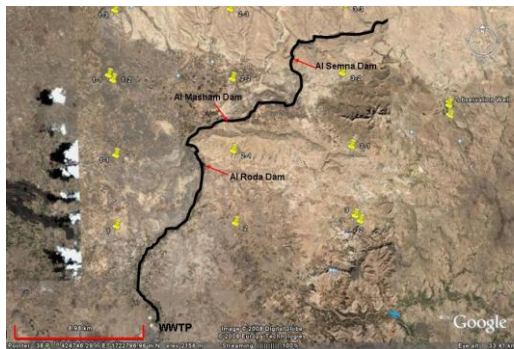


Figure 6-125 Treated wastewater passage



Figure 6-126 Treated wastewater passage just downstream from Sana'a WWTP



Figure 6-127 The road culvert in the Bani-Garmouz area. Al-Mosayerka Dam is 1.5 km downstream



Figure 6-128 Upstream view from the Bani Garmouz road culvert



Figure 6-129 Downstream view of the Bani Garmouz road culvert



Figure 6-130 Flow downstream from the road culvert at Bani Garmouz



Figure 6-131 Flow downstream from the road culvert at Bani Garmouz



Figure 6-132 Google Earth image showing the Al-Moseyreka Dam Lake, just downstream from the Bani Garmouz road culvert



Figure 6-133 Google Earth image showing the Al-Masham Dam Lake, just downstream from Al-Mosyeraka Dam



Figure 6-134 Panorama of Al-Semna Dam Lake, downstream from Al-Masham Dam

6.18 Final Surface Runoff Monitoring Stations

Table 4 shows the final locations for Surface Water Runoff Stations throughout the entire Sana'a Basin. Figure 260 presents a map of these final locations. Note that there are also three more stations to be installed along the treated wastewater passage.

| Ser No. | Wadi Name | UTM E | UTM N | GPS Level (m) | Station Cross-section Description |
|---------|------------------|--------|---------|---------------|-----------------------------------|
| 1 | Sanhan | 426052 | 1685774 | 2355 | Road Culvert |
| 2 | Ghayman | 429534 | 1687768 | 2411 | Dam Lake |
| 3 | Shahik | 427870 | 1696144 | 2410 | Road Culvert |
| 4 | Sa'awan | 419444 | 1702761 | 2274 | Open Channel |
| 5 | Al-Furs | 426000 | 1710625 | 2274 | Road Culvert |
| 6 | Al-Sirr | 432849 | 1713362 | 2253 | Open Channel |
| 7 | Thuma | 428835 | 1726392 | 2064 | Open Channel |
| 8 | Al-Kharid Bridge | 441456 | 1734314 | 2034 | Bridge Opening |
| 9 | Khulaqah | 437089 | 1734937 | 1925 | Road Culvert |
| 10 | Al-Kharid Outlet | 436758 | 1739964 | 1825 | Weir |
| 11 | Al-Melaiky | 415755 | 1686539 | 2331 | Road Culvert |
| 12 | Zahr | 405858 | 1707154 | 2262 | Open Channel |
| 13 | Iqbal | 408986 | 1714085 | 2242 | Ground Reservoir |
| 14 | Al-Mawrid | 415475 | 1700396 | 2255 | Bridge Opening |

Table 6-1 Final locations and coordinates of the Surface Water Runoff Stations for the Sana'a Basin

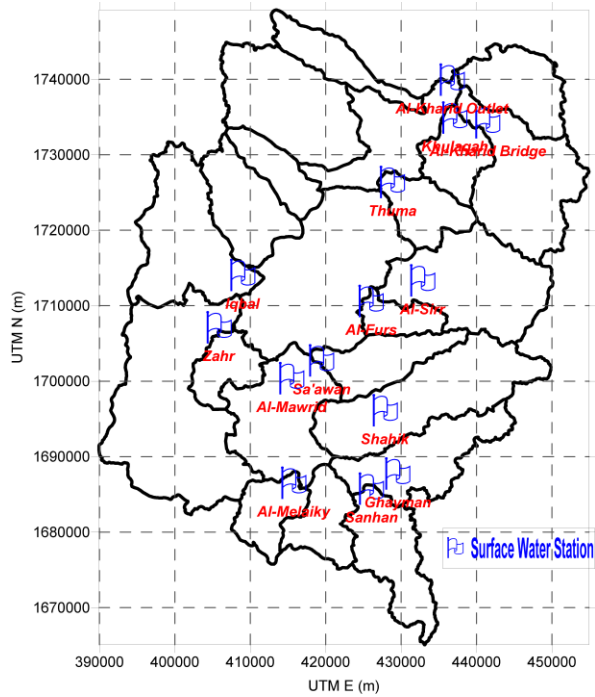


Figure 6-135 Locations of surface water runoff stations for the Sana'a Basin